Pigment dispersing factor: Transcriptional regulation and its role in metabolism in *Drosophila melanogaster*

A Dissertation Presented for the
Doctor of Philosophy
Degree
The University of Tennessee, Knoxville

Sudershana Nair
August 2016

Copyright © 2016 by Sudershana Nair.
All rights reserved.

ACKNOWLEDGEMENTS

This work would not have been possible without the guidance and help of many individuals. First and foremost, I would like to thank my advisor, Dr. Jae H. Park, for his guidance and support throughout my tenure. I will always be grateful to him for letting me choose my thesis project and giving me the freedom to pursue various projects. Dr. Gyunghee Lee deserves mention for being the constant knowledge resource on *Drosophila* genetics and behavior. I would like to thank all the past and current members of the Park lab, including Dr. Zixing Wang, Dr. Kai Sha, Ritika Sehgal, Katherine Stefanski and Dr. Siuk Yoo for support and advice. I would also like to thank my committee members, Drs. Bruce D. McKee**,** Ranjan Ganguly, Rebecca Prosser and Juan Luis Jurat-Fuentes for their willingness to serve on my committee and for their advice and discussion. I really appreciate the help from members of McKee and Labrador lab for sharing reagents and protocol. Additionally, I would also like to thank all members of the Prosser Lab for fun time at circadian rhythm conferences.

A number of talented undergraduates have assisted me in many aspects of my work. Rebecca Murdaugh and Thong Luong, who have moved on for their graduate studies deserve a special mention for their hard work and enthusiasm for science. Shannon Smith, Abigail Stidham, Gloria Kwak, Haylie Lam, Yoonjee Kim, James Ray and William Guthrie are among the multitude of undergraduates who have contributed to the lab morale.

Finally, I would like to thank my family and friends who did not contribute in the scientific aspect of this work yet this journey would not have been possible without them. My Mom and Dad for their continuous support and for instilling the value of hard work that has served me well as a scientist. I will always be grateful to my friends Nozomi Shirato, Dhivya Kumar, Amrita Sherlekar, Shih-Jui Hsu, Kristen Holbrook, Badri Krishnan, Snehal Joshi and Sujith Raj for inspiration and constantly reminding me not to take life too seriously.

ABSTRACT

Almost all living organisms have circadian clocks coordinating physiology and behavior, and an innate molecular clock drives rhythmic changes by integrating environmental and metabolic stimuli to generate 24 hour timing. *Drosophila melanogaster* has proved to be an excellent model organism with a well-characterized circadian clock and the neural circuits underlying clock have been intensely investigated. The neuropeptide pigment-dispersing factor (PDF) plays an essential role in maintaining circadian rhythmicity and synchronizes circadian clock neurons. However, the regulation of *Pdf* has been a black box with no known protein identified that directly regulates it, and its role in metabolism hasn't been looked into. In addition, the role of different signaling pathways that work in the PDF expressing neurons to integrate circadian period also needs to be explored. The collection of work presented here addresses some of these concerns. Chapter II outlines the role of a transcription factor in spatially restricting *Pdf* expression to the ventral lateral neurons that express this neuropeptide. We have identified a cis-regulatory element in the promoter of *Pdf* that is sufficient for its expression in the ventral lateral neurons. In addition, we have identified a novel homeodomain transcription factor scarecrow (scro) that directly binds and negatively regulates *Pdf*. Chapter III aims to characterize the function of *scro* in tissue identity and specification during *Drosophila* development. Here, we have outlined the possible mechanism by which *scro* plays a role in proper development of tissues. Chapter IV addresses the role of transforming growth factor – beta (TGF-β) in PDF neurons. Furthermore, we have identified a Type I receptor in this signaling pathway that

downregulates *Pdf* and is key to maintaining circadian rhythmicity. Finally, Chapter V addresses the role of PDF signaling pathway in caffeine metabolism, thus linking central clock to metabolism. We hypothesize the importance of PDF in regulating *cytochrome* genes induced in response to caffeine. Taken collectively, this body of work enhances our present understanding of *Pdf* regulation in addition to identifying the role of TGF-β signaling in the PDF expressing neurons. This study also identifies novel role of *scro* during *Drosophila* development.

TABLE OF CONTENTS

CHAPTER 1: INTRODUCTION 1
Circadian Rhythms *2*
Neuropeptide: Pigment dispersing factor *4*
TGF- β signaling and the circadian clock *10*
Circadian clock and metabolism *12*
CHAPTER 2: *SCARECROW* NEGATIVELY REGULATES *PDF* NEUROPEPTIDE GENE IN THE CIRCADIAN PACEMAKER NEURONS IN *DROSOPHILA MELANOGASTER* 15
Abstract *16*
Introduction *17*
Materials and Methods *19*
Results *27*
Discussion *56*
CHAPTER 3: CHARACTERIZING THE FUNCTION OF *SCARECROW* IN DEVELOPING TISSUES 60
Abstract *61*
Introduction *61*
Materials and Methods *64*
Results *65*
Discussion *81*
CHAPTER 4: TGF- β SIGNALING IN PIGMENT DISPERSING FACTOR (PDF) EXPRESSING SMALL VENTRAL LATERAL NEURONS 88
Abstract *89*
Introduction *89*
Materials and Methods *93*
Results *94*
Discussion *106*
CHAPTER 5: MECHANISM FOR CAFFEINE RESISTANCE IN P*IGMENT DISPERSING FACTOR* (*PDF*) MUTANTS 113
Abstract *114*
Introduction *115*
Materials and Methods *118*
Results *121*
Discussion *132*
CHAPTER 6: CONCLUSIONS 137
LIST OF REFERENCES 141
APPENDIX 159
VITA 163

LIST OF TABLES

Table 2.1: Primers used for *scro* transgenic constructs 25
Table 2.2: Locomotor activity analysis of *scro* driven by specific Gal4 constructs 47
Table 2.3: Mutation frequencies of *scro* induced by Cas9 52
Table 4.1: Locomotor activity assay for TGF-β components.....108

LIST OF FIGURES

Figure 1.1 Organization of circadian neurons in the *Drosophila* brain 5
Figure 1.2 *Drosophila* oscillator model 6
Figure 2.1 *Pdf-Gal4* constructs 30
Figure 2.2 GFP expression in the larval CNS driven by *Pdf-Gal4*s 31
Figure 2.3 *GFP* expression in the adult CNS driven by various *Pdf-Gal4*s 32
Figure 2.4 Alignment of *PRE* from different *Drosophila* species. 34
Figure 2.5 Isolation of SCRO as a *PRE* binding factor 35
Figure 2.6 Expression of *Pdf* in response to ectopic *scro* expression 39
Figure 2.7 Suppression of *Pdf* expression by SCRO 40
Figure 2.8 PDF-immunoreactivity in adult brain. 41
Figure 2.9 SCRO is not cytotoxic to the neurons 44
Figure 2.10 PDF immunoreactivity in the adult brain resulting from the transgenic expression of mutant *scro* and *vnd* 45
Figure 2.11 Locomotor activity rhythms of flies expressing *scro* 48
Figure 2.12 No ectopic *Pdf* expression was detected after *scro* knockdown. 50
Figure 2.13 Generation of *scro* mutant using CRISPR. 53
Figure 2.14 Expression pattern of *scro* in the larval, pupal and adult CNS 55
Figure 3.1 Eye imaginal disc in the third instar larvae. 68
Figure 3.2 Ectopic expression of *scro* during late eye development 70
Figure 3.3 Overexpression of *scro* causes apoptosis in the developing eye. 71
Figure 3.4 Regions expressing Gal4 drivers in the wing disc. 73
Figure 3.5 Drosophila adult wing and leg phenotypes resulting from overexpression of *scro* 76
Figure 3.6 Ectopic *scro* expression in the wing pouch leads to transformation of halteres to wings 77
Figure 3.7 Overexpression of *scro* leads to increased apoptosis in the developing wing 78
Figure 3.8 Overexpression of *scro* leads to abnormal terminalia 80
Figure 3.9 SCRO does not downregulate transcription of dsx^{M} 82
Figure 3.10 Expression pattern for *scro* in different tissues 83
Figure 3.11 Hypothetical model for the role of *scro* in regulating Bithorax complex 87
Figure 4.1 Expression of Pdf in response to knockdown of type I receptor $babo_a$ 97
Figure 4.2 Knockdown of $babo_a$ isoform leads to lack of PDF expression in the s-LNvs and arrhythmicity 99
Figure 4.3 Knockdown of $babo_b$ and $babo_c$ led to misrouting phenotype 101
Figure 4.4 Cell autonomous role of $babo_a$ in the PDF positive neurons. 103
Figure 4.5 Type I receptors *punt* and *wit* affect PDF expression. 105
Figure 4.6 Knockdown of dSmad2 and Medea affect development of the PDF neurons 107
Figure 4.7 Model for TGF- β signaling in the PDF expressing s-LNvs 110
Figure 5.1 Average survival rate (%) for *CS* and Pdf^{01} at different concentrations of caffeine 124
Figure 5.2 Average survival rates of different genotypes in 1.2 mg/ml caffeine 127

Figure 5.3 Measurement of food consumption using CAFE assay 128
Figure 5.4 Measurement of food consumption using feeding assay 129
Figure 5.5 Locomotor activity for CS and *Pdf*^{01} flies..... 131
Figure 5.6 RT-PCR results show higher expression of *cyp6a8*..... 133
Figure 5.7 Model for the role of PDF pathway in regulating caffeine induced gene *cyp 6a8* 136
Figure A1: Overexpression of *Gro* led to aberrant phenotype of the s-LNv dorsal projections. 161
Figure A2: Ectopic expression of *Gro* led to abnormal eye phenotype 162

CHAPTER 1: INTRODUCTION

Circadian Rhythms

Circadian clocks synchronize the physiology, behavior and metabolism of organisms to their environment thus helping them adapt and maximize their chances of survival. The core clock or the central oscillator consists of genes that interact with each other in a feedback loop to generate circadian rhythms that oscillate with a period of approximately 24 hours, and this information is then handed down to clock regulated downstream genes. This oscillator is resynchronized everyday by Zeitgebers (time giver in German) like light intensity, temperature, food availability and social interactions and is capable of sustaining itself even in the absence of external time cues (Dubruille and Emery, 2008).

Genetic studies in *Drosophila* identified several clock genes that form transcriptional-translational feedback loops that lead to rhythmic accumulation of clock genes, RNA and proteins. A model for the *Drosophila* oscillator is provided in Figure 1.2. The first feedback loop involves basic helix loop helix (bHLH) and Per-Arnt-Sim (PAS) domain containing transcription factors Clock (CLK) and Cycle (CYC) that form a heterodimer and bind to an enhancer box (E-box) on the promoter of the genes *period* (*per*) and *timeless* (*tim*). Some eukaryotic genes have an E-box in their promoter region with a canonical sequence of CACGTG that is recognized by bHLH-PAS transcription factors (He et al., 1992). PER and TIM proteins form heterodimers and enter the nucleus during nighttime to inhibit CLK/CYC that will, in turn, prevent transcription of *per* and *tim*. The light dependent degradation of PER and TIM restores CLK and CYC activity during daytime (Allada et al., 1998; Darlington et al., 1998; Hao et al., 1997; McDonald et al.,

2001; Rutila et al., 1998). Light activates Cryptochrome (CRY), a blue-light photoreceptor that binds to TIM and targets it for degradation (Stanewsky et al., 1998).

The circadian pacemaker in *Drosophila* and other organisms consists of conserved transcriptional and post-transcriptional regulators. A set of kinases and phosphatases regulate the precise timing of activation and repression of PER and TIM. PER and CLK phosphorylation is regulated by Doubletime (DBT), with DBT closely attached to PER during nuclear translocation of the PER/TIM complex. Casein kinase II regulates PER phosphorylation, whereas protein phosphatase 2A regulates both PER and CLK. The ortholog of glycogen synthase kinase SHAGGY (SGG) and protein phosphatase I regulate phosphorylation and dephosphorylation of TIM respectively (Fang et al., 2007; Martinek et al., 2001). CLK/CYC compete with clockwork orange (cwo), a bHLH transcription factor to bind to the E-box region of *per* and *tim* and regulate their transcription, thus forming a second feedback loop (Kadener et al., 2007; Matsumoto et al., 2007). CLK and CYC activate *vrille* (*vri*) and *Par domain protein* (*Pdp1*), and VRI and PDP1 in turn regulate CLK (Glossop et al., 1999; Hardin, 2006). However, the function of this interlocked feedback loop remains unclear.

Neuroanatomy of pacemaker neurons

Clock genes are expressed in approximately 150 neurons in the adult *Drosophila* brain (Kaneko and Hall, 2000; Nitabach and Taghert, 2008; Rieger et al., 2006; Shafer et al., 2006). These neurons are divided into six clusters based on their anatomical position:

ventrolateral neurons (LNvs), dorsolateral neurons (LNds), 3 groups of dorsal neurons (DN1, DN2 and DN3) and the lateral posterior neurons (LPNs) (Figure 1.1). LNvs are further divided into 4 small LNvs (s-LNvs) and 4-5 large LNvs (l-LNvs) that express the neuropeptide pigment-dispersing factor (PDF) and a single PDF-negative s-LNv (Kaneko, 1998) that expresses ion transport peptide (ITP) (Hermann-Luibl et al., 2014). Three to four LNds express the photoreceptor Cryptochrome (CRY) (Picot et al., 2007; Rieger et al., 2006; Yoshii et al., 2008) and one LNd expresses ITP (Hermann-Luibl et al., 2014). All of these neurons have a dedicated role in controlling circadian behavior.

Wild type flies are active at dawn and dusk but relatively inactive at midday and midnight when kept under 12hr: 12hr light-dark (LD) conditions. When subjected to constant conditions (DD), the wild-type flies display activity bouts at approximately the same time each day reflecting a period close to 24 hours. The LNvs play a crucial role in maintaining rhythms under constant conditions and control the morning peak and hence are called M-cells (Stoleru et al., 2004). LNds, 5^{th} s-LNv and 2 DN1s control evening activity peak and hence are referred to as E cells (Stoleru et al., 2004). LPNs express TIM and PER and have a role in temperature entrainment of the clock (Miyasako et al., 2007; Yoshii et al., 2005).

Neuropeptide: Pigment dispersing factor

Neuropeptides are ubiquitous and diverse signaling molecules present in multicellular organisms and regulate a wide range of biological processes.

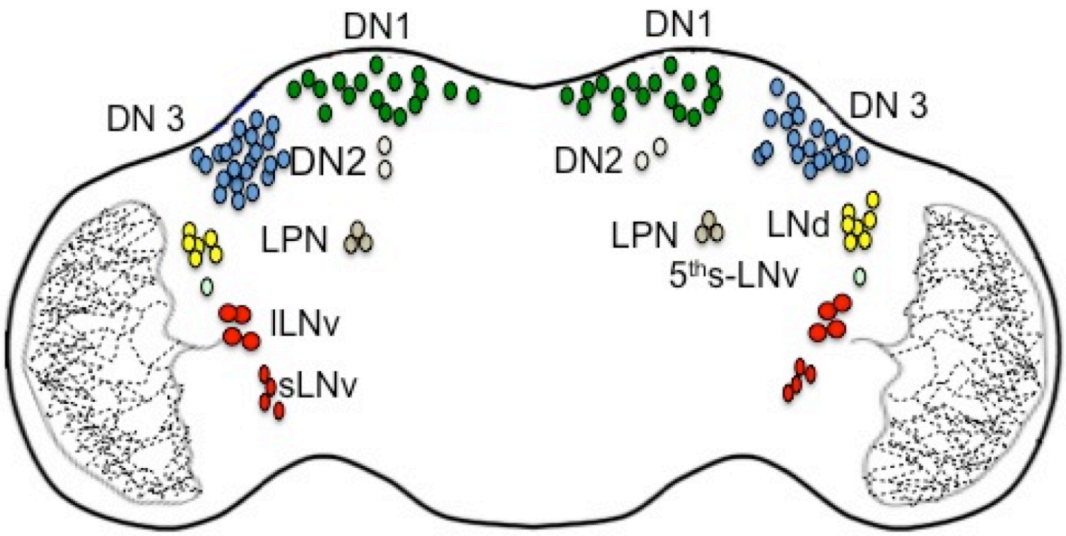


Figure 1.1 Organization of circadian neurons in the *Drosophila* brain

The s-LNvs and l-LNvs (red) are the only neurons that express the neuropeptide PDF. The fifth s-LNv (aqua green) does not express PDF. The LNds (yellow) and the LPN (brown) represent the rest of the lateral neurons in the adult brain. The dorsal neurons DN1 (green), DN2 (white) and DN3 (blue) are shown in the anterior brain.

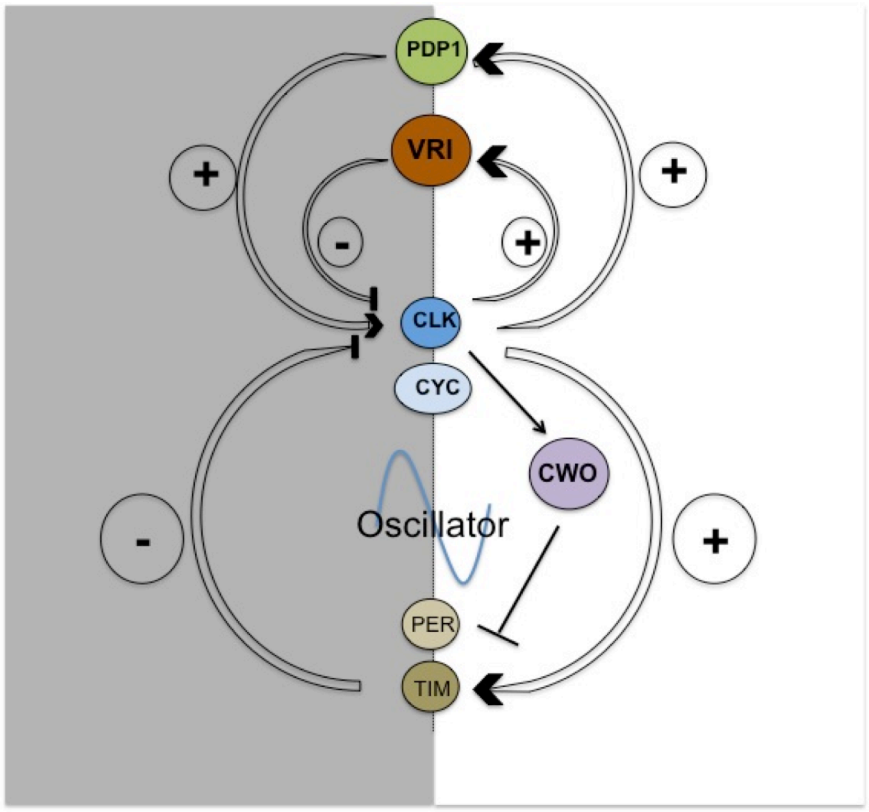


Figure 1.2 *Drosophila* oscillator model. The core molecular clock consists of CLK and CYC proteins that form a heterodimer and bind to E box on the promoters of *per* and *tim* to activate their transcription. PER and TIM form a complex and enter the nucleus and inhibit their activation by blocking the activity of CLK and CYC forming a feedback loop. CWO competes with CLK and CYC to bind to the promoters of *per* and *tim* forming a second feedback loop. In addition, there exists a feedback loop that regulates *Clk* transcription with VRI and Pdp1 but the function of this interlocked loop is not clear.

In *Drosophila melanogaster* there are 42 known neuropeptide precursor genes that regulate development, longevity, circadian rhythms, metabolism and ecdysis behavior among many other functions (Hewes and Taghert, 2001; Nassel and Winther, 2010; Vanden Broeck, 2001). Pigment-dispersing factor (PDF) is one of the neuropeptides well studied for its role in circadian rhythms in *Drosophila melanogaster*. PDF is structurally homologous to the crustacean pigment-dispersing hormone (PDH) and has been identified in various insects (Rao and Riehm, 1993). In crustaceans, PDH functions in the dispersion of pigment within chromatophores and induce light adaptive movement of screening pigment in the distal eye (Rao, 2001). However, there is no functional similarity between PDF and its crustacean counterpart PDH. Subsequently, PDF immunoreactivity was observed in the LNvs that express the clock gene *per* (Helfrich-Forster, 1995) and that was the first clue for the role of PDF in the circadian clock. Also behaviorally arrhythmic *disconnected* (*disco*) mutants lacked PDF immunoreactivity (Helfrich-Forster, 1995), further providing support for a possible role for PDF in circadian rhythms.

More definitive evidence came from genetic and behavior studies on PDF null mutants (Pdf^{01}) that exhibit abnormal circadian rhythms (Renn et al., 1999). Pdf^{01} flies lack the morning anticipation peak in addition to having a phase advance in the evening activity peak under LD conditions. When these flies were shifted to DD, they gradually become arrhythmic within the initial 3 days. *Pdf* transcripts or peptide levels do not oscillate in a circadian manner. However, there is a diurnal variation in PDF immunohistochemistry in the dorsal projections emanating from the s-LNvs (Park et al., 2000) indicating that

rhythmic release of PDF is essential for maintaining circadian rhythms (Nitabach et al., 2006; Park et al., 2000). Several papers have demonstrated s-LNvs are circadian pacemaker neurons essential for locomotor activity rhythms (Grima et al., 2004; Lin et al., 2004; Peng et al., 2003; Renn et al., 1999).

Pdf in *D. melanogaster* is an intronless gene encoding a 102 amino acid neuropeptide precursor that consists of a signal peptide (first 16 amino acids), PDF associated peptide (63 amino acids) followed by mature PDF (18 amino acids). In between the PDF associated peptide and PDF, there is a proteolytic processing site (Lysine-Arginine) that undergoes cleavage to yield the mature PDF peptide. PDF exists as an alpha-amidated peptide (Park and Hall, 1998). Peptidyl glycine alpha-amidating monooxygenase (PAM) mediates alpha-amidation, a C-terminal modification that is crucial for signal transduction function of the peptides (Bradbury and Smyth, 1991; Eipper et al., 1985).

There are four lateral neurons (LNs) in each brain lobe that express PDF in the larval brain in addition to 6-8 abdominal neurons. Larval LNs are differentiated neurons that become adult small ventral lateral (s-LNv) neurons. During metamorphosis PDF is expressed in two distinct clusters of ventral lateral neurons, namely s-LNvs and large ventral lateral neurons (l-LNvs). PDF is also expressed in a pair of neurons located in the tritocerebrum (Helfrich-Forster, 1997) in the adult brain. However, the neurons in the tritocerebrum undergo programmed cell death and disappear shortly after 24 hours of eclosion (Lee et al., 2013; Renn et al., 1999). The l-LNvs send projections ipsilaterally into the medulla and also contralaterally via the posterior optic tract (POT) whereas the

s-LNvs have their axon terminals projecting into the superior protocerebrum (Helfrich-Forster, 1995; Helfrich-Forster and Homberg, 1993; Nassel et al., 1993).

Given the importance of PDF in the regulation of circadian locomotor activity rhythms, maintenance of PDF levels in the s-LNvs is essential for the circadian clock function. Of significance, *Pdf* transcription and post-translational regulation is affected by core-clock factors. Interestingly, Pdf expression also seems to be differentially regulated between l-LNvs and s-LNvs. In Clk^{Jrk} and cyc^{0} mutants, there is no PDF expression in the s-LNvs implying that both CLK and CYC are positive transcriptional regulators. However, the lack of a consensus E-box in the *Pdf* regulatory sequence suggests that CLK and CYC are only indirectly associated with *Pdf* transcription. Indirect activation of *Pdf* could involve PER and TIM as they are regulated by CLK and CYC. However, the transcript levels of *Pdf* are not affected in per^{01} and tim^{01} mutants, indicating the presence of additional factors involved in transcriptional regulation of *Pdf* (Park et al., 2000).

PDF has an evolutionarily conserved function in regulating circadian rhythms in a distant species *D. virilis,* which diverged from *D. melanogaster* 63 million years ago (Bahn et al., 2009). PDF is expressed only in the l-LNvs in *D. virilis* as opposed to the l-LNvs and s-LNvs in *D. melanogaster*, indicating a difference in transcriptional regulation of *Pdf* between the two species. *D.virilis* shows locomotor activity patterns similar to Pdf^{01}, which could be explained by the lack of PDF expression in the s-LNv like neurons in *D. virilis* (Bahn et al., 2009). PDF has no homolog in mammals; however, vasoactive intestinal polypeptide (VIP) performs a similar function as PDF. It synchronizes

individual clock neurons and maintains circadian rhythmicity. The receptor for VIP is VAPC (2) and both VIP and VAPC (2) are expressed in the suprachiasmatic nucleus (SCN), the master clock in the mammalian brain (Aton et al., 2005). In *D. melanogaster*, the PDF receptor is a G-protein coupled receptor that is coupled to the activation of adenylyl cyclase/cAMP (Hyun et al., 2005; Lear et al., 2005; Mertens et al., 2005) and is expressed in non-clock cells, all non-PDF expressing clock neurons and s-LNvs except the l-LNvs (Shafer et al., 2008).

PDF has been at the center of intense analysis for close to two decades, yet little is known about its transcriptional regulation. Transcriptional gene regulation is primarily governed by an interaction between *cis*-regulatory elements and their cognately binding trans-factors. The presence of these trans-acting factors might be the primary mechanism restricting neuropeptide expression to a defined set of neurons in the central nervous system.

TGF-β signaling and the circadian clock

Transcription factors that act as activators or repressors dictate the ability of the cell to grow and differentiate, thus playing a key role in development (Busser et al., 2008; Davidson and Levine, 2008; Deplancke, 2009). One of the signaling pathways that play a key role during development is transforming growth factor beta (TGF-β) signaling. The TGF-β superfamily encompasses a large group of secreted proteins that fine tune signals between cells to coordinate development across the animal kingdom. Members

of this superfamily play a role in cellular proliferation and cell death in addition to concentration gradient driven specification of multiple cell fates (Derynck and Akhurst, 2007).

In *D. melanogaster*, members of TGF- β superfamily are categorized into two distinct branches namely, Bone morphogenetic protein (BMP) and Activin. The BMP signaling pathway components contribute to patterning and growth of imaginal discs (adult precursor tissues) and synapse development (Parker et al., 2004). In contrast, the role of the activin pathway in differentiation and growth of adult tissues is not well understood. However, the majority of mutant studies have found a significant role of the pathway in neuronal proliferation, wiring, axon guidance and remodeling of neurons during metamorphosis (Parker et al., 2006; Serpe and O'Connor, 2006; Zheng et al., 2003; Zheng et al., 2006).

A key to neuronal assembly and communication is anterograde (communication from neurons to their postsynaptic targets) and retrograde (communication from target cells to the presynaptic neurons) signaling (Fitzsimonds and Poo, 1998). BMP is a well-conserved retrograde signaling pathway that influences synaptic connectivity and is well studied at the larval neuromuscular junction in *Drosophila* (Marques et al., 2002; McCabe et al., 2003). Interestingly, PDF is known to synchronize clock neurons, but the underlying neuronal connectivity in the adult brain among the circadian clusters is not well understood. The presence of the components of the BMP signaling pathway in PDF neurons was recently reported where activation of the BMP pathway components

caused a long period phenotype (Beckwith et al., 2013). Assembly of circadian neuronal clusters relies on information from the network and environmental signals in addition to specific signal transduction pathways. Characterizing the role of various signal transduction pathways and how that impacts the molecular clock will be key to understanding neuronal circuits underlying circadian rhythms (Muraro et al., 2013).

One of the inherent properties of the circadian clock is the ability to respond to environmental changes, and signal transduction pathways are capable of altering neuronal connectivity within the circadian network in response to a changing environment. In mammals, TGF-β/activin signaling is capable of resetting the circadian clock independent of *Per*, but rather through induction of *Dec1* (Kon et al., 2008). *Dec1* is a homolog of *clockwork orange* (*cwo*) in *Drosophila*. CWO is part of the second interlocked transcriptional feedback loop that regulates CLK. However, no role for TGF-β signaling in circadian clock in *Drosophila* has been reported.

Circadian clock and metabolism

Circadian rhythms regulate metabolic pathways and organ function, and disruption of circadian rhythms can have adverse effects on metabolic function and eventually health (Maury et al., 2010). Several epidemiological studies indicate that restricting sleep leads to increased insulin sensitivity and long-term alteration in the circadian rhythms increases the risk of obesity (Gangwisch, 2009). Metabolic stress usually triggers the production of detoxifying enzymes, which are commonly thought to have a constant

level of expression. However, some recent reviews suggest that genes encoding xenobiotic enzymes have cyclical gene expression (Levi and Schibler, 2007). However, the function of these genes and their association with the circadian clock is little understood. It is conceivable that induction of detoxification in response to the altered clock function is key to removal of accumulated toxic materials.

The major organ responsible for detoxification of xenobiotics is liver in mammals, and functionally equivalent organ in insects is the fat body. It is well known that clock proteins are expressed in metabolically important tissues like the fat body in *Drosophila* (Giebultowicz, 2000) and that they exhibit a circadian pattern in their feeding behavior (Xu et al., 2008). The cyclical expression of *Clk* in the fat body is evidence of the existence of peripheral clocks (Xu et al., 2008). In *Drosophila*, clock controlled cycling genes (CCGs) are widely involved in physiological processes such as metabolism and several CCGs have been identified using transcriptome analysis by DNA microarray analysis and RNA sequencing. Detoxification enzymes especially Cytochrome P450 (CYP) enzymes are also under circadian control, with several *cyp* genes expressed in the PDF expressing l-LNvs and s-LNVs (Kula-Eversole et al., 2010; Nagoshi et al., 2010).

The effects of several toxic substances have been studied in *Drosophila*. Among these, caffeine has been looked into for its role as a transcriptional regulator of *cyp* genes (Willoughby et al., 2006). Caffeine has been shown to induce similar effects in insects and vertebrates. Caffeine leads to mutagenesis (Kuhlmann et al., 1968), inhibition of

feeding and sleep (Shaw et al., 2000) and increased heart rate(Zornik et al., 1999) in insects. In *Drosophila*, several gustatory receptors have been shown to be caffeine sensitive and hence the wild type flies usually exhibit aversive behavior (Ebbs and Amrein, 2007) to caffeine. Interestingly, caffeine has been shown to promote wakefulness, and the PDF expressing l-LNvs are wake promoting neurons in *Drosophila* (Wu et al., 2009). With the PDF expressing ventral neurons also showing cyclical expression of several *cyp* genes (Nagoshi et al., 2010), this could explain the possible link between circadian rhythms and caffeine metabolism.

The collection of work provided here addresses (1) the transcriptional regulation of the neuropeptide pigment dispersing factor (PDF) by a homeodomain transcription factor; (2) characterizing the role of a homeodomain transcription factor scarecrow during *D. melanogaster* development; (3) testing the role of TGF-β signaling in the development of PDF expressing s-LNvs and (4) linking the circadian clock to caffeine metabolism through regulation of *cyp* genes. Though seemingly disparate, each chapter is an attempt at furthering our understanding of the clock network circuitry and its regulation of metabolic behavior with a focus on the neuropeptide PDF.

CHAPTER 2: *SCARECROW* NEGATIVELY REGULATES *PDF* NEUROPEPTIDE GENE IN THE CIRCADIAN PACEMAKER NEURONS IN *DROSOPHILA MELANOGASTER*

A version of this chapter is currently under revision in *Plos Genetics*.

Sudershana Nair, Jae Hoon Bahn, Gyunghee Lee and Jae H. Park (under revision) *Plos Genetics*, 2016.

Abstract

Transcriptional regulation contributes to intracellular timekeeping mechanisms in all organisms. In *Drosophila melanogaster*, Pigment dispersing factor (PDF) is the major neuropeptide that is produced by central clock cells called latero-ventral neurons (LN_vs). PDF synchronizes other clock neurons thereby playing an essential role in the maintenance of circadian rhythms. Core clock transcription factors have been shown to regulate *Pdf* expression indirectly in the LN_vs. However, the underlying molecular mechanisms of restricted *Pdf* expression to the LN_vs are little understood. Here, using *Pdf* promoter-bashing experiment, we have identified *cis*-acting *Pdf* regulatory element (*PRE*) that is sufficient for driving *Pdf* expression in the LN_vs. We have further identified a homeobox transcription factor, SCARECROW (SCRO) that binds to *PRE*. Transgenic expression of *scro* in the clock neurons with *timeless-Gal4* abolished *Pdf* expression and circadian locomotor activity rhythms. Such repression of *Pdf* requires DNA-binding homeodomain of SCRO, but not other conserved domains. These results suggest that *scro* encodes a novel transcriptional regulator repressing *Pdf* expression in non-PDF expressing clock neurons.

Introduction

Cell autonomous clock comprising of transcriptional and translational feedback loops drives biological rhythms in almost all living organisms (Dunlap, 1999). Transcriptional feedback loops in *Drosophila melanogaster* consist of two interlocking molecular loops involving core-clock regulators, Period (Per), Timeless (Tim), Clock (Clk) and Cycle (Cyc) proteins. The loops are initiated by Clk and Cyc that bind to E boxes of *per* and *tim* in the *per/tim* feedback loop and *vrille (vri)* and *Par domain 1* ε*(Pdp1* ε*)* in the *Clk* feedback loop. Several post-translational modifiers involving kinases and phosphatases, in turn, regulate stability and activity of PER and TIM. This intracellular network of feedback loops generates output rhythms that manifest in physiology and behavior of animals by regulation of clock-controlled genes and through extracellular signaling between cells using secreted neuropeptides (Edery, 2011).

Pigment dispersing factor (PDF) is a well-studied neuropeptide in *Drosophila* that exhibits structural homology to crustacean pigment-dispersing hormone (PDH). Transcription of *Pdf* gene is restricted to sixteen neurons out of the approximately 150 clock neurons in the adult brain, and these neurons consist of two groups; the small and large lateral neurons ventral (s- and l-LN_vs) (Helfrich-Forster, 1998). PDF peptide and PDF-neurons are critical to the maintenance of circadian locomotor activity rhythms (Park et al., 2000; Renn et al., 1999). *Pdf*-null mutants (Pdf^{01}) are largely arrhythmic under constant darkness (DD), and the rhythmic Pdf^{01} flies have shorter free-running periods than wild-type flies do (Renn et al., 1999). Additionally, PDF receptor mutants exhibit behavioral defects similar to that of Pdf^{01}, further providing evidence for the

crucial role of PDF signaling in regulating circadian rhythms (Hyun et al., 2005; Lear et al., 2005; Mertens et al., 2005).

Given the importance of PDF in the regulation of circadian locomotor activity rhythms, maintenance of PDF levels in the s-LN_vs is essential for the circadian clock function. In this regard, *Pdf* transcription and post-translational regulation are affected by core-clock factors. Previously we have shown that *Pdf* mRNA expression in the s-LN_vs is largely absent in the Clk^{Jrk} and cyc^{0} mutants, implying that Clk and Cyc proteins act as positive transcriptional regulators of the *Pdf* gene. However, lack of cognate sequence for the Clk and Cyc, called E-box, in the *Pdf* regulatory sequence suggests that Clk and Cyc are indirect regulators (Park et al., 2000). It is likely that Per and Tim can play a role in such indirect activation, as Clk and Cyc positively regulate them (Allada et al., 1998; Rutila et al., 1998). However, transcript levels of *Pdf* are not affected in per^{01} and tim^{01} mutants, indicating the presence of additional factors involved in transcriptional regulation of *Pdf* (Park et al., 2000). In the larval lateral neurons vrille, a bZIP transcriptional repressor has been previously shown to suppress PDF peptide and not *Pdf* mRNA levels (Blau and Young, 1999).

In addition to the positive regulation, our previous *trans*-specific studies imply that *Pdf* expression is negatively regulated, limiting the expression to the s- and l-LN_vs. The transgenic introduction of *Pdf* gene isolated from *D. virilis* (for short, *DvPdf*) to the *D. melanogaster* genome resulted in *Pdf* expression in non-PDF clock neurons, LN_ds and 5^{th} s-LN_v, in addition to the endogenous PDF-producing neurons (Bahn et al., 2009).

Such ectopic expression suggests that *Pdf* transcription is normally repressed in the LN_ds and 5^{th} s-LN_v in *D. melanogaster*. Thus, spatial regulation of *Pdf* expression seems to require both positive and negative aspects of gene regulation. To gain insight into the transcriptional regulatory mechanisms of *Pdf*, we first identified the minimal regulatory region required for *Pdf* expression. Furthermore, we found a transcription factor, *scarecrow* (*scro*) that binds to this region. Transgenic expression of *scro* downregulates *Pdf*, suggesting that SCRO plays a role as a negative *Pdf* regulator.

Materials and Methods

Fly stocks

All fly stocks were reared on standard cornmeal-yeast-agar medium and maintained at 25°C. The following transgenic lines were employed in this study: *scro-Gal4* (Vienna-VT 208008) (Kvon et al., 2014); *y w*; *Pdf-Gal4* (Park et al., 2000); *yw, DvPdf-Gal4* (Bahn et al., 2009); *y w*; *tim-Gal4*-62 and *y w; tim-Gal4*-86 (Kaneko and Hall, 2000); *y w; tim-Gal4, Pdf-Gal80*/*CyO*; *Pdf-Gal80*/*TM6B* (Murad et al., 2007) and *y w;; UAS-vnd* (Yu et al., 2005), *scroRNAi* lines (Bloomington stock numbers 29387 and 33890).

Immunocytochemistry

Fly brains were dissected and fixed in 4% paraformaldehyde, 7.5% picric acid and phosphate buffer (0.1 M, pH 7.4) for 2 h at room temperature. Fixed tissues were washed in phosphate buffer followed by TNT (0.1 M Tris-HCl, 0.3M NaCl, 0.5% Triton X-100). The brains were blocked in 5% normal donkey serum (Jackson

ImmunoResearch Laboratories) and subsequently incubated with primary antibody [rat anti-PDF (1:300)] at 4°C overnight. After washing with TNT, the brains were incubated with TRITC- or FITC-tagged secondary antibody at 1:200 for 1 h at room temperature. Following this, the brains were washed three times with TNT followed by phosphate buffer before being mounted in a quenching medium (0.5% n-propyl gallate in 90% glycerol and 10 mM phosphate buffer, pH 7.4). Fluorescent signals were captured using Olympus BX-61 microscope equipped with a CCD camera. Images were processed using ImageJ (v1.47b; National Institutes of Health).

Pdf Promoter constructs

***Pdf*^{356} and *Pdf*^{155}**: Previously described ~0.8-kb *Pdf* upstream sequence in the pBluescript (Park et al., 2000) was digested with *Swa*I/*Sma*I. The vector was purified and re-ligated intra-molecularly, from which XbaI/EcoRI fragment (*Pdf*^{356}) was purified and inserted into the pPTGAL vector. The *Pdf*^{155} fragment was obtained by PCR using forward (5'-GCTCTAGAGGGCTGAAGGACCGCCGCTG, XbaI site underlined) and reverse (5'-GCGAATTCAGCAGGAGACTTGCG, EcoRI site underlined) primers. The PCR product was digested with XbaI and EcoRI, and then inserted into the pPTGAL vector.

***Pdf*$^{524\Delta}$**: Targeted mutagenesis was applied to delete putative enhancer element from the *Pdf*^{524} construct (see Fig. 1). The *Pdf*^{524}-SK construct was employed as a PCR template using reverse (5'-CAGCGGCGGTCCTTCAGCCC) and T3 primers. Another PCR was performed using forward (5'-CCGATACTGACGCTCTTGGG) and T7 primers. The former product was digested with EcoRI and the latter with XbaI; subsequently the

digested fragments were inserted at XbaI/EcoRI sites of the pBluescript via three-way ligation. Following transformation into *E. coli* (DH5α), plasmids were purified and digested with XbaI/EcoRI. The resulting fragment (*Pdf*$^{524\Delta}$) was gel-purified, and then cloned into pPTGAL4 vector.

Internal 80-bp fragments: An 80-bp fragment including *PRE* was amplified by PCR with forward (5'-GGGCTGAAGGACCGCCGCTG) and reverse (5'-CGCAACCCAAGAGCGTCAGT) primers. The PCR product was cloned into the pGEM-T easy vector (Promega) and positive plasmid clones were identified by PCR using T7 and SP6 primers. The PCR product was cut with EcoRI and then inserted into the pPTGAL4 vector. Sequencing of the recombinant plasmids identified three different clones; a single 80-bp fragment inserted in forward direction (*Pdf*^{80F}), the same in reverse orientation (*Pdf*^{80R}), and a dimer of *Pdf*^{80F} with a 20-bp spacer that was derived from the pGEM-T Easy vector. This clone is designated as *Pdf*^{80D} (see Fig. 1 for schematic).

All these above-mentioned *Pdf-Gal4* constructs were injected into the *yellow white* (*y w*) mutant embryos, along with helper *pUChsΔ2-3* plasmid. Individual *Pdf-Gal4* transgenic lines were crossed to a *UAS-mCD8-GFP*, and F1 progeny were dissected to assess *GFP* expression in the CNS. At least three independent lines for each construct were tested and at least five CNS specimens from each cross were examined.

***Pdf-GFP*:** Previously described 1-kb *Pdf* upstream sequence (Park et al., 2000) was inserted into pGreen Pelican vector at XbaI/XhoI for germline transformation.

T7 phage display screening

T7 phage cDNA library was constructed from *eya*^{1} mutant fly head mRNA using a commercial kit (T7 Select System, Novagen). Total RNA was extracted from *eya*^{1} adult heads, and then subsequently poly-A RNA was further purified using Qiagen Oligotex kit. Approximately 500 ng of poly-A RNA was subjected to reverse transcription reaction using random primers. The resulting cDNA was ligated with linkers (5' with EcoRI linker and 3' with HindIII linker), digested with EcoRI and HindIII, and then inserted into T7 Select10-3b vector. Following *in vitro* packaging the T7 phages were amplified through infection with *E. coli* (*BLT5403*) strain, which resulted in 5x10^{9} PFU/ml. For the bait, the *Pdf*^{80D} was amplified and labeled with biotin by PCR using forward and the biotin-labeled reverse primers whose sequences were as described for the 80-bp fragment. The biotin-labeled *Pdf*^{80D} was mixed into 1mg of streptavidin-magnetic beads (Dynal Biotech), and then incubated for 30 min at room temperature to immobilize it. The beads were washed three times with 1ml washing/binding buffer and 2 ml TENT buffer (10mM Tris-HCl, pH 8/1mM EDTA/250 mM NaCl/0.5% Triton X-100) to remove unbound DNA probe. The T7 phage library (1.5 X 10^{10} pfu/3 ml) was incubated with the probe-laden beads for 1 h at room temperature. Following washing three times with 1ml TENT buffer, the bound phages were amplified by plaque amplification method (Danner and Belasco, 2001) and then used for the next round of screening. After a total of five rounds of screening, phage-plaques were randomly selected for DNA analysis. Phage DNA was purified using a commercial kit (Wizard lambda kit, Promega), digested with EcoRI and HindIII, and then the EcoRI/HindIII fragment (i.e., cDNA insert) was cloned into the pBluescript for sequencing.

Electrophoretic mobility shift assay (EMSA)

The phage clone was allowed to infect 50mL *E. coli* (BLT5403) culture according to the manual. Infected cell lysate was centrifuged at 7000 x *g* for 10 min at 4°C to remove cell debris. Final concentration of 500mM NaCl, 10%PEG 8000 was mixed with supernatant and incubated at 4°C overnight. Following centrifugation at 7000 x *g* for 10 min at 4°C, the pellet was resuspended with 1mL of 1M NaCl, 10mM Tris-HCl, pH8.0, 1mM EDTA and sonicated for 10s at 30% amplitude. EMSA was performed by incubating 1μg of the phage extract in binding buffer containing 1mg/ml BSA and 1 μg of poly dI/dC for 5 min on ice. It was then mixed with 20 fmol of biotin-labeled Pdf^{80D} fragment for 20 min at room temperature. For a competition experiment, 4 pmol of unlabeled Pdf^{80D} was pre-incubated with the phage extracts for 10 min. Samples were mixed with 2X gel loading buffer and run on a 6% TBE-PAGE gel. The electrophoresed samples were transferred to Nylon membrane, and then cross-linked on UV trans-illuminator for 10 min. The biotin-labeled DNA was detected using streptavidin-HRP system (Pierce) on X-ray film.

Yeast one hybrid assay

Pdf^{80D} was subcloned into the *pHIS2* bait vector (*PRE-HIS2*). *Scro* cDNA identified from the phage display screening was amplified by using T7SelectUP and T7SelectDOWN primers (Novagen) and then subcloned into pGADT7-Rec[2] vector (Clonetech) at EcoRI/BamHI sites. The *PRE-HIS2* and *scro*-pGAD-Rec[2] constructs were co-transformed into Y187 yeast strain using Matchmaker yeast one hybrid system (Clonetech). To suppress leaky expression of the *HIS3* gene, the transformed yeast

cells were grown in -His/-Trp/-Leu dropout medium containing 50 mM 3-amino-1,2,4-triazol (3-AT) (Sigma).

Construction of mutant *scarecrow* (*scro*)

Generation of *UAS-scro*: RNA was extracted from wild type (*Canton-S*) adult heads and reversely transcribed to make cDNA. The *scro* open reading frame (ORF) was amplified by RT-PCR using forward (5'- ATGAGAATTC**ATG**TCATCGCACGGCCTT GCTTACAC, EcoRI site underlined) and reverse (5'-ATGCTCTAGATTAggcggcgtagtc gggcacgtcgtaggggtaCCATGCCCGGCCTTGTAAGGGCAG, XbaI site underlined, HA in small-cases) primers**.** The PCR products were subcloned into pUAST vector at EcoRI/XbaI sites for germ-line transformation.

***UAS*-mutant *scro* lacking TN, HD and NK2 domains:** Three *scro* cDNAs, each lacking TN, homeodomain (HD) or NK2 domains, respectively, were constructed by site-directed mutagenesis. For this, overlapping 5' and 3' fragments were generated by PCR with *UAS-scro* vector template, and then a fusion PCR was done to stitch these PCR fragments. For instance, to delete HD, 5' fragment was generated by PCR with HD-f/UAS-r primers, and 3' fragment with HD-r/UAS-f (Figure 2.10A). The two PCR products were mixed and used as a PCR template for UAS-f/UAS-r primers. The resulting PCR products were ligated into pGEMT-easy vector for sequencing. Deletions of TN and NK2 domain were done similarly. The resulting constructs were subcloned into pUAST vector at EcoRI/XbaI sites. Primers used for generating *scro* mutant constructs are listed in Table 2.1.

Table 2.1: Primers used for scro transgenic constructs

Primer Name	Sequence (5'→3')
TN-f	AGTAATCACTCAACACCCAGTCCAATTGAAGAATCG
TN-r	CGATTCTTCAATTGGACTGGGTGTTGAGTGATTACT
HD-f	CAGTTTCCTTTAGCACAA……..AGAAATGGCTG
HD-r	TTGTTCAGCCA……..CTAAAGGAAACTG
NK2-f	CATAATCAGCCTGCA……..GTTCAAGTCAA
NK2-r	TTGACTTGAACTG…….CAGGCTGATTATG
UAS-f	GAATACAAGAAGAGAACTCTG
UAS-r	GTCCAATTATGTCACACCAC
Y54M-f	CACAGAATGAAATGTAAAAGACAAGCG
Y54M-r	CGCTTGTCTTTTACATTTCATTCT
scro-frwd	CACCATGTCATCGCACGGCCTTG
scro-rev	CCATGCCCGGCCTTGTAAGGGCAG

(……..) represent the nucleotides in the deletion region for each of the domains.

***UAS-scro^{WT}*-Venus and *UAS-scro^{Y54M}*-Venus constructs:** The *scro* cDNA was amplified by PCR using scro-frwd and scro-rev primers, and then cloned into entry vector pENTR/D-TOPO (Invitrogen). The cDNA was then recombined into the Gateway P-element vector pPWV 1094 (Drosophila Genomics Resource Center), which contains a C-terminal Venus tag and UAS sequences using Gateway LR Clonase II Enzyme Mix (Invitrogen). This is referred to as *UAS-scro^{WT}*-Venus. And then site-directed mutagenesis was performed to generate *scro^{Y54M}* mutant construct, substituting tyrosine residue at position 54 of the HD for methionine (*UAS-scro^{Y54M}-Venus*). The resulting constructs were used for germ-line transformation.

Analysis of the circadian locomotor activity rhythms

Flies were entrained to four cycles of 12-h light: 12-h dark (LD) conditions and then subjected to constant darkness (DD) for 7 days. Locomotor activities during 30-min intervals were collected using Trikinetics Drosophila activity monitors. Rhythmicity was analyzed with Clocklab software (Actimetrics), as described previously (Bahn et al., 2009).

Scanning electron microscopy

Adult flies were dehydrated in 95% ethanol and dried. Each fly head was mounted, sputter-coated, and visualized using a Leo 1525 Gemini scanning electron microscope (Zeiss, Thornwood, NY).

scro mutant generation using CRISPR

The genomic target sequence for *scro* was identified using flyCRISPR Optimal Target finder tool (Gratz et al., 2014). Targeting gRNAs were annealed and cloned into pU6-BbsI-chiRNA via BbsI restriction sites. We co-injected two gRNAs and each gRNA was injected at a concentration of 100ng/ul into y[1] M(vas-Cas9)ZH-2A w[1118]/FM7c (Bloomington stock – 51323) flies using standard protocols. Individual G0 flies that were viable were crossed to third chromosome balancer and fertility was scored. Genomic DNA was isolated from the G1 flies and single fly PCR was performed using primers flanking the targeted locus. Genomic PCR products encompassing the gRNA-targeted sites and deletions were confirmed by sequencing.

Target sequence 1 - GGTTATGAGTTTATCTCCAA [AGG] with oligonucleotides CTTC GGTTATGAGTTTATCTCCAA and AAAC TTGGAGATAAACTCATAACC
Target sequence 2 - GTTGATGTAGTTAATGTTCC [AGG] with oligonucleotides CTTC GTTGATGTAGTTAATGTTCC and AAACGGAACATTAACTACATCAAC
The following primers were used to detect the deletion in *scro* CRISPR mutants - 5' ATGTCATCGCACGGCCTTGCT 3' and 5' GGTCGTTAGCTGTTGATCCGT 3'.

Results

Identification of *cis*-acting element for *Pdf* expression

In *Drosophila* larvae, PDF is expressed in 4 lateral neurons (LNs) in each hemisphere and 6-8 abdominal neurons. In the adult brain there are four groups of PDF expressing neurons; 4 large (l) and 4 small (s) LN_vs in each hemisphere, a pair of tritocerebral

neurons which die of apoptosis shortly after eclosion, and 4-6 in the abdominal ganglia (Helfrich-Forster, 1998; Lee et al., 2013). Previously we have shown that 524-bp sequence in the 5' upstream region is sufficient for driving *Pdf* expression in the larval LNs (but not in the Ab neurons) and in all endogenous *Pdf* neurons in the adult CNS (Park et al., 2000). To identify minimal *cis*-acting element(s) required for the *Pdf* expression, we dissected the 524-bp sequence using the Gal4/UAS system. For this, various upstream regions were fused with Gal4 coding sequence (Figure 2.1A), and then these Gal4 drivers were crossed to a UAS-mCD8-GFP reporter line to examine green fluorescent signals.

First, two smaller 356-bp and 155-bp sequences were examined. The Pdf^{356} produced *GFP* expression similar to Pdf^{524} in both larval (Figure 2.2C) and adult CNS (Fig. 2.3Ba). Pdf^{155}-directed *GFP* expression was also observed in larval LNs but with weaker intensity (Figure 2.2 D, n=6). Weak staining intensity was also observed in the adult s-LN_vs (Figure 2.3 Ca, n=6). These results indicate that essential regulatory information responsible for directing *Pdf* expression lies within 155-bp upstream region and the genomic region upstream of the 155 bp is required for optimal levels of expression. The 155-bp sequence includes an interesting sequence motif consisting of a tandem repeat of 13-bp sequence separated by a 9-bp space. The repeat contains TGAC tetra-nucleotide, which was shown to be important for the acquisition of FMRFamide neurochemical phenotypes in a set of neurons during metamorphosis (Taghert et al., 2000). To test the significance of this region, 35-bp sequence encompassing both repeat and spacer was removed from the Pdf^{524} construct (Figure 2.1A and 2.1B).

Intriguingly, the resulting *Pdf*$^{524\Delta}$-*Gal4* lines failed to produce *GPF* expression in both larval and adult CNS (Figure 2.2E and 2.3Da). Since three independent lines showed identical results, the absence of *GFP* signals is unlikely due to positional effect of the transgene. Immunohistochemistry also revealed intact lateral neurons in the adult brains (Figure 2.3E). Because this 35-bp region is essential for *Pdf* expression, we now refer to this sequence as *Pdf regulatory element* (for short, *PRE*).

To confirm the role of *PRE* for *Pdf* expression, we generated *Gal4* lines bearing 80-bp sequence, which contains the *PRE* in the center (*Pdf*^{80F}-*Gal4*, Figure 2.1A). *Pdf*^{80F}-*Gal4* drivers were able to produce *GFP* expression in both larval LNs (Figure 2.2 F) and adult s/l-LN$_v$s (Figure 2.3Fa). Intriguingly, expression driven by a reversely oriented 80-bp fragment (*Pdf*^{80R}) was similar to *Pdf*^{80F} (Figure 2.2 G and Figure 2.3 Ga). Moreover, a dimer of the two 80Fs (*Pdf*^{80D}) produced stronger *GFP* signals than each of the monomers (Figure 2.2H and Figure 2.3Ha). These data support that *PRE* is necessary and sufficient for directing lateral neuron-specific *Pdf* expression.

PRE is conserved in other species related to *D. melanogaster* (Figure 2.4). We found an identical sequence in *D. simulans Pdf* gene and a slightly diverse one in *D. erecta* gene. In the case of *D. virilis*, similarity of the *PRE*-like sequence is modest, containing imperfect repeats, shorter interval between the repeats, and a substantial gap before the repeats. Such divergence raises the possibility of differential regulatory mechanisms of *Pdf* between *D. melanogaster* and *D. virilis*.

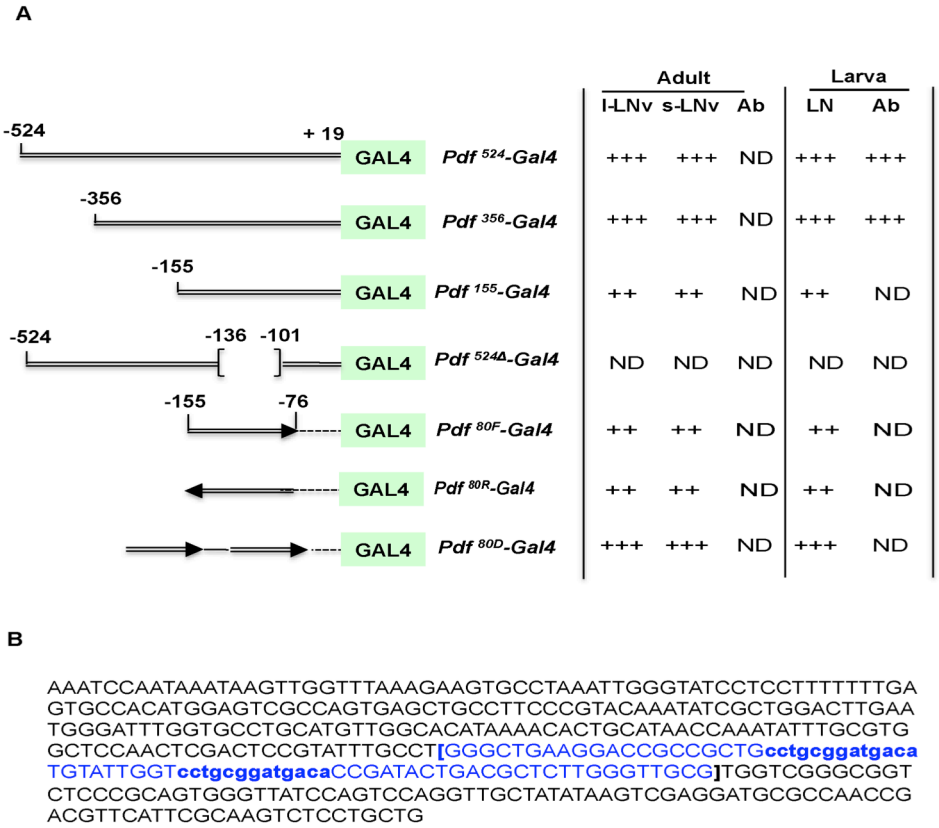


Figure 2.1 *Pdf-Gal4* constructs (A) Various *Pdf* upstream regions (double lines) fused to the *Gal4* coding sequence. Numbers indicate nucleotide positions relative to the transcription start site (+1). Arrows indicate directions of the 80-bp element, and a thin line between the two arrows indicates spacer sequence. Broken lines are 3' deletion region and bracket indicates the deletion from *Pdf*^{524} sequence. Expression of mCD8GFP driven in each cell group by a Gal4 line is indicated by '+' sign. ND, not detectable. (B) Nucleotide sequence of the *Pdf* ^{356}. Tandem 13-bp repeats are shown in lower-case letters. Sequence within the brackets indicates the 80-bp element.

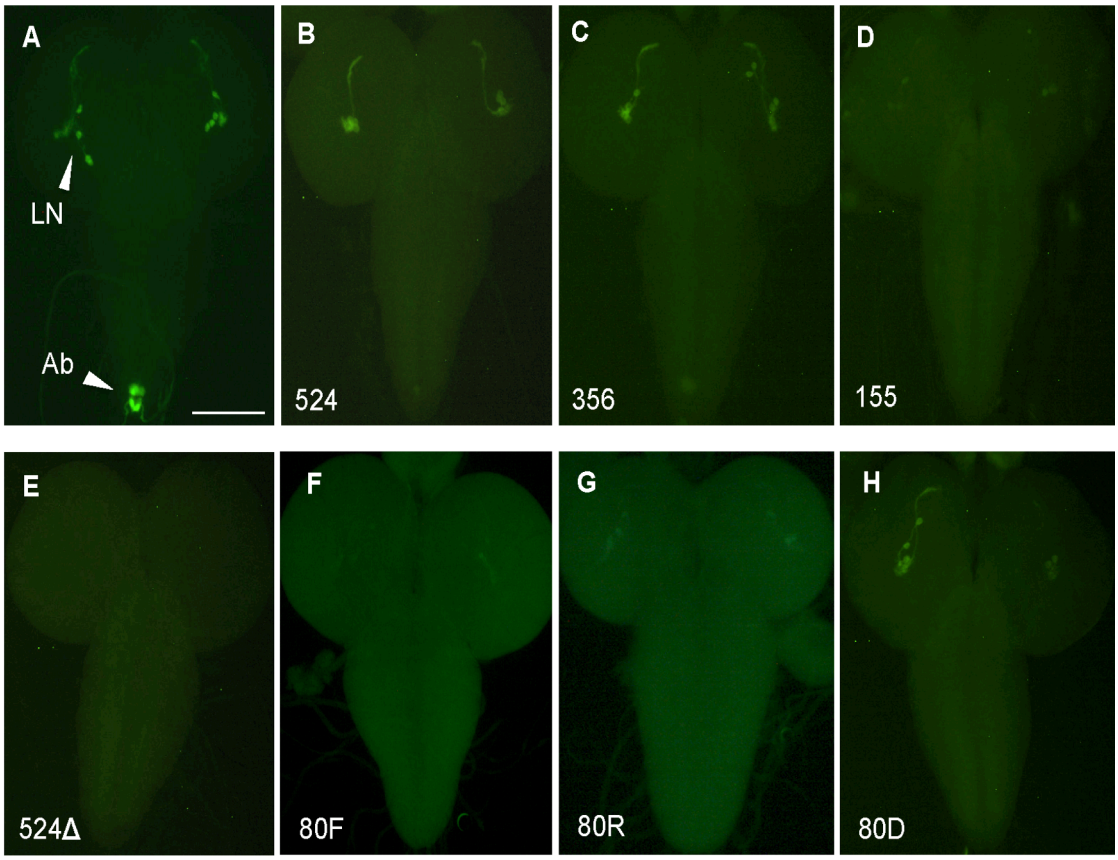


Figure 2.2 GFP expression in the larval CNS driven by *Pdf-Gal4*s (A) *Pdf* 2.4-kb *Gal4*, which recapitulates all endogenous *Pdf* expressing neurons (Park et al., 2000) LN, lateral neurons; Ab, abdominal ganglionic neurons. (B) Pdf^{524}–*Gal4*. Notice that *GFP* expression in Ab neurons is missing. (C) Pdf^{356}–*Gal4*. (D) Pdf^{155}–*Gal4*. (E) $Pdf^{524\Delta PRE}$–*Gal4*. No *GFP* expression is observed. (F) Pdf^{80F}*-Gal4.* (G) Pdf^{80R}*-Gal4*. (H) Pdf^{80D}*-Gal4*. Scale bar = 100 μm.

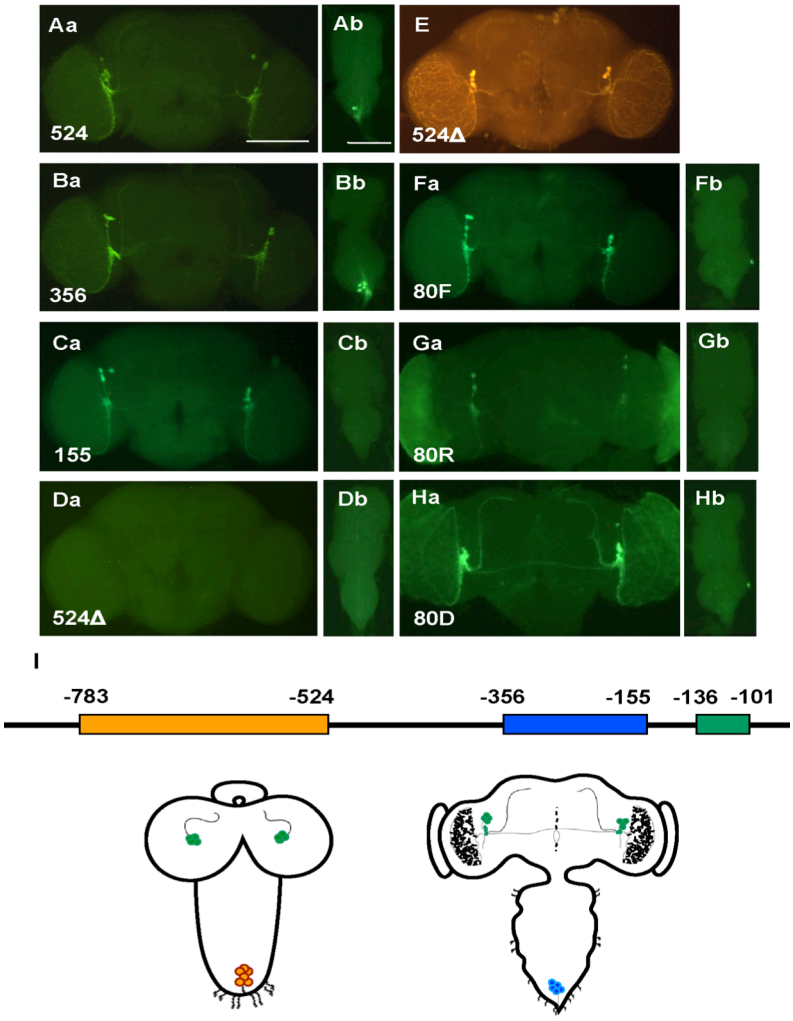


Figure 2.3 *GFP* expression in the adult CNS driven by various *Pdf-Gal4*s. (Aa-Da, Fa-Ha) protocerebrum. Scale bar = 100 μm. (Ab-Db, Fb-Hb) ventral nerve cord. Scale bar = 50 μm. (E) PDF immunostaining of the brain from Da. (I) Schematic of *Pdf* regulatory regions that direct developmental and cell specific expression. Orange box, larval Ab-specific; blue box, adult Ab-specific; green box, *Pdf* regulatory element for LNv specific expression. This is also required for adult Ab.

Distinct regulatory element for the abdominal ganglionic neurons

Pdf^{524} construct is unable to activate *Pdf* transcription in a cluster of Ab neurons in the larval abdominal ganglion (Figure 2.2B *vs.* Figure 2.2A). Interestingly however, *Pdf* expression in corresponding adult neurons is unaffected (Figure 2.3Ab), indicating differential regulatory mechanisms between the two developmental stages. Similar results were obtained with *Pdf*^{356} construct (Figure 2.3Bb), while *Pdf*^{155} failed to drive Ab expression in adults (Figure 2.3Cb).

Since *Pdf*^{783} drives Ab expression in both larval and adult tissues (Park et al., 2000), the larva-specific Ab regulatory element must be present in the region between -783 and -524, while the adult-specific one between -356 and -155 (Figure 2.3I). The latter, however, seems to require *PRE*, because *Pdf*$^{524\Delta}$ failed to express *GFP* in the adult Ab neurons (Figure 2.3Db). This is supported by the fact that all of the 80-bp sequences (80F, 80R, and 80D) were unable to drive *GFP* expression in the adult Ab neurons (Figure 2.3Fb-Hb). Overall, the regulatory mechanisms for *Pdf* expression in Ab neurons are distinct between larval and adult stages (Figure 2.3I).

Identification of the *PRE*-binding protein

To further elucidate the mechanisms of *Pdf* regulation, we attempted to identify *trans*-acting factors binding to the *PRE*. We made a cDNA library from the heads of *eyes-absent* mutant (*eya*^{1}) to enrich LN_vs mRNA fraction in the total head-derived mRNAs.

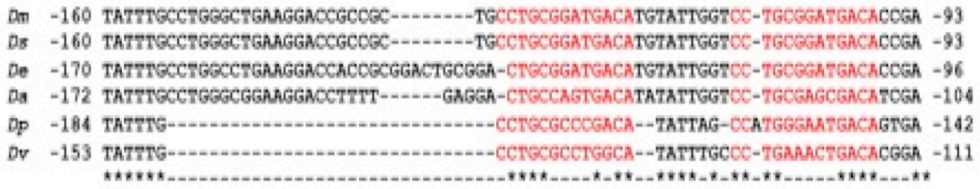


Figure 2.4 Alignment of *PRE* from different *Drosophila* species. Numbers indicate nucleotide positions relative to the transcription start sites. Asterisks indicate identical nucleotides. (Abbr. Dm, *Drosophila melanogaster*; Ds, *D. simulans*; De, *D. erecta*; Dv, *D. virilis*). IDs of the *DmPdf*-homologous genes are as follows: Dsim\GD18125 for *DsPdf*; Dere\GG12188 for *DePdf*. For *DvPdf*, see (Bahn et al., 2009). The *PRE* sequence found for the *DePdf* locates in the intron, according to the annotated gene structure in Flybase. However, according to our experimental data the *DePdf* is a single-exon gene, as is the case for *DmPdf* and *DsPdf*. The positions indicated here are based on our own 5'-RACE data.

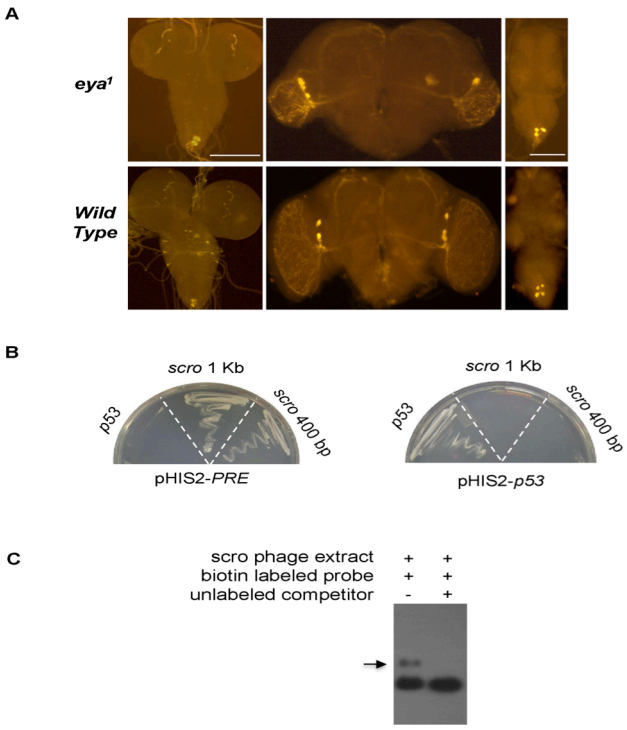


Figure 2.5 Isolation of SCRO as a *PRE* binding factor. (A) Intact PDF immunoreactivity in *eya*^{1} mutant as compared to wild-type (WT) in larval and adult brains. Scale bar = 100μm. Scale bar = 50μm for adult ventral nerve cord stained for PDF. (B) Yeast one-hybrid assay. (left) Cell growth resulting from the interaction between 80-bp *Pdf* bait and SCRO. (right) p53 positive control, showing cell growth as a result of the interaction between p53 and its binding sequence. (C) Electrophoretic mobility shift assay. Protein extracted from 1-kb *scro* phage clone induced mobility shift (arrow), which was not seen in the presence of competitor.

PDF-immunoreactive s/l-LN_vs are intact in the *eya*^{1} mutant brains, although the optic lobe medulla is severely reduced (Figure 2.5 A). We then performed yeast one hybrid screenings using the aforementioned 80-bp bait and *eya*^{1} head cDNA library. However, too many false positives disallowed us to find any significant results.

As an alternative approach, we performed phage display screening. After five rounds of screening, ten plaques were randomly picked for a diagnostic PCR using T7SelectUP and T7SelectDown primers included in the kit. We frequently found two phage clones, which produced *ca*. 400-bp and 1-kb PCR product, respectively. Sequences of both PCRs match *scarecrow* cDNA (*scro*, CG17594) and the 400-bp one is a truncated version of the 1-kb sequence, each encoding partial SCRO protein. SCRO is likely to be a transcription factor as it is a member of the NK2 family of DNA-binding homeodomain (HD) proteins (Kim and Nirenberg, 1989; Zaffran et al., 2000).

To gain more evidence for the interaction between 80-bp *PRE* as bait and SCRO, we performed yeast-one hybrid assay. Robust growth of yeast cells was observed on positive plate with *PRE* as bait (Figure 2.5B left) but none on negative control plate with p53-binding sequence as bait (Figure 2.5B right). These results strongly support specific interaction between SCRO and the *Pdf* regulatory region. EMSA result is also consistent and supports molecular interaction between SCRO and *PRE* (Figure 2.5C).

SCRO negatively regulates *Pdf*

Functions of SCRO are little understood; however, ventral nerve cord defective (VND), the closest relative of SCRO (Zaffran et al., 2000), was characterized to be a transcriptional repressor in the developing fly embryos (Koizumi et al., 2003). Based on the similarity between SCRO and VND, we hypothesized that SCRO functions as a *Pdf* repressor. To test this, we generated *UAS-scro* transgenic lines. Transgenic expression of *scro* with *Pdf-Gal4* did not affect *Pdf* mRNA (Figure 2.6B) and peptide (Figure 2.6E) expression in adult neurons, as compared to wild-type controls (Figure 2.6A and 2.6D). It also did not affect PDF-immunoreactivity in larval LNs. (Figure 2.6H *vs.* 2.6G). A possible explanation is that transgenic production of SCRO represses both endogenous *Pdf* gene and *Pdf-Gal4* transgene. The latter event attenuates *scro* expression, which in turn de-represses *Pdf* expression.

It has been shown previously that altered Pdf expression is indicative of arrhythmic locomotor activity. We tested locomotor activity rhythms of *scro* overexpression using *DvPdf-Gal4*. As expected acute downregulation of *Pdf* using *DvPdf-Gal4* shows higher arrhythmicity as compared to Pdf^{01} (Figure 2.6, Table 2.2 and Figure 2.11). We also employed another LN_v-driver, *timeless-Gal4* (*tim-Gal4*). Since *tim* regulatory region does not have *PRE*-like sequence, we expected that SCRO would not affect *tim-Gal4* activities. Remarkably, *tim-scro* resulted in a complete lack of *Pdf* expression in all LNs in the larval brain (Figure 2.6I) and s/l-LN_vs in the adult brain (Figure 2.6C and 2.6F). As a complementary experiment, we examined *Pdf*-driven *GFP* expression in *tim-scro* CNS. In the control larval and adult CNS, we detected GFP signals in all endogenous

PDF neurons (Figure 2.7A and C). However, such signals in the lateral neurons were abolished by *tim-scro* (Figure 2.7B and D). Together, our data strongly support that SCRO represses *Pdf* transcription. Since *tim-Gal4* is a broad driver than *Pdf-Gal4*, *Pdf* downregulation by *tim-scro* could take place in cell non-autonomous way. To test this possibility, we employed 3 copies of *Pdf-Gal80* to repress *tim-Gal4* in PDF neurons (Murad et al., 2007). As compared to control (Figure 2.8A and Figure 2.8A'), PDF-immunoreactivity was restored in about two s-LN_vs (± 1, n=10) and in all l-LN_vs (Figure 2.8B and Figure 2.8B'), supporting that *Pdf* downregulation by *scro* is LN_v-autonomous.

Another concern about the lack of *Pdf* expression by *tim-scro* is that SCRO might have altered developmental lineage of PDF neurogenesis during embryonic development. To address this question, we manipulated expression of *scro* post-embryonically using Gal80ts, a temperature-sensitive Gal4 repressor (McGuire et al., 2003). The flies bearing all three transgenes (*tub-Gal80ts, tim-Gal4, UAS-scro*) were maintained at permissive temperature (18°C) until adults are emerged. Under this condition, PDF-immunoreactivity is normal, indicating that Gal80ts represses Gal4 effectively (Figure 2.8C). On the other hand, the same flies were placed at 30°C starting 3 days old pupal stage to inactivate Gal80ts, thereby permitting *tim*-induced *scro* expression. As a result, we observed no *Pdf* expression in 2-3 day old adult flies (Figure 2.8D). These data strongly support that SCRO does not alter developmental pathway of PDF neuronal lineage, but functions as a negative transcriptional regulator of *Pdf.*

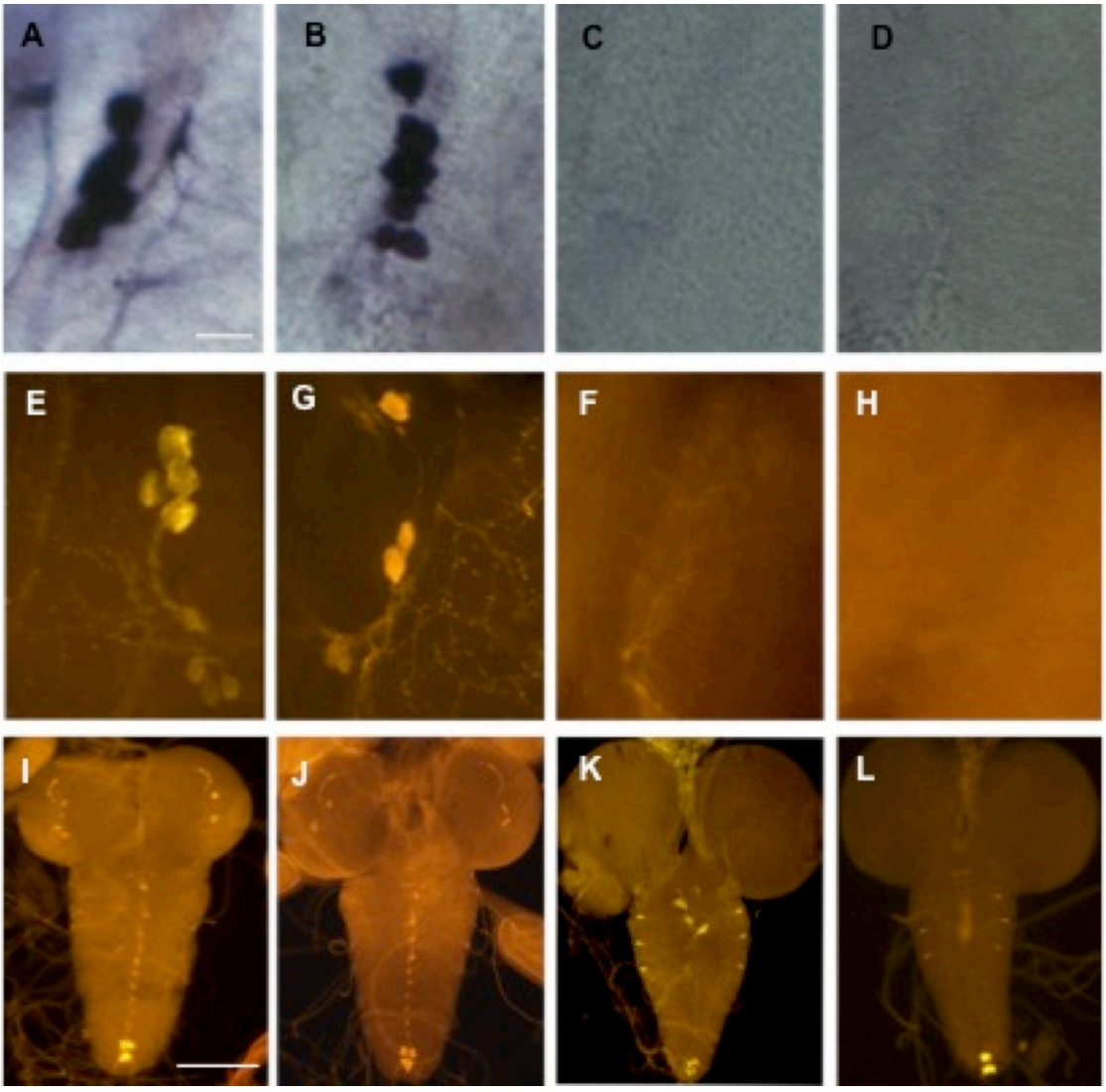


Figure 2.6 Expression of *Pdf* in response to ectopic *scro* expression. (A-D) *Pdf* in situ hybridization in the adult brain. (E-H) PDF immunoreactive LN_vs in adult brain. Sm, small LN_vs; Lg, large LN_vs. Scale bar = 50μm. (I-L) PDF immunoreactivity in larval CNS. Scale bar = 100 μm. (Genotypes for A, E, I, Canton-S, n=6; B, G and J *y w; Pdf-Gal4/+; UAS-scro/+*, n=8; C, F and K, *DvPdf-Gal4/+*;; *UAS-scro/+*, n=8; D, H and L, *y w; tim-Gal4/+*; *UAS-scro/+,* n=8).

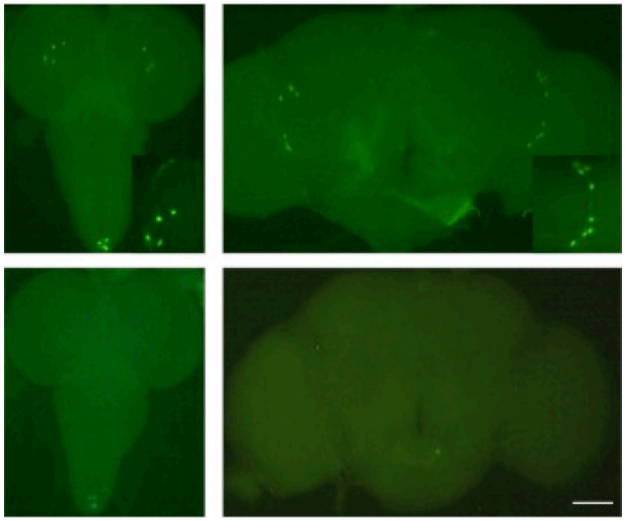


Figure 2.7 Suppression of *Pdf* expression by SCRO. Top panel shows GFP expression in the larval CNS and adult brain for the genotype *Pdf-GFP, tim-gal4/+*. Bottom panel shows lack of GFP expression in the larval LNs and adult s- and l-LNvs for the genotype *Pdf-GFP, tim-gal4/+*; *UAS-scro*/+. All images are representative of at least four samples. Scale bar = 100 μm.

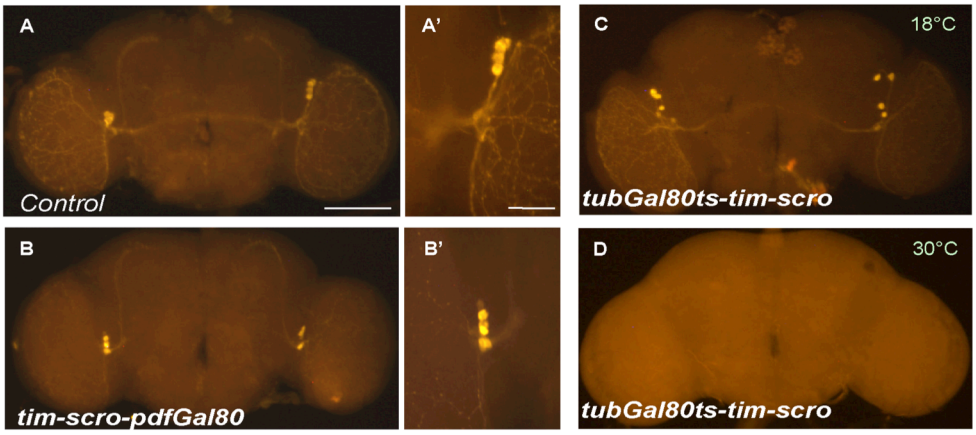


Figure 2.8 PDF-immunoreactivity in adult brain. (A, A') Control (genotype: *+/CyO; UAS-scro/Pdf-Gal80*^{3X}). n=7. (B, B') *tim*-driven *scro* expression (genotype: *tim-Gal4/+; UAS-scro/Pdf-Gal80*^{3X}). n=6. PDF expression is restored, suggesting that SCRO downregulates *Pdf* in a cell-autonomous way. (C) Flies (*tub-Gal80ts/tim-Gal4; UAS-scro/+*) were maintained at 18°C throughout their development. Intact PDF immunoreactivity was observed in adult brain (n=8) (D) The same flies as (C) were shifted to 30°C to activate *tim-Gal4* during pupal development. PDF immunoreactivity was absent (n=8), suggesting that SCRO does not affect developmental progress of PDF neurons. Scale bar = 100 μm.

SCRO does not cause cell death in PDF expressing lateral neurons

Ectopic expression of VND was reported to cause cell death in the photoreceptors (Jong-cheol Lee 2014). Since SCRO is the closest relative of VND, we wondered if *scro* also induces cell death of neurons. To test this possibility, *UAS-mCD8GFP* and *UAS-scro* were co-expressed using the *tim-Gal4*. As shown, *tim-GFP* signals overlap with PDF in the larval LNs (Figure 2.9A-C). In response to *scro* expression, no PDF immunoreactivity but normal *GFP* expression was observed in all larval LNs (Figure 2.9D-F). Expression of *scro* in another set of peptidergic bursicon neurons also did not cause the cell death (Figure 2.9G and H). From these results, we concluded that ectopic SCRO expression does not cause cell death of neurons.

Homeodomain is essential for SCRO's negative function

SCRO contains three conserved domains; homeodomain (HD), TN/eh1 and NK2-specific domain (Jagla et al., 2001). According to our data so far, we hypothesize that SCRO interacts with *PRE* through its DNA-binding HD. To test this, we generated a mutant SCRO construct lacking 60-aa HD ($scro^{\Delta HD}$) (Figure 2.10A). In contrast to wild-type SCRO, *tim-Gal4* driven expression of $scro^{\Delta HD}$ showed normal *Pdf* expression (Figure 2.10B). These data suggest that HD is critical for SCRO's activity as a *Pdf* repressor. Interestingly, expression of VND also abolished PDF immunoreactivity (Figure 2.10C). Because HDs in these two members of NK2 family are highly conserved (98%) (Zaffran et al., 2000), our data support the importance of HD for binding *PRE*. Previous studies on VND demonstrated that Y54 residue within the HD is essential for DNA binding, and Y54M mutation abolished VND's negative function (Koizumi et al.,

2003). To test whether this is true for SCRO, we generated a similar mutation in SCRO HD (HD^{Y54M}). Intriguingly, expression of *UAS-scro*^{HDY54M} was unable to suppress *Pdf* expression (Figure 2.10D), further supporting that HD-mediated DNA binding to *PRE* is critical for SCRO-mediated *Pdf* repression.

In addition to HD, NK2 family proteins have two other conserved domains; eh1/TN and NK2-specific domain or NK2-box (Zaffran et al., 2000). The eh1/TN domain, consensus sequence being FxIxxIL, interacts with co-repressor GROUCHO (GRO) to regulate its target genes (Cowden and Levine, 2003; Jennings et al., 2006). NK2-box was also reported to be important for GRO-dependent repressor activity of VND (Uhler et al., 2007). To assess the roles of eh1/TN and NK2-box domains, we made two transgenic lines carrying mutant *scro*. Expression of *scro* lacking eh1/TN domain ($scro^{\Delta TN}$) eliminated *Pdf* expression, as observed with wild-type *scro* (Figure 2.10E). In addition, expression of wild-type *scro* in *gro*^{C105} mutant background resulted in the lack of *Pdf* expression, implying that GRO is not required for SCRO's action (Figure 2.10F). These results therefore suggest that eh1/TN domain is not necessary for SCRO's repressor function. We also found that expression of NK2-box deletion mutant (*scro*$^{\Delta NK2}$) abolished *Pdf* expression similar to wild-type SCRO, suggesting that NK2 box is not important for SCRO-mediated repression of *Pdf* (Figure 2.10G).

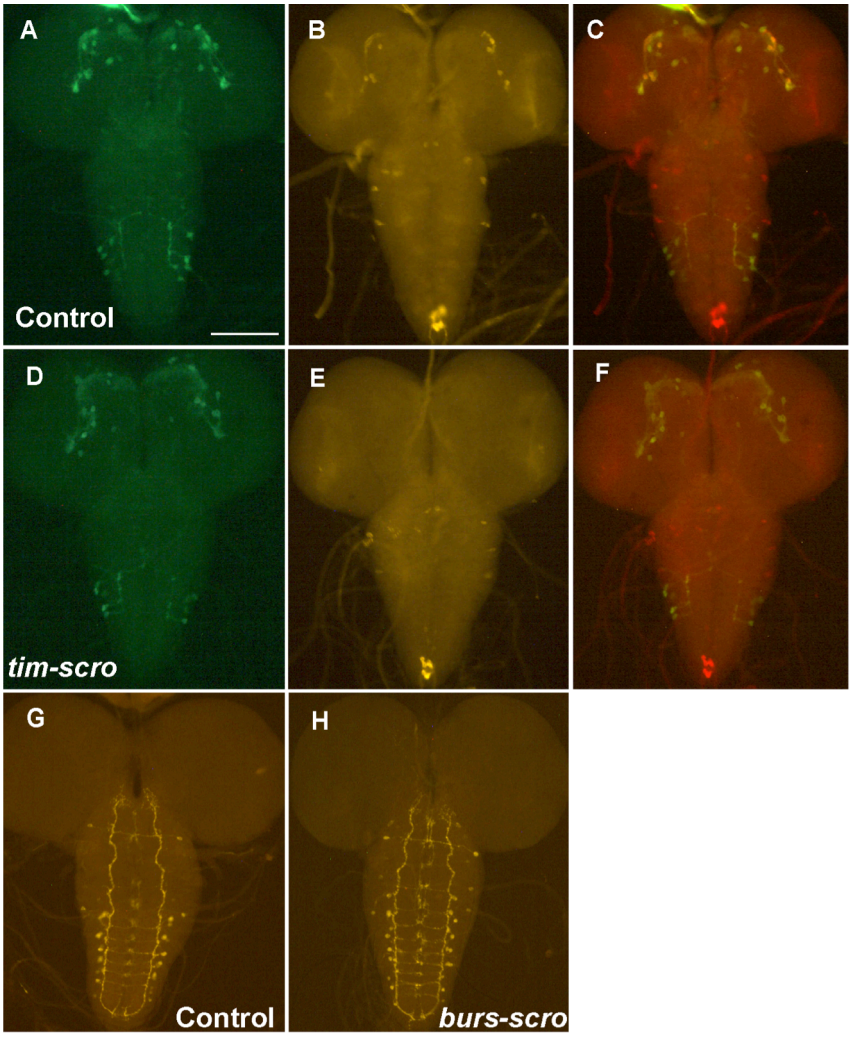


Figure 2.9 SCRO is not cytotoxic to the neurons. (A-C) Control larval CNS with *GFP*-reported *tim* expression (genotype: *UAS-mCD8GFP; tim-Gal4/+*). (A) GFP signals. (B) Immunostaining of PDF. (C) Merge of A and B. (n=5). (D-F) Overexpression of *scro* in tim neurons (genotype: *UAS-mCD8GFP; tim-Gal4/+; UAS-scro/+*). (n=5). (G, H) bursicon-immunoreactivity of larval CNS. (G) Control (*bursicon-Gal4/+*, n=5). (H) Ectopic expression of *scro* in bursicon neurons (genotype: *bursicon-Gal4/+; UAS-scro/+*, n=5). Scale bar = 100 μm.

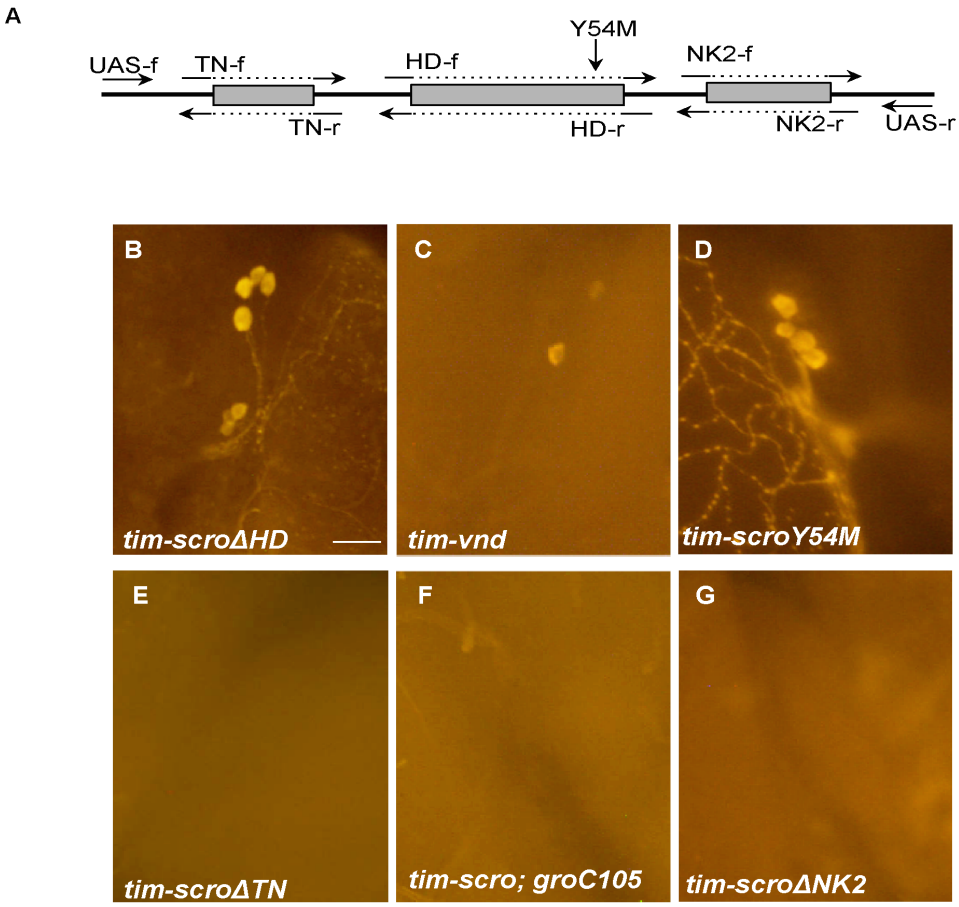


Figure 2.10 PDF immunoreactivity in the adult brain resulting from the transgenic expression of mutant *scro* and *vnd* (A) Schematic of SCRO domains and PCR primers used for site-directed mutagenesis. (B-G) Representative images of PDF-immunoreactivity in the l-LN$_v$s and s-LN$_v$s. (Genotypes: B, *tim-Gal4/+; UAS-scro*$^{\Delta HD}$/+ (n=5); C, *y w; tim-Gal4/+; UAS-vnd/+* (n=7); D, *y w; tim-Gal4/UAS-scro*^{HDY54M} (n=5); E, *tim-Gal4/+; UAS-scro*$^{\Delta TN}$/+ (n=6); F, *tim-Gal4/UAS-scro*; *gro*^{C105} (n=9); G, *tim-Gal4/+; UAS-scro*$^{\Delta NK2}$/+ (n=6). Scale bar = 50 μm.

Overexpression of *scro* causes arrhythmicity

Since PDF is required for circadian locomotor activity rhythms (Renn et al., 1999), we measured the rhythms of flies expressing of various *scro* constructs. Typically, wild-type flies have two activity peaks, each at dusk and dawn under 12-hr light: 12-hr dark (LD) condition. And then single peak activities continue under constant darkness (DD) with approximately 24-h rhythmicity (Figure 2.11A and Table 2.2). Consistent with the immunohistochemistry results, flies expressing wild-type *scro* using *Pdf-Gal4* (*Pdf-scro*) seem to show normal rhythmicity (Figure 2.11B). However, under DD conditions, rhythmicity dampened after 4 DD days. This could be due to accumulation of SCRO, which then reduces *Pdf* expression. In support of this notion, doubling dosage of the *UAS-scro* accentuated arrhythmicity (Figure 2.11C and Table 2.2).

As expected from the lack of PDF, free-running behaviors of all *tim-scro* flies were arrhythmic in DD (Figure 2.11D and Table 2.2). Additionally, *tim-scro* flies displayed abnormal LD behavior; flies don't seem to anticipate light-on and light-off changes, as flies show startle responses to lights on. They also maintained relatively higher levels of activities during the night and midday. Such abnormal LD patterns might indicate that ectopic expression of *scro* in tim-neurons affects cellular physiology of other non-PDF clock neurons. As expected, expression of $scro^{\Delta TN}$ and $scro^{\Delta NK2}$ using *tim-Gal4* produced behavioral results comparable to that of wild-type *scro* (Table 2.2). In contrast, normal rhythmicity was observed for the flies expressing $scro^{\Delta HD}$ (Figure 2.11E and Table 2.2).

Table 2.2: Locomotor activity analysis of *scro* driven by specific Gal4 constructs

Genotype	n	R	WR	AR	Period (h) Mean±S.D.
Wild-type	25	24	1	0	24.25±0.31
Pdf-Gal4/+; UAS-scro/+	54	28	6	20	23.25±3.01
UAS-scro/Pdf-Gal4; UAS-scro/+	31	0	3	28	23.67±0.76
DvPdf-Gal4/+;; UAS-scro/+	42	0	0	42	-
tim-Gal4/+; UAS-scro/+	35	0	0	35	-
tim-Gal4/+; UAS-scro$^{\Delta TN}$/+	68	0	0	68	-
tim-Gal4/+; UAS-scro$^{\Delta HD}$/+	23	23	0	0	24.06±0.73
tim-Gal4/+; UAS-scro$^{\Delta NK2}$/+	14	0	0	14	-
Pdf-Gal4/+;UAS-scroRNAi(I)/+	19	18	1	0	23.93±0.49
DvPdf-Gal4/+;UAS-scroRNAi(I)/+	19	19	0	0	23.61±0.32
tim-Gal4/+;UAS-scroRNAi(I)/+	19	17	1	1	24.15±0.46
Pdf-Gal4/+;UAS-scroRNAi(II)/+	20	17	2	1	23.88±0.42
DvPdf-Gal4/+;UAS-scroRNAi(II)/+	19	17	1	1	23.76±0.40
tim-Gal4/+;UAS-scroRNAi(II)/+	15	11	3	1	23.25±0.58

n, number of flies tested; R, rhythmic (power≥10); WR, weakly rhythmic (0<power<10); AR, arrhythmic.

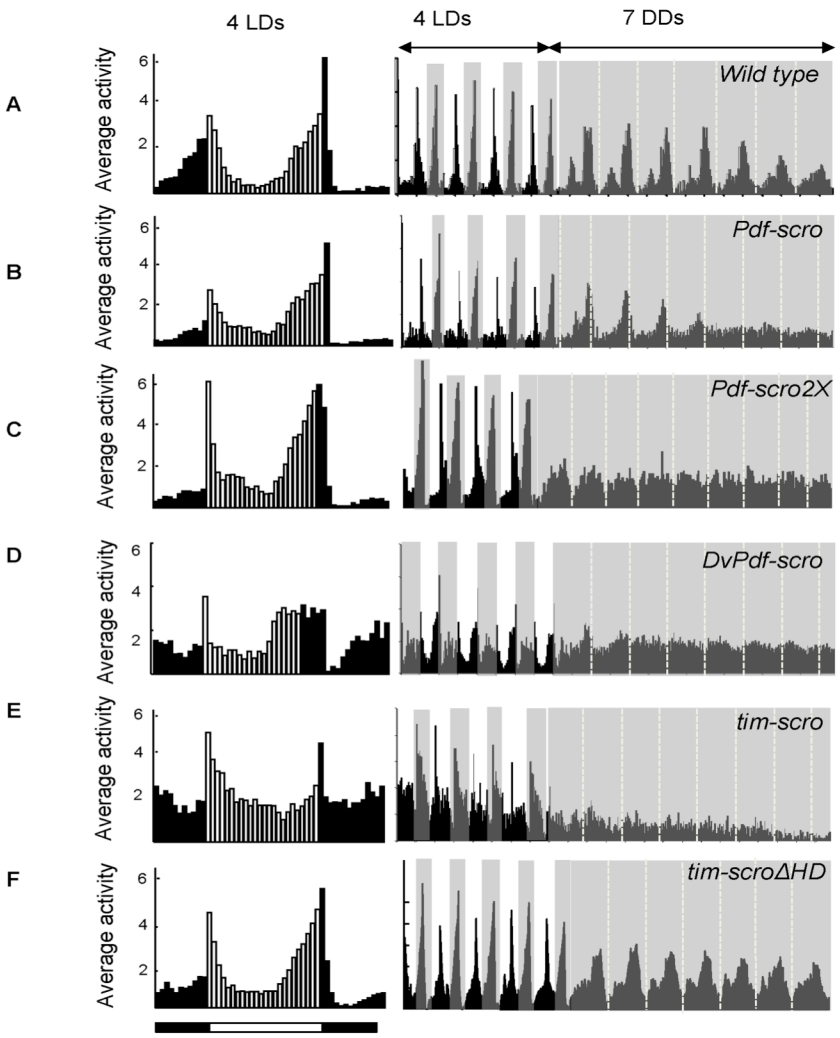


Figure 2.11 Locomotor activity rhythms of flies expressing *scro*. Histograms on the left show average activities of 4 LD cycles (activities in dark phase are in black and those in light phase are in white). Plots on the right show average daily activity patterns. (A) Wild type flies (n=25) (B) *y w; Pdf-Gal4/+; UAS-scro/+* (n=54) (C) *y w*; *UAS-scro*/*Pdf-Gal4*; *UAS-scro*/+ (n=31) (D) *y w, DvPdf-Gal4/+*;; *UAS-scro/+* (n=35) (E) *y w; tim-Gal4/+*; *UAS-scro/+* (n=35) (F) *y w; tim-Gal4/+; UAS-scro*$^{\Delta HD}$*/+* (n=23).

Knockdown of *scro* using RNAi lines does not show ectopic PDF immunohistochemistry

Scro is located in the heterochromatin region (3LHet) and has no known mutant alleles, except for one P-element insertion line. We performed RT-PCR analysis on this insertion line and found that it does not affect transcriptional activity of the *scro*. Hence, we decided to test two different transgenic RNAi lines available at the Bloomington Stock Centre expressing double stranded RNA of *scro* under UAS control. We refer to these lines as *UAS-scro*RNAi I and II (Stock 29387 and Stock 33890 respectively). To test the efficacy of the RNAi lines, we used *act5c-Gal4* and *tub-Gal4* drivers to ubiquitously knockdown *scro* in all the cells. We found larval lethality at L3 stage when we drove both $scro^{RNAi}$ lines. When expressed using *Pdf-Gal4* driver PDF expression was observed in both subsets of LNvs (Figure 2.12 A and C). We monitored adult locomotor activity and found that overexpression of *UAS-* $scro^{RNAi}$ transgene using circadian clock-related Gal4 drivers had no apparent effect on circadian behavior (Table 2). Knockdown of *scro* in the non-PDF expressing clock neurons should lead to ectopic *Pdf* expression based on our hypothesis that *scro* represses *Pdf*. We tested the effect of *scro* knockdown using *scro-RNAi* lines and overexpressing these by UAS-Gal4 system. We ectopically expressed *scro-RNAi* using *tim-Gal4* that is expressed in a wide set of clock neurons. However, but did not find any ectopic PDF staining in the non-PDF expressing clock neurons (Figure 2.12 B and D). This could be attributed to partial knockdown of *scro* in the RNAi lines.

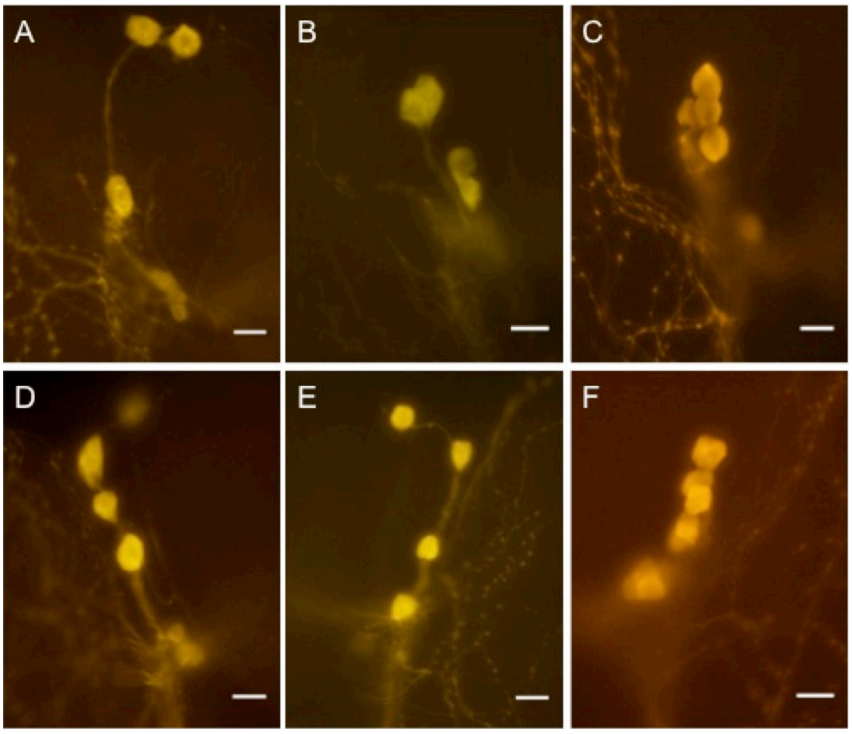


Figure 2.12 No ectopic *Pdf* expression was detected after scro knockdown.

(A-D) Representative images of PDF-immunoreactivity in the l-LN$_v$s and s-LN$_v$s for these genotypes: (A) *Pdf-Gal4/+; UAS-scro*$^{RNAi(I)}$/+ (n=5); (B) *DvPdf-Gal4/+;; UAS-scro*$^{RNAi(I)}$/+ *(n=5);* (C) *tim-Gal4/+; scro*$^{RNAi(I)}$/+ (n=7); (D) *Pdf-Gal4/+; UAS-scro*$^{RNAi(II)}$/+ (n=5); (E) *DvPdf-Gal4/+;; UAS- scro*$^{RNAi(II)}$/+ *(n=5);* (F) *tim-Gal4/+; scro*$^{RNAi(II)}$/+ (n=6). Scale bar = 50 μm.

Deletion of *scro* using CRISPR leads to embryo lethality

In order to further understand endogenous function of *scro*, we attempted to generate *scro*-null mutant. Using CRISPR, we intended to remove an internal part of coding sequence as illustrated in Figure 2.13. To perform this, we identified two sequences for potential guide RNA targets and these sequences were individually inserted into pU6-BbsI-chiRNA vector (Gratz et al., 2013; Gratz et al., 2014). The resulting plasmids were together injected into y^1 w^{1118} M (vas-Cas9) ZH-2A embryos that express Cas9 nuclease under the control of *vasa* regulatory region specifically in the female germline.

Out of 45 viable G0 adult flies obtained after injection, we found only 7 fertile lines. We found greater percentage of sterile flies than the typical ~30% sterility usually observed with P-element germline transformation. Ten G1 males from each G0 (total 7 independent G0 lines) line were individually crossed to the third chromosome balancer stock. After larvae started hatching, the male from each individual crossing was sacrificed to perform single fly PCR. The results confirm deletion of 330 bp of the genomic DNA between the two guide RNA-targeted sequences as shown in Figure 2.13 and we identified eight G1 stocks bearing targeted deletion. Sequence analysis of all the eight stocks showed similar results. All these eight lines were homozygous lethal during embryonic development, indicating that *scro* has a crucial role in embryonic development. We immunostained the heterozygous larval brain and found normal PDF immunoreactivity (Figure 2.13).

Table 2.3: Mutation frequencies of *scro* induced by Cas9

gRNA concentration	Embryos injected	Larvae survival Rate	Adults survival rate	Total fertile G0 lines	Total heterozygous lines
100 ng/µl	300	100/300	45/300	7/45	8/70 G1 crosses
		(33.33%)	(15%)	(15.21%)	

7 fertile G0 lines – 10 males per line were individually crossed to balancer stock and hence a total of 70 crosses.

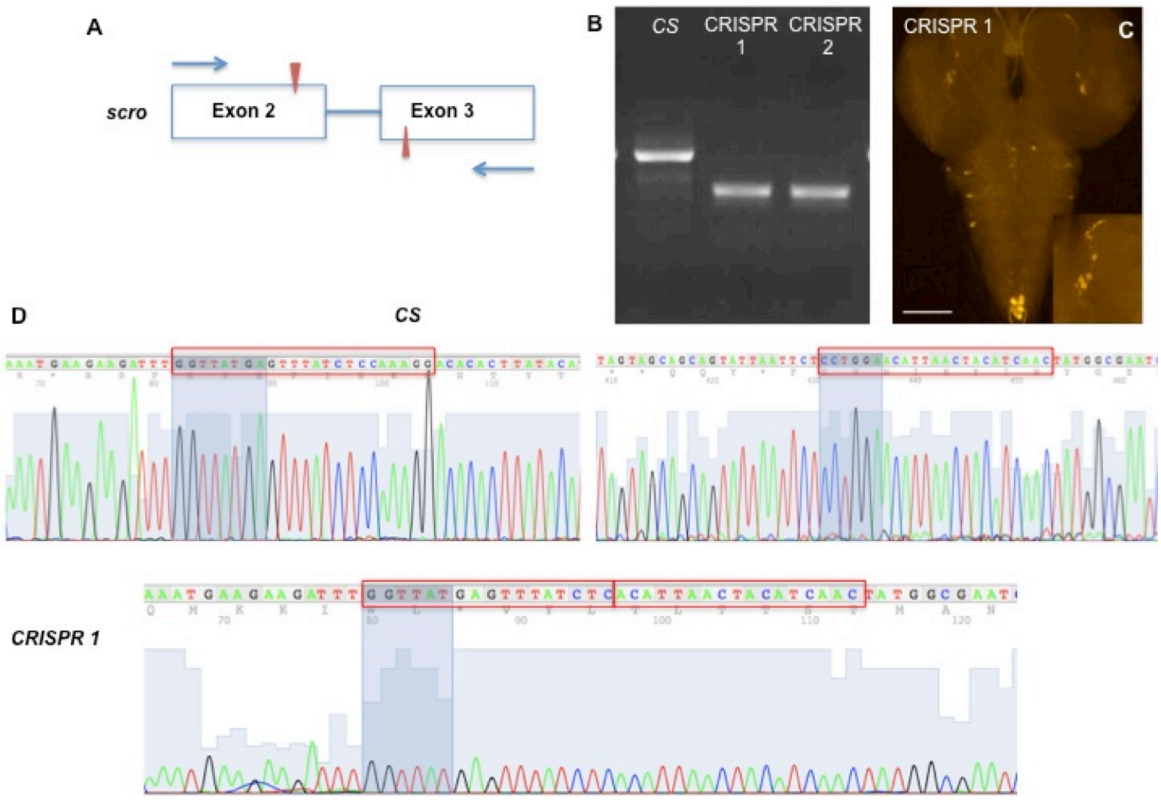


Figure 2.13 Generation of *scro* mutant using CRISPR (A) Schematic for position of gRNA in the *scro* genomic region. Red arrowheads indicate the position of two different gRNA sequences on Exon 2 and Exon 3 with the blue arrows indicating position of primers. (B) PCR products confirming deletion of 300 bp as compared to *CS* (wild type control). (C) CRISPR heterozygous larval brain stained for PDF. (D) Sequence analysis between wild type control *CS* and the CRISPR 1 mutant for *scro*. In the wild type, the gRNA sequence is highlighted in red box. Whereas, in CRISPR 1, there is a precise deletion of the target region in *scro* indicated by two red boxes that represent the remainder of the gRNA sequence after deletion.

Expression of *scro* and *Pdf* do not overlap in the *Drosophila* brain

In situ hybridization shows *scro* expression in the brain and ventral nerve cord in developing embryos, implying that *scro* functions are associated with neural development in *Drosophila* (Zaffran et al., 2000). In addition to the embryonic function, our data with overexpression studies clearly indicates post-embryonic roles of SCRO particularly in the CNS. In order to better understand post-embryonic expression of *scro* we utilized a *scro-Gal4* line (Kvon et al., 2014). Using *UAS-Red-stinger* that expresses nucleus *Ds-Red*, we looked at the *scro* expression patterns in the larval, pupal and adult brain. Interestingly, *scro* is expressed a wide set of neurons in the third instar larval brain and ventral nerve cord excluding neurons in the optic lobe (Figure 2.14A). Even 12-24 hour after puparium formation, there is wide spread *scro* expression in the pupal brain and ventral nerve cord with a group of neurons near the calyx showing increased staining (Figure 2.14B). Figure 2.14C indicates scro expression in the calyx in the pupal brain in 50-60 hour pupa and this expression pattern is maintained in the adult stage (Figure 2.14D). Interestingly, in the adult ventral nerve cord, *scro* expression is predominantly restricted to the abdominal neurons (Figure 2.14E) very different than the larval and pupal stage ventral nerve cord expression.

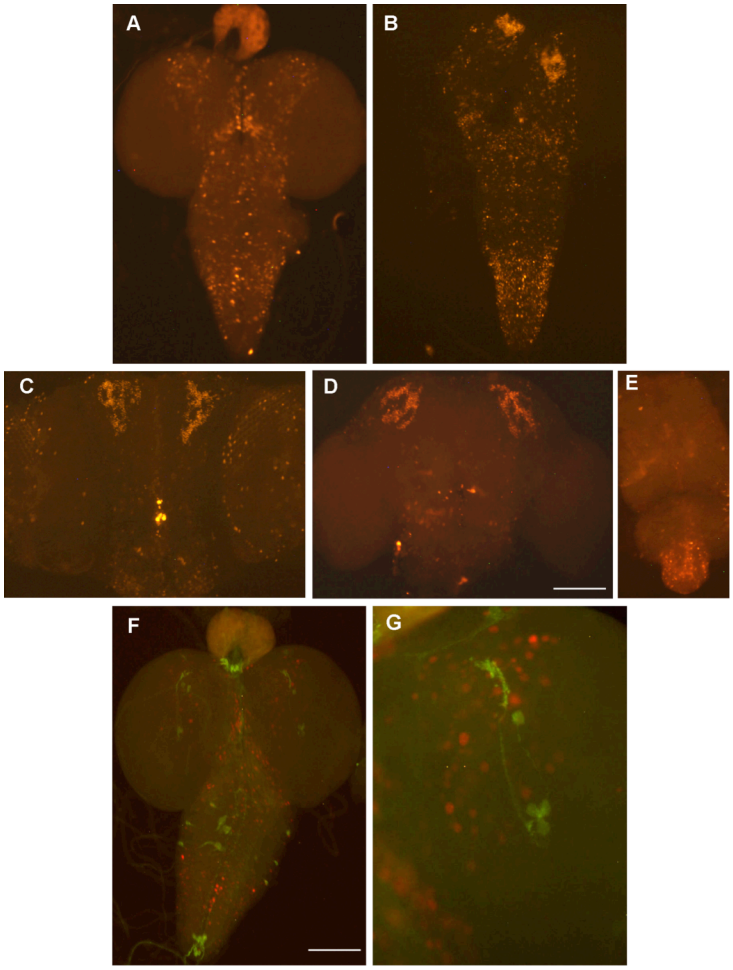


Figure 2.14 Expression pattern of *scro* in the larval, pupal and adult CNS Nuclear *Ds-Red* staining in neurons expressing *scro* in (A) third instar larval stage, (B) 12-24 hour after puparium formation (C) 50-60 hour after puparium formation, (D) adult brain and (E) adult ventral nerve cord. Labeling for PDF in the flies expressing nuclear Ds-Red under the control of *scro* clearly indicates no overlap of *scro* and Pdf (F and G) suggesting that *scro* is not expressed in the LNs.

Discussion

Transcriptional gene regulation is primarily governed by the interaction between *cis*-regulatory elements and their cognate binding factors. Neuropeptide gene expression is stereotypically restricted to defined sets of neurons in the CNS (Nassel and Winther, 2010). In the larval CNS, *Pdf* expression is found in only two groups of neurons, LNs in the brain lobe and Ab in the abdominal ganglion. During metamorphosis, the LNs persist to form s-LN_vs, while a new cluster with larger somata and much stronger *Pdf* expression (l-LN_vs) emerge in the vicinity of the s-LN_vs (Helfrich-Forster et al., 2007). Interestingly, Clk^{Jrk} and cyc^{0} mutations abolish *Pdf* expression mostly in s-LN_vs, not l-LN_vs (Park et al., 2000), suggesting that transcriptional regulatory mechanisms are different between the two neuronal groups. Such cell type-specific regulation of a neuropeptide gene has been well studied for *FMRFamide* (Benveniste and Taghert, 1999; Benveniste et al., 1998).

Subsets of these neurons, called OL neurons, begin to produce FMRFamide during metamorphosis, and such transcriptional activation requires a regulatory sequence consisting of 10-bp tandem repeats (Taghert et al., 2000). The anatomical position and developmental acquisition of the neuropeptide phenotype is similar between FMRFamide-OL neurons and PDF l-LN_vs. Another similarity is the 13-bp tandem repeats in the *PRE* and hence it was proposed to play a role for *Pdf* expression in l-LN_vs during metamorphosis (Taghert et al., 2000). Our experiments, however, revealed that *PRE* is necessary for the expression of *Pdf* not only in l-LN_vs but also in s-LN_vs. Thus we have not been able to separate regulatory elements for these two types of neurons.

In contrast, our data show that *Pdf* expression in a group of Ab neurons is controlled by distinct *cis*-acting elements from those for LN_vs. What's more complicated is that *Pdf* expression in Ab neurons is controlled differentially between larva and adult stages, as we found different regulatory regions acting in the two developmental stages. Why does a transcriptional switch function to control the expression of the same neuropeptide differentially in separate life stages? According to developmental studies, PDF immunoreactivity in Ab neurons changes noticeably during metamorphosis. The larval immunoreactivity is severely weak or even absent during first half of pupal development, and then adult-like immunoreactivity appears at later pupal stage (Helfrich-Forster, 1998). Such a developmental gap might indicate transcriptional reorganization during metamorphosis to control the appropriate production of PDF for adult-specific functions.

Spatial control of gene expression requires both positive and negative elements in which the latter is to repress ectopic expression. However, the mechanisms of the negative regulation are in general not well understood as compared to positive regulation. Previously, we have shown that *D. virilis Pdf* transgene in the *D. melanogaster* genome produces ectopic *Pdf* expression in 3-4 LN_ds and 5^{th} s-LN_v in addition to endogenous PDF neurons (Bahn et al., 2009). These results led us to propose that *Pdf* is normally repressed in these ectopic clock neurons. In line with this, a previous study showed that abnormally developed LN_ds are PDF-immunoreactive (Helfrich-Forster et al., 2007). These observations further support the importance for the negative regulation of *Pdf* to restrict its expression to LN_vs.

Although our intent was to find a direct activator of *Pdf*, our work led to identifying SCRO as a novel transcriptional repressor of *Pdf*, which to our knowledge has yet to be described in *D. melanogaster*. SCRO is a member of the NK2 homeobox family, members of which are widespread in vertebrates and invertebrates (Kim and Nirenberg, 1989; Zaffran et al., 2000). Other *Drosophila* NK families include *NK4/tinman* (*tin*), *NK3/bagpipe* (*bap*), and *NK2/ventral nervous system defective* (*vnd*). The closest vertebrate homolog of SCRO is Nkx2.1, which is also referred to as TTF1 (thyroid transcription factor 1) (Harvey, 1996; Zaffran et al., 2000). Nkx2.1/TTF1 is important for the development of lung and thyroid glands and causally associated with the oncogenic development of lung adenocarcinoma (Fernandez et al., 2015; Yamaguchi et al., 2013). The Nkx2.1/TTF1 is also important for the CNS development, as it is required for the migration of interneurons from medial ganglionic eminence to the striatum and cerebral cortex in the developing telencephalon. Humans bearing mutations in the Nkx2.1/TTF1 develop various symptoms such as congenital hypothyroidism, infant respiratory distress syndrome (IRDS) and benign hereditary chorea (Carre et al., 2009).

Little is known about the biological function of SCRO. Previous work has suggested that *scro* is expressed in the brain and ventral nerve cord in developing embryos (Zaffran et al., 2000). According to high-throughput RNA-seq data, the larval CNS and adult heads are major tissues expressing *scro* (Gelbart, 2013), suggesting that *scro* functions in the post-embryonic nervous system. We further confirmed using *scro*-Gal4 that *scro* is expressed in a wide set of neurons in the larval, pupal and adult brain. In addition, scro is also not expressed in the PDF expressing LNs suggesting that scro is

required to suppress *Pdf* in the non-PDF expressing neurons. The molecular mechanisms of SCRO-mediated downregulation of *Pdf* expression are only beginning to be understood. As expected we confirmed the importance of DNA-binding homeodomain while the other two domains, NK2 and TN, conserved in NK2 members do not play a role in *Pdf* repression. In the case of VND, the TN domain was shown to interact with GRO, a global corepressor thereby playing a critical role in VND's transcriptional repression of several target genes that are required for embryonic development (Cowden and Levine, 2003). Moreover, the NK2 domain seems to stabilize GRO-VND interaction (Uhler et al., 2007). However, our genetic data indicate that SCRO-mediated *Pdf* repression does not involve GRO, suggesting that the modes of SCRO action are dissimilar to those of VND. SCRO perhaps interacts with other proteins to function as a repressor and identification of such molecular partners will be important to understand SCRO's function.

Finally, we have questioned how *DvPdf* transgene led to ectopic PDF expression in the non-PDF clock neurons. A possible explanation is that SCRO is unable to repress *DvPdf* in these neurons. This can be further supported by the fact that *PRE*-like region in *DvPdf* is substantially diverse from *D. melanogaster PRE*. Such sequence divergence might weaken *D. melanogaster* SCRO's interaction with *DvPdf PRE*, thus disabling it to repress *Pdf* in non-PDF clock neurons. Further dissection and molecular analysis of *PRE* will be needed to reveal the exact binding site of SCRO.

CHAPTER 3: CHARACTERIZING THE FUNCTION OF *SCARECROW* IN DEVELOPING TISSUES

Abstract

The *Drosophila* larval imaginal disc is a great model system to study tissue and organ development. Several patterning genes that regulate organ size and shape rely on cell proliferation and differentiation. Homeodomain containing proteins are involved in the development process, with some involved in segment identity. In this work, we characterize the function of a homeodomain containing gene *scro*. Expression of *scro* in the embryo is localized to the brain, pharynx and ventral nerve cord. We show *scro* expression in wing imaginal disc, adult testis in addition to being expressed in a wide set of neurons in the larval brain and ventral nerve cord. When expressed in the wing pouch using *MS1096-Gal4* we observe the transformation of haltere to wing tissue with bristles, a phenotype described in Ultrabithorax (*Ubx)* mutants in addition to overexpression of *miR-iab4-5p*. The locus *miR-iab4* encodes for this microRNA that influences *abdominal-A* (*Abd-A)* and attenuates *Ubx*. We provide evidence for the defective development of gonads by ectopically expressing *scro* in cells that express the sex determination gene *doublesex* (*dsx*). Furthermore, microRNA interaction database suggests an interaction between *scro* and *miR-iab4*. Based on these results we hypothesize that *scro* influences miR-iab4 to affect *Ubx* and *Abd-A* expression.

Introduction

Gene expression depends on synergistic binding of transcription factors and co-factors and how these factors regulate enhancer function is one of the most important questions in biology (Rosenfeld et al., 2006). Transcription factors are grouped based

on their DNA-binding domains and factors with similar DNA-binding domains could have distinct binding specificity. The homeodomain is a self-folding 60 amino acid DNA-binding domain with three helices that form a helix-turn-helix motif (Gehring et al., 1994). Homeodomains are 180 base pair homeobox regions that are evolutionarily conserved. These regions were first identified in genes that control morphogenesis in *D. melanogaster* (McGinnis et al., 1984a; McGinnis et al., 1984b; Scott and Weiner, 1984). Homeobox genes are capable of autoregulation in addition to regulating other homeobox genes to control gene expression patterns in spatial and temporal manner (Hayashi and Scott, 1990).

Homeobox genes are divided into different clusters based on the specificity of the sequences they bind. There exists *Hox* gene cluster that are highly conserved and determine development of structures along the antero-posterior (A/P) axis. In *Drosophila*, these are divided into Bithorax (BX-C) complex and Antennapedia (Antp) complex. BX-C comprises of *Ultrabithorax* (*Ubx*), *abdominal-A* (*abd-A*) and *abdominal-B* (*abd-B*) (Lewis, 1978; Sanchez-Herrero et al., 1985). Antp consists of the genes *labial* (*lab*), *proboscipedia* (*pb*), *Deformed* (*Dfd*), *Sex combs reduced* (*Scr*), and *Antennapedia* (*Antp*) (Kaufman et al., 1980; Scott et al., 1983).

In addition to the BX-C and Antp, there is a NK (Nirenberg and Kim) cluster of homeobox genes located on the chromosomal region 93DE (Kim and Nirenberg, 1989). This cluster consists of six genes namely *msh*, *tinman* (NK4), *bagpipe* (NK3), *ladybird late* (NKch4), *ladybird early*, *C15* (93Bal) and *slouch* (NK1). These genes determine

pattern formation and development of the mesoderm (Jagla et al., 2001). The NK2 family is a part of the NK superfamily and is characterized by two additional domains in the N and C-terminal regions in addition to the homeodomain (Harvey, 1996). Interestingly, two NK2 homeobox genes, ventral nerve cord defective (*vnd*) and scarecrow (*scro*) are located elsewhere in the genome away from the NK cluster of homeobox genes. The NK2 family is highly conserved with human genome coding for seven of these genes. They are further divided into NK2-1 family (*scro* in *Drosophila*) with *NKX2-1* and *NKX2-4*, NK2-2 family (*vnd* in *Drosophila*) with *NKX2-2* and *NKX2-8* and the NK4 family *(tinman* in *Drosophila)* with *NKX2-3*, *NKX2-5* and *NKX2-6 (Holland et al., 2007)*.

The NKX2-1 homolog *scarecrow* (*scro*) was named because of its sequence similarity to *tinman*. *In situ* hybridization in *Drosophila* embryo first detects *scro* expression in pharynx followed by embryonic head and brain and in the later stages in ventral nerve cord (Zaffran et al., 2000). At stage 15, *scro* is detected in neuronal precursors anterior to the neuronal precursors of engrailed and lateral to even-skipped. Based on this it was deduced that scro expressing neurons were derived from lateral cells of neuroblast row 5 (Zaffran et al., 2000). In addition, scro was reported in a screen that identified transcription factors involved in dendritic patterning (Iyer et al., 2013) further supporting the possible role for *scro* in neuronal patterning. Transcription factors that act as activators or repressors dictate the ability of the cell to grow and differentiate thus playing a key role during development (Busser et al., 2008; Davidson and Levine, 2008; Deplancke, 2009). These factors that determine cell fate usually involve coordination of

cellular proliferation and differentiation to maintain tissue homeostasis. These data suggest a possible role for *scro* in determining cell fate during development and hence we decided to further characterize the function of *scro* in developing tissues.

Materials and Methods

Fly stocks

The following transgenic flies were used in this study. *UAS-scro*, *UAS-scro*$^{\Delta TN}$, *UAS-scro*$^{\Delta HD}$, *UAS-scro*$^{\Delta NK2}$ were previously described in Chapter 2 of this thesis. *Short GMR-Gal4 (Hay et al., 1997)*; *MS1096-Gal4* (Stock 8860)*; wg*$^{sp-1}$*; dpp-Gal4/TM6B,Tb* (Stock 1553); *vg-Gal4* (stock 6819); *en-Gal4* (Stock 30564) and *dsx-Gal4* (Robinett et al., 2010) was obtained from the Bloomington Stock Centre. *UAS-p35* (Hay et al., 1995), *scro-Gal4* (Vienna-VT 208008) (Kvon et al., 2014).

X-gal staining

Dissected wing imaginal disc from third instar larvae and adult testis were fixed in 1X PBS and glutaraldehyde. The dissected tissues were incubated in 0.02% X-gal solution overnight. The *β* - galactosidase staining in these tissues were then visualized using Olympus BX16 microscope.

Acridine orange staining

Acridine orange staining was used to detect dying cells. Eye and wing imaginal discs were dissected from third instar larvae and then incubated for 2-3 min in 0.5-µg/ml

acridine orange/1XPBS solution. These samples were rinsed in 1X PBS before observation. Images were taken within 10 minutes of staining due to the transient staining of acridine orange.

Scanning Electron Microscope

Adult male flies that were 4-5 days old were dehydrated in 95% ethanol and dried. Each fly head was mounted, sputter-coated, and visualized using a Leo 1525 Gemini scanning electron microscope (Zeiss, Thornwood, NY).

RT- PCR

For semi quantitative reverse transcription-PCR (RT-PCR), total RNA from whole adult flies was isolated using TRIzol (Invitrogen). After the removal of contaminating genomic DNA by DNase I digestion, RNA was reverse transcribed with GoScript reverse transcriptase and oligo (dT) primers according to the manufacturer's instructions (Promega). The cDNA was amplified by PCR using gene specific primers as previously mentioned (Lee et al., 2002). PCR products were resolved on 1% agarose gel.

Results

The best approach to study function of a transcriptional regulator or for that matter any gene would be to look at its loss of function phenotype. However, approximately 75% of *Drosophila* genes using loss of function do not show a phenotype (Miklos and Rubin, 1996) or are lethal and hence overexpression studies using the powerful UAS-GAL4

system (Brand and Perrimon, 1993) provide an alternative to study the function of transcription factors in a tissue specific manner. We used CRISPR to generate a *scro* mutant but the homozygous mutants do not survive past the embryo stage. Hence, we decided to overexpress scro using *UAS-scro* transgenic lines generated in the lab and drove its expression using tissue specific Gal4 lines.

Overexpression of *scro* in the photoreceptor neurons lead to abnormal eye

The compound eye of *Drosophila* has 800 eye units or ommatidium arranged hexagonally and has mechanosensory bristles at the anterior of each ommatidium (Kumar, 2012). The eye is an example of a simple nervous system and is ideal to identify developmental genes. Each ommatidium is composed of 8 photoreceptor neurons, R1-R6 on the outside and R7 and R8 at the centre. The adult antennal eye disc is single layered and the ommatidium arises from cells within the morphogenetic furrow. In the developing embryo, 8-9 cells represent the presumptive eye disc and it undergoes increase in cell size during first and second instar larval stage. It is only during the third instar larval stage that the morphogenetic furrow forms and undifferentiated cells differentiate and get organized in rows (Figure 3.1). This is followed by a second mitotic wave that generates cells required to form a mature ommatidium.

GMR-Gal4 driver has been used widely to induce expression of several transgenes in the cells posterior to the morphogenetic furrow in the developing eye. *GMR-Gal4* contains glass multimer response element from the promoter of Rh1 opsin gene

(Freeman, 1996). We decided to use *GMR-Gal4* to ectopically express *scro* in the developing eye. Interestingly, when ectopically expressed *scro* shows alteration of the adult eye morphology with over proliferation of ommatidium and no mechanosensory bristles (Figure 3.2 B, B' and B") as compared to Figure 3.2 A, A' and A''.

However, two copies of *scro* led to severe degeneration of the ommatidia with several regions of the eye showing complete lack of ommatidia and reduced eye phenotype (Figure 3.2 C, C' and C''). We have made *scro* mutants with deletions of the N-terminal TN domain and C-terminal NK2 domain. Ectopic expression of *scro-TN* shows a much more severe phenotype than wild-type *scro* overexpression. TN deletion shows a layer of tissue with no ommatidia and presence of a few bristles but they are disrupted (Figure 3.2 D, D' and D''). Ovexpressing *scro* with NK2 domain deletion shows abnormal cells with holes in adult eye. In addition, there is a small black dot of dead cells with reduced eye phenotype (Figure 3.2 E, E' and E'').

Cell proliferation and tissue patterning are crucial to building functional units of the tissue and organ. As differentiation and patterning begin in late larval eye disc, there is extensive regulation of the cell cycle followed by cell death that controls the cell number (Baker, 2001). Based on the abnormal eye morphology for ectopic *scro* expression it is possible that it inhibits differentiation of photoreceptors cells or causes cell death. We decided to check if overexpression led to extensive apoptosis of the eye imaginal disc.

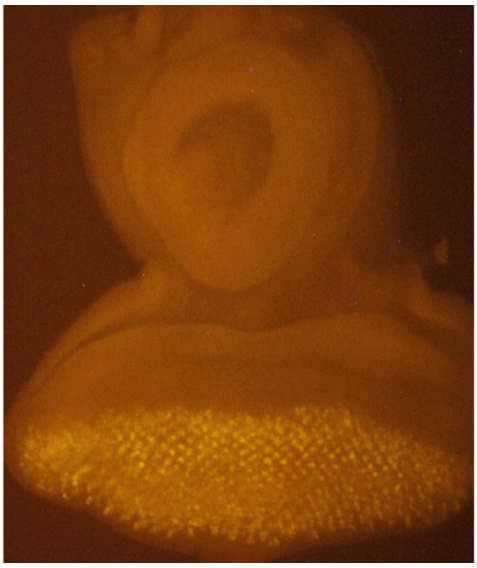


Figure 3.1 Eye imaginal discs in the third instar larvae. Dissected eye imaginal disc showing cells stained with HA antibody when *scro* is overexpressed in the morphogenetic furrow using *GMR-Gal4*.

We dissected eye imaginal disc from the third instar larvae and performed acridine orange (AO) staining to detect apoptosis. Slight staining is detected in living cells however dying cells show much brighter staining as altered pH causes the dying cells to retain the dye (Robbins and Marcus, 1963). Staining with AO showed an increase in dying cells when *scro* was overexpressed (Figure 3.3 A) as compared to the homeodomain deletion (Figure 3.3 C). AO staining was observed in the posterior part of the eye disc. Interestingly, TN domain deletion shows increased staining consistent with the severe adult eye phenotype but most of the cells in the anterior region are also stained (Figure 3.3 B). Similar to the TN domain deletion, NK2 deletion also shows cells in the posterior and anterior region of the eye disc stained strongly with AO (Figure 3.3 D).

These results suggest that overexpressing *scro* shows increased cell death. Activation of caspases, a family of cysteine proteases is crucial to apoptosis. We co-expressed *UAS-p35*, a baculovirus that inhibited caspases to verify if apoptosis was caspase dependent or independent. When co-expressed with *scro*, 30% (n=60) of the flies were rescued with normal eye morphology but the rest of the flies still exhibited over proliferation of the ommatidia cells. Similarly, when *scro-TN* deletion line was co-expressed with *p35*, we observed 35% rescue phenotype and with NK2 deletion line it was 30% rescue. These results indicate that the abnormal eye phenotype partially is due to caspase dependent apoptosis.

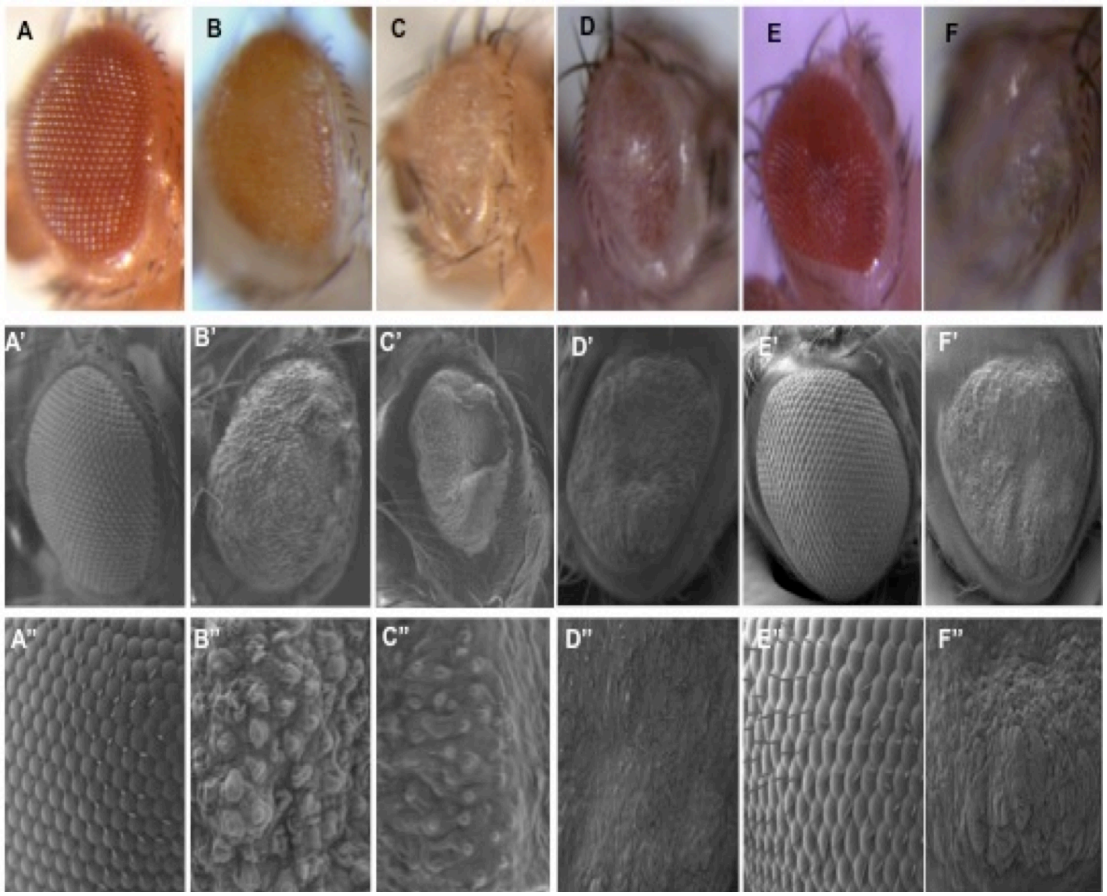


Figure 3.2 Ectopic expression of *scro* during late eye development. GMR-Gal4 driven expression of control *GMR/+* (A, A', A''), *GMR-Gal4/+;;UAS-scro/+* (B, B' and B''), *GMR-Gal4/+;UAS-scro/+;UAS-scro/+* (C, C', C''), *GMR-Gal4/+;UAS- scro* $^{\Delta TN}$*/+* (D, D' and D''), *GMR-Gal4/+;UAS-scro* $^{\Delta HD}$*/+* (E, E', E''), *GMR-Gal4/+;; UAS-scro* $^{\Delta NK2}$*/+* (F, F', F''). Top: Adult eyes using a dissecting light microscope. Middle: Scanning electron micrographs of fly heads Bottom: Magnified Scanning electron micrographs.

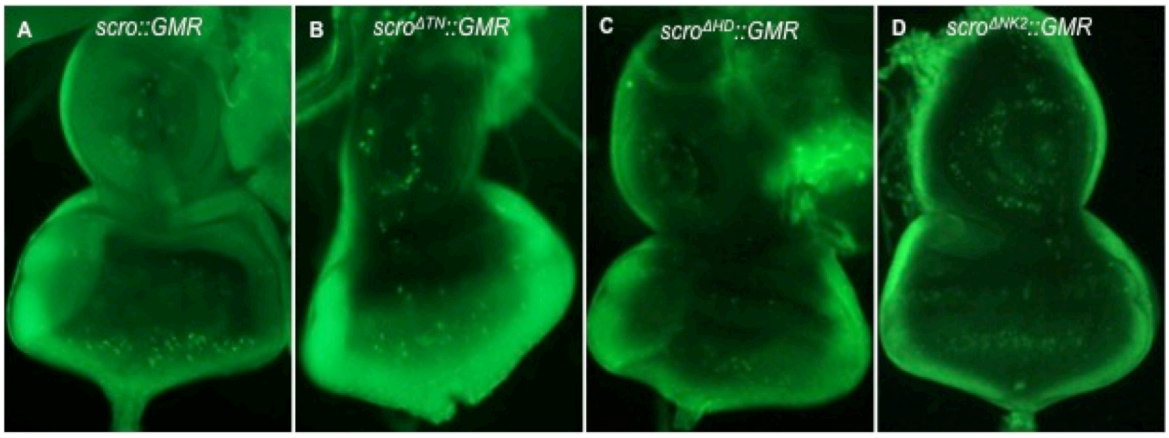


Figure 3.3 Overexpression of *scro* causes apoptosis in the developing eye.

Acridine orange staining showing increased number of dying cells stained with the dye (A) *GMR-Gal4/+;;UAS-scro/+* , (B) *GMR-Gal4/+;UAS- scro* $^{\Delta TN}$/+, (C) *GMR-Gal4/+;UAS-scro* $^{\Delta HD}$/+, (D) *GMR-Gal4/+;; UAS-scro* $^{\Delta NK2}$/+.

In apoptosis-induced proliferation, cells undergoing apoptosis are capable of inducing proliferation of the neighboring healthy cells (Fan et al., 2014) and these apoptotic cells exhibit both caspase dependent and independent apoptosis. Based on our results we suggest that a caspase independent cell death pathway and explains why we couldn't rescue the abnormal eye morphology.

Ectopic *scro* expression affects development of wings

The *Drosophila* wing represents an appropriate system to investigate development and patterning with phenotype that can be easily visualized. The molecular mechanisms of establishment of the dorsal-ventral and anterior-posterior and how morphogens provide positional information in pattern formation is well established. Engrailed, hedgehog and dishevelled establish the anterior-posterior (A-P) axis with *engrailed* expression in the posterior compartment of the wing. A stripe of cells expresses the morphogen *decapentaplegic* in the A-P compartment boundary of the wing. The dorso-ventral (D-V) axis is established by *vestigial*, key for wing and hinge development. To assess the role of *scro* in wing development, we chose four different Gal4 drivers. A schematic for Gal4 drivers and the regions in the wing they affect are explained in Figure 3.4.

We ectopically expressed *scro*, TN deletion, homeodomain deletion and NK2 deletion lines using *engrailed-Gal4* (*en-Gal4*). This Gal4 drives expression in the posterior compartment of the wing disc. Overexpression of *scro*, $scro^{\Delta TN}$, $scro^{\Delta HD}$ and $scro^{\Delta NK2}$ leads to 100% lethality at late pupal stage. These results indicate a possible role for *scro* in the posterior compartment of the wing in addition to its role during development.

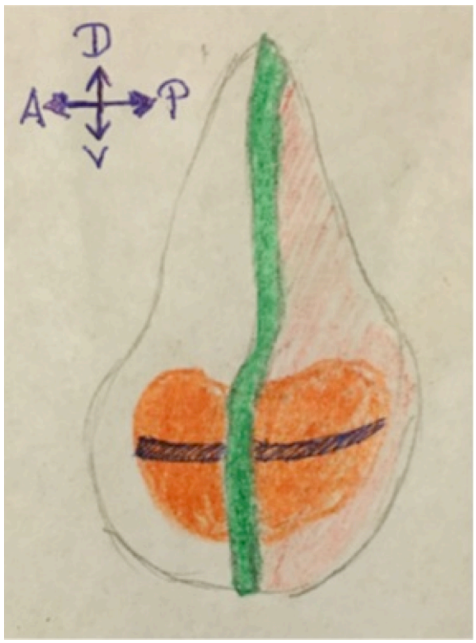


Figure 3.4 Regions expressing Gal4 drivers in the wing disc. Green represents *dpp-Gal4* whereas orange region represents *MS1096-Gal4*. Blue shaded region is *wingless* expression pattern and red region is *en-Gal4* expression pattern.

We used *vestigial-Gal4* (*vg-Gal4*) to drive expression in the dorso-ventral boundary. Interestingly, none of the overexpression lines showed any wing abnormality. This suggests that overexpression of *scro* in the dorsal-ventral boundary did not affect development. Decapentaplegic (dpp) is a morphogen that is required for regulating disc size in addition to patterning along the antero-posterior (A/P) axis. Dpp forms a long-range activity gradient and all cells along the A/P axis have to transduce signal for correct patterning (Teleman and Cohen, 2000). We ectopically expressed *scro* using the driver *dpp-Gal4 (wg^{sp-1}; dpp-Gal4/TM6B, Tb)*. This Gal4 is combined with *wingless* gene and can be distinguished based on stenopleural (sp) marker. We observe a severe reduction in size of the wings (Figure 3.5 B). However, overexpression of TN and NK2 deletion did not affect wing morphology. When we expressed two copies of *scro*, we observe a much stronger phenotype with truncated appendages (Figure 3.5 C). Either all three pairs of legs were affected or in some flies predominantly the third pair was affected (Figure 3.5 B' and C') compared to that of the control flies (Figure 3.5 A'). These results suggest that misexpression of *scro* in *dpp* cells leads to reduction in size of the wings but when dosage of *scro* is increased it leads to truncated legs as was previously observed in dpp^{d8}/ dpp^{d10} mutants (Sopory et al., 2010).

Lastly, we used *MS1096-Gal4* to drive *scro* expression in the entire wing pouch. Overexpression of *scro* using *MS1096-Gal4* leads to severe reduction of wing size. Interestingly, the halteres show sensory bristles that are usually present in the wing (Figure 3.6 A-A'''). This phenotype is seen in *Ubx* loss of function mutations (Weatherbee et al., 1998) and indicates haltere to wing transformation. Wild type

halteres show presence of small sensilla but lack bristles like the wing (Figure 3.6 C-C'''). In addition, we found TN deletion line also shows severe reduction in the wing phenotype and presence of ectopic bristles on the halteres, which is increased in size (Figure 3.6 B-B'''). However, no abnormal phenotype was observed when homeodomain and NK2 domain were deleted. The transformation of halteres might be due to downregulation of *Ubx*, however that does not explain the severe wing phenotype as *Ubx* is expressed only on the outer edges of the larval wing imaginal disc but is not necessary for proper wing development.

In order to understand the wing phenotype observed upon ectopic expression of the *scro* transgene, we examined apoptosis in wing imaginal discs by staining with acridine orange. Using *MS1096-Gal4*, we observe an increased staining in dying cells in the wing pouch when we overexpress *scro* and *scro-TN* deletion transgene (Figure 3.7 B and C) as compared to the control (Figure 3.7 A). However, deletion of homeodomain and NK2 domain do not show increased staining of apoptotic cells (Figure 3.7 D and E).

Overexpression of *scro* causes rotation of the adult male terminalia

In *Drosophila*, genital disc is sexual dimorphic and gives rise to internal and external genitalia and analia collectively known as terminalia (Carr et al., 2006). The genital disc is formed by the fusion of female primordium (derived from embryonic abdominal segment A8), male genital primordium (derived from A9) and anal primordium (A10-11) (Sanchez and Guerrero, 2001).

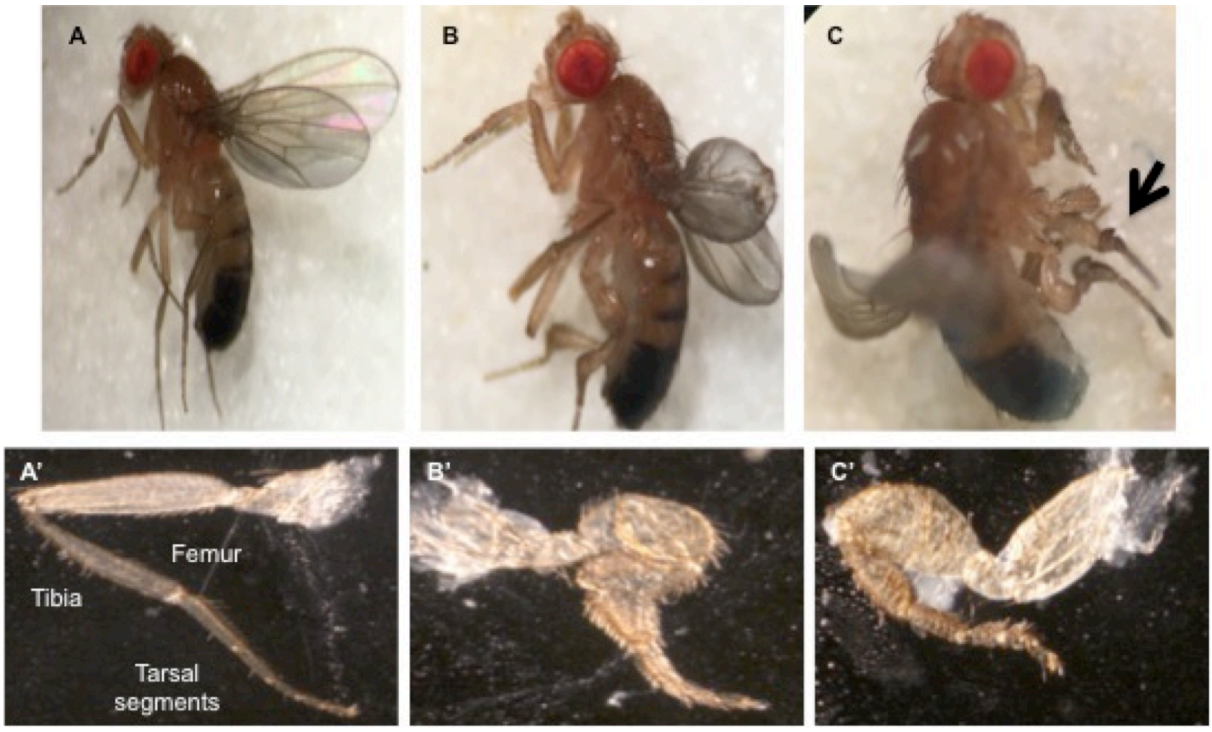


Figure 3.5 *Drosophila* adult wing and leg phenotypes resulting from overexpression of *scro*. (A) *wg^{sp-1}; dpp-Gal4/+* show normal wing and leg phenotype. (A') Leg appendage with femur, tibia and tarsus are labeled. (B) *wg^{sp-1}/+; UAS-scro/dpp-Gal4* shows reduced wing phenotype. (B', C and C') w*g^{sp-1}/UAS- Scro; UAS-scro/dpp-Gal4* result in short and thick legs as compared to A'. The short and curved legs are indicated by an arrow in C.

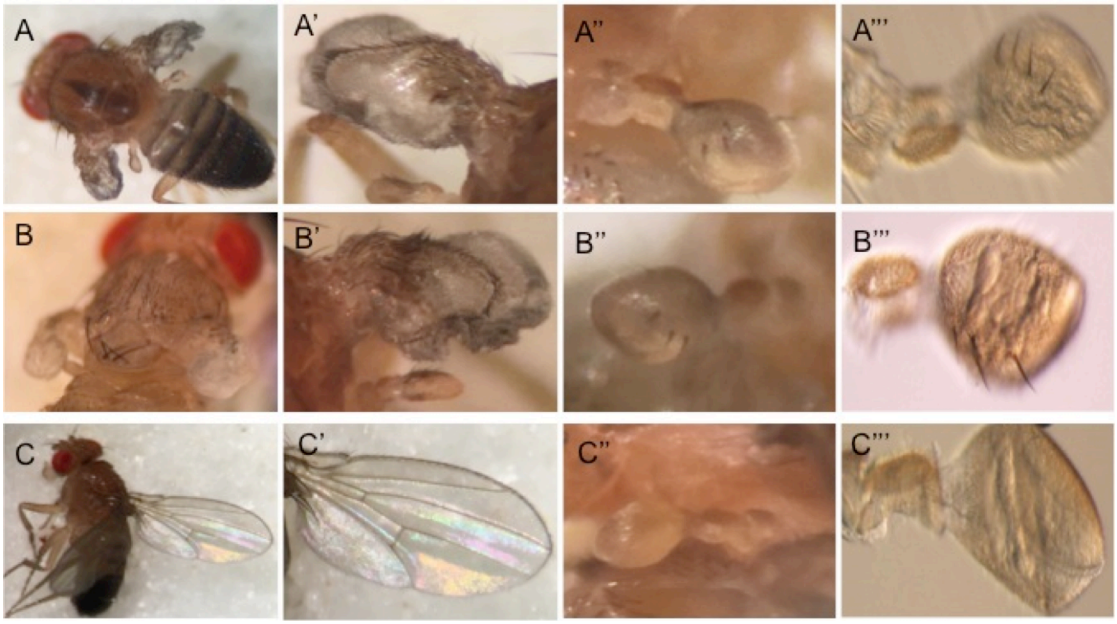


Figure 3.6 Ectopic *scro* expression in the wing pouch leads to transformation of halteres to wings. (A, A') *MS1096-Gal4/+;;UAS-scro/+* show reduced wing phenotype with presence of bristles on the halteres (A'' and A''') that resemble wing tissue. (B-B''') *MS1096-Gal4/+; UAS- scro* $^{\Delta TN}$*/+* show reduced wing and altered halteres (C-C''') MS1096-Gal4/+ show normal wing and haltere phenotype.

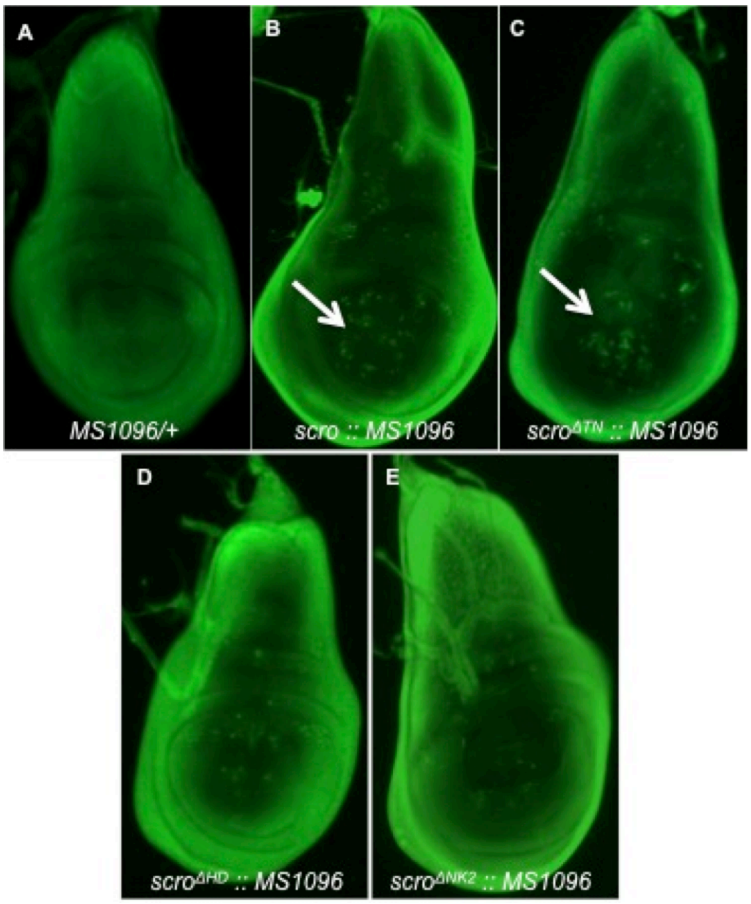


Figure 3.7 Overexpression of *scro* leads to increased apoptosis in the developing wing. (A) *MS1096-Gal4/+*, (B) *MS1096-Gal4/+;;UAS-scro/+*, (C) *MS1096-Gal4/+;UAS-scro $^{\Delta TN}$/+*, (D) *MS1096-Gal4/+;UAS-scro $^{\Delta HD}$/+*, (E) *MS1096-Gal4/+;; UAS-scro $^{\Delta NK2}$/+*. B and C show increased AO staining shown by brighter spots (arrow indicating apoptosis).

Development of the genital disc requires genetic interaction between homeotic gene *Abdominal-B* and sex determination gene *doublesex*. Homeotic genes *abd-A* and *Abd-B (I)* specify different parts of segment A8, while *Abd-B (II)* specifies segment A9. Dsx regulates both growth and differentiation by modulating homeotic genes in the genital primordia (Keisman et al., 2001).

We ectopically expressed *scro* and drove its expression utilizing *dsx-Gal4* and examined the adult flies. 25% (n=50) of the adult male flies had abnormally positioned terminalia (Figure 3.8B) whereas 75% of them show no external genitalia. Figure 3.8B shows the anal region represented as A and penis as P and the rotation is 90 degrees as compared to the control (Figure 3.8C). The position of the genitalia and analia occurs during pupal development. Interestingly, these flies lack sex combs on the first pair of legs. We also dissected the testis and observe arrested development of the testis, as the adult testis resembles larval gonads.

Doublesex male form (Dsx^M) is required to form male specific structures and is crucial for sex comb (comb like structure on the basotarsus) formation on the first pair of legs in the adult male flies (Marin and Baker, 1998). We dissected the testis from the adult male flies and saw structures resembling male gonads seen at the larval stage. We ectopically expressed *scro-TN* deletion transgene in dsx cells and found complete absence of male terminalia and the male flies showed female like terminalia. In addition, the male flies had weakly stained dorsal cuticle plates (sterni) and no sex combs on the foreleg. The adult male testis resembled larval male gonads.

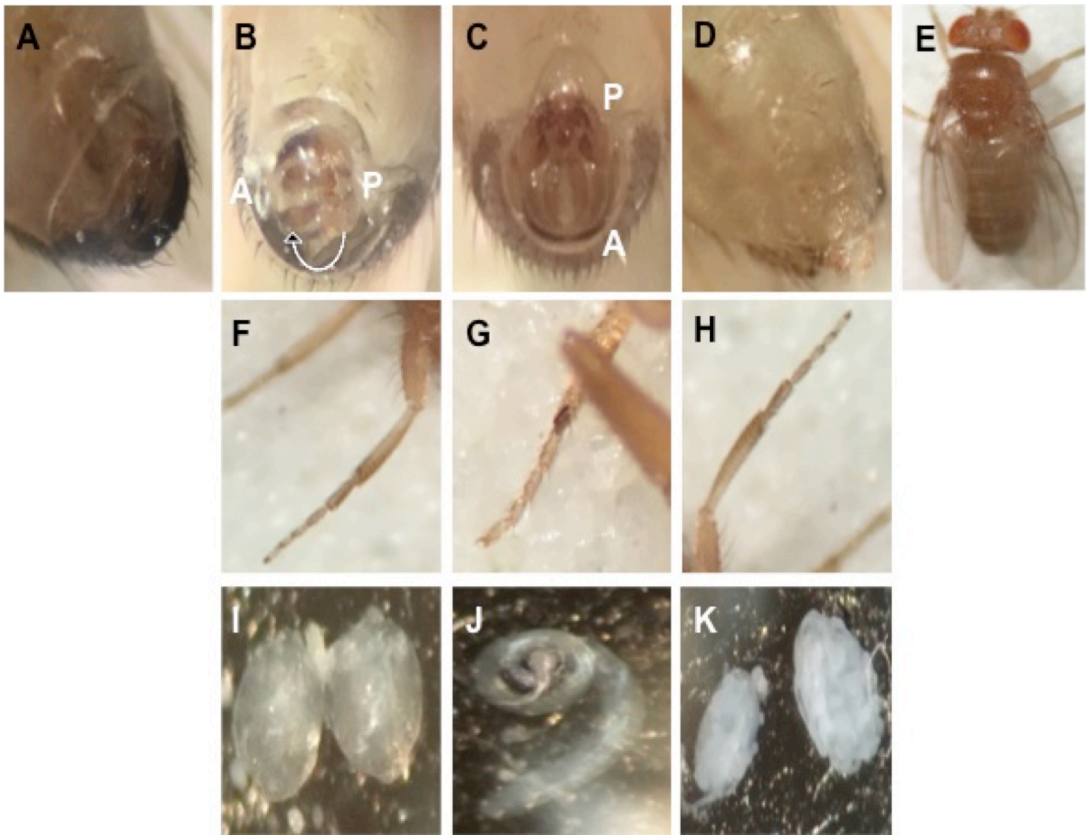


Figure 3.8 Overexpression of *scro* leads to abnormal terminalia. (A and B) *UAS-scro/dsx-Gal4* shows abnormal rotation of the terminalia whereas normal terminalia is seen in *dsx-Gal4/+* (C). *UAS-scro* $^{\Delta TN}$*/+; dsx-Gal4* flies show complete absence of male terminalia and show similarity to female external genitalia (D). However, the male fly shows darker abdominal segments (E). *UAS-scro/dsx-Gal4 and UAS-scro* $^{\Delta TN}$*/+; dsx-Gal4* flies lack sex combs on the first pair of legs (F and H) as compared to *dsx-Gal4/+ flies* (G). Both *UAS-scro/dsx-Gal4 and UAS-scro* $^{\Delta TN}$*/+; dsx-Gal4* flies show arrested development of the testis (I and K respectively) as compared to normal adult testis (J).

Female flies did not exhibit any abnormality. However, loss of homeodomain and NK2 domain showed no abnormal phenotype. These results suggested that ectopic *scro* expression modulates Dsx^M function. To test if *scro* regulates dsx^M, we extracted RNA from whole adult male flies of the genotype *UAS-scro/dsx-Gal4; UAS-scro*$^{\Delta HD}$*/dsx-Gal4 and UAS-scro/+; UAS-scro/dsx-Gal4*. We performed RT-PCR using primers designed for dsx^M transcripts. However, we did not observe a downregulation of dsx^M in *scro::dsx* flies as compared to the control (Figure 3.9).

Based on our observations, we hypothesize that *scro* modulates Dsx^M probably by interacting with another protein to regulate Dsx^M. Further experiments would be able to provide a clear picture on how *scro* is able to modulate Dsx^M to affect formation of male specific structures. Preliminary analysis using *scro-Gal4,* we observed *scro* expression in adult testis (Figure 3.10) indicating it plays a role in testis development.

Discussion

Before initiating metamorphosis, *Drosophila* larval tissue or imaginal disc undergo an increase in mass, size and development with the help of genetic and external environmental signals. Regulating organ size and shape rely on territorial specification in addition to cell proliferation and differentiation. In this work, we tested the effect of overexpression of *scro* in three different tissues.

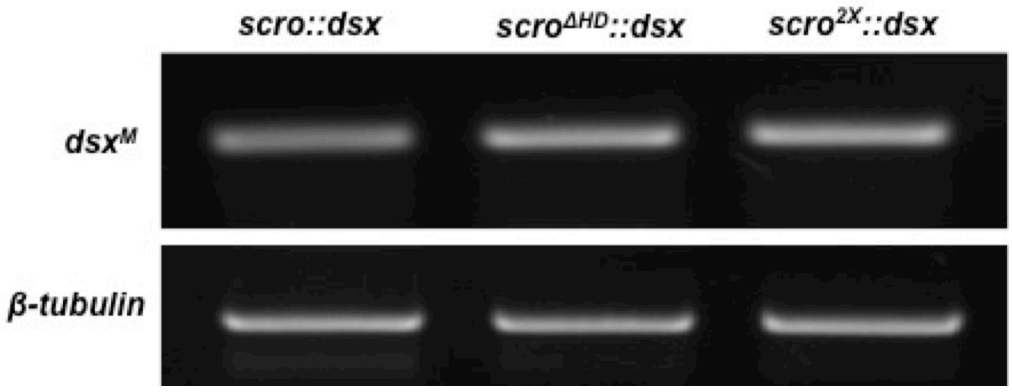


Figure 3.9 SCRO does not downregulate transcription of *dsx^{M}*. The top panel represents RT-PCR products derived from *UAS-scro/dsx-Gal4; UAS-scro$^{\Delta HD}$/dsx-Gal4 and UAS-scro/+; UAS-scro/dsx-Gal4*. Bottom panel shows *β-tubulin* as a loading control.

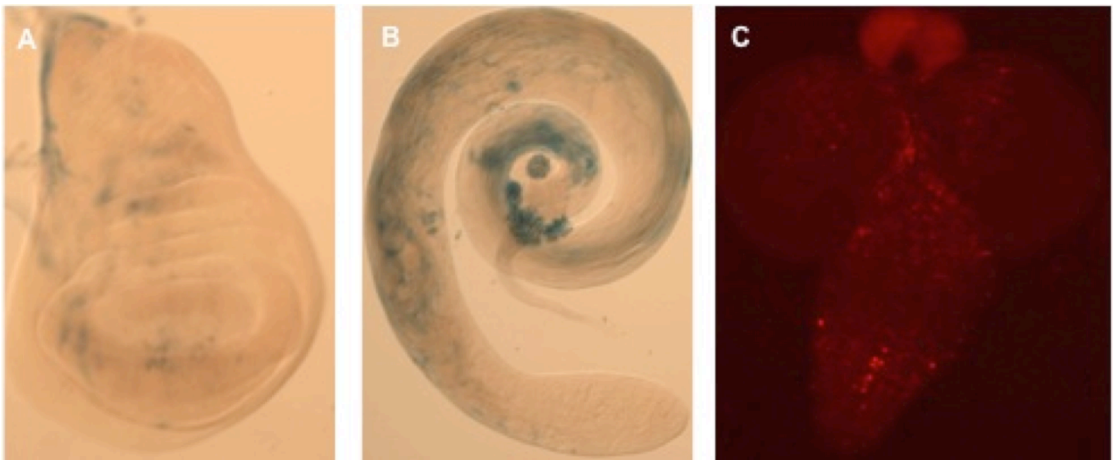


Figure 3.10 Expression pattern for *scro* in different tissues. (A) β-galactosidase staining reveals expression of *scro* in the wing pouch (B) adult male testis. (C) Expression of *UAS-RedStinger* (nuclear DsRed reporter) using *scro-Gal4* in the larval CNS.

Ectopic expression of *scro* led to an overproliferation phenotype in the adult eyes, and what initially looked like apoptotic phenotype. Similar phenotype was observed for N and C-terminal deletions of *scro*. However, there were approximately 30% of the flies that could be rescued by expression of *P35*, a caspase inhibitor. This phenotype could be explained by apoptosis that is independent of caspase accompanied by overproliferation. These results also suggest that the phenotype observed could be an effect of ectopic *scro* on its own, or that it likely forms heterodimer with bHLH protein that could be necessary for cell proliferation. Previously, it has been shown that at stage 14 in the *Drosophila* embryos, *scro* is expressed cells anterior to the cells that will form the optic lobe (Zaffran et al., 2000). This could explain the overexpression phenotype we observe for *scro* and indicates regulation of genes important in patterning the developing eye.

In addition to the eye imaginal disc, we tested if *scro* had a role in wing patterning or development. When we tested for *scro* expression using *scro-Gal4*, we found *scro* is expressed in the wing imaginal disc with most of the staining in the wing pouch. Ectopic expression of *scro* using *en-Gal4* showed a severe phenotype. Engrailed is a segment polarity gene involved in a multitude of processes and that explains the severe phenotype. However, using *dpp-Gal4* that affects wingless gene expression, we observed reduction of wing size. Furthermore, increasing dosage of *scro* led to truncated wings and legs. *Decapentaplegic* is a morphogen crucial for patterning imaginal disc that form organs in the adult fly and that explains that *scro* might play a crucial role in regulating patterning genes.

Using *MS1096-Gal4* that drives expression in the wing pouch, we expressed *scro* in a larger area in the wing imaginal disc. Interestingly, overexpression led to severe reduction in the wing tissue, however wing margins were still intact. When stained with acridine orange, an increased number of cells were stained indicative of apoptosis. This phenotype was also observed with deletion of N-terminal TN domain, in addition to loss of bristles in the mesothorax. Massive cell death alone after ectopic *scro* expression should not lead to this severe wing phenotype indicating *scro* might target genes that play a role in wing patterning. We also observed transformation of the halteres to wing, with the halteres developing wing like bristles usually not seen in wild type. This is extremely interesting as loss of function of *Ultrabithorax* (*Ubx*) leads to this transformation and has been previously reported for *Ubx* mutants (Weatherbee et al., 1998) and microRNA-iab4 that interferes with the *Ubx* locus (Ronshaugen et al., 2005).

In *Drosophila,* pole cells and somatic cells form the gonads. Pole cells give rise to germ line and mesoderm of abdominal segments 5-8 gives rise to soma. Formation of the gonads depends on *abdominal-A* (*abd-A*), a homeotic gene and if *abd-A* is removed the other genes of the Bithorax complex namely *Ubx* and *Abd-B* cannot substitute for development of the gonads (Greig and Akam, 1995). Overexpression of *scro* affects gonad development in cells that express sex determination gene *doublesex*. They also show developmental arrest of adult male testis that resembles larval gonads. Deletion of the N-terminal TN domain shows a more dramatic phenotype with adult male flies showing no external genitalia. In addition to this using *scro-Gal4*, we found *scro*

expression in adult male testis. Based on these results, *scro* does seem to have a role in gonad development.

We observed two phenotypes that were specifically interesting, transformation of the halteres to wing and development of gonads. Transformation of the halteres to wing indicates a role in downregulation of *Ubx* and development of the gonads probably indicates regulation of *abd-A*. However, the mechanism of how *scro* regulates both *Ubx* and *abd-A* is not clear. Bithorax Complex encodes homeotic genes *Ubx*, *abd-A* and *abd-B* in addition to noncoding RNAs. One of them is *miR-iab-4-5p* homologous to the Hox gene *miR-196* in vertebrates and has been previously shown to downregulate *Ubx* and cause homeotic transformation of haltere to wing (Ronshaugen et al., 2005). The iab-4 locus that encodes this microRNA regulates *abd-A* expression as well (Karch et al., 1994). We found the gene *scro* has been predicted to interact with miR-iab4 (Murali et al., 2011). The phenotype observed for overexpression of *scro* and *miR-iab4* is similar. Hence, we propose a model based on the preliminary evidence that *scro* might control miR-iab4 locus and hence attenuates *Ubx* and *abd-A* leading to transformation of halteres and developmental arrest in the gonads.

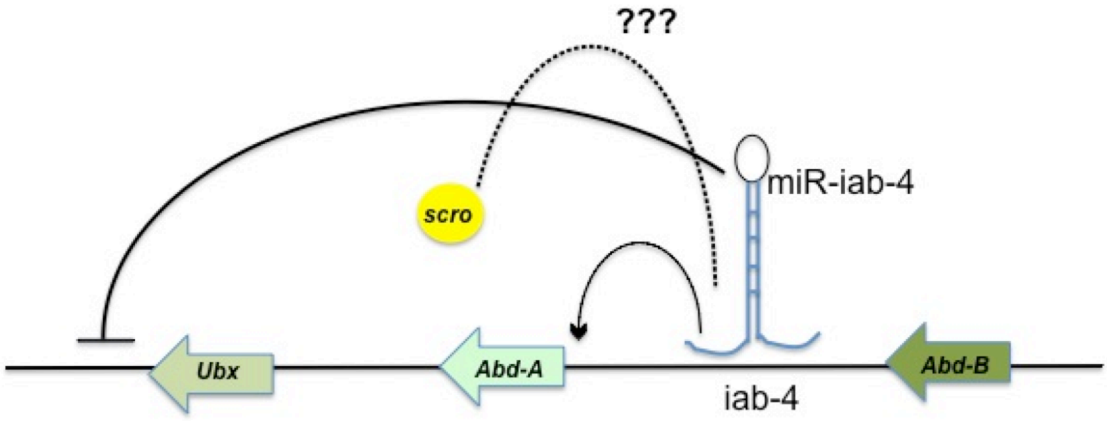


Figure 3.11 Hypothetical model for the role of *scro* in regulating Bithorax complex (BX-C) Based on the predicted interaction between *miR-iab-4* and *scro*, we propose that both of these form a complex to attenuate *Ubx* in the halteres leading to the haltere to wing transformation. It has been previously shown that miR-iab-4 influences *Abd-A* and *Abd-B* expression that controls genital disc development.

CHAPTER 4: TGF- β SIGNALING IN PIGMENT DISPERSING FACTOR (PDF) EXPRESSING SMALL VENTRAL LATERAL NEURONS

Abstract

TGF-β signaling controls many fundamental processes including nervous system development. The molecular mechanisms involved in establishment and changes in neuronal connections are not well understood. In the *Drosophila* circadian cluster, the small ventral lateral neurons (s-LNvs) play a crucial role in maintaining circadian rhythmicity. These neurons in addition to the large ventral lateral neurons express a neuropeptide pigment-dispersing factor (PDF). Here we demonstrate that type I receptor babo mediated TGF-β signaling plays a central role in development of the s-LNvs. We find that elimination of the Activin/TGF-β type I receptor babo isoform-a leads to downregulation of *Pdf* thus modulating the endogenous circadian period. This modulation is in a cell-autonomous manner. The knockdown of $babo_a$ in the clock neurons causes arrhythmicity and is similar to the *Clk* mutant. Elimination of the downstream transducer *dSmad2* causes misrouting of the dorsal projections emanating from the s-LNv neurons indicating of downregulation of *Pdf* in these neurons. The TGF-B pathway activation seems to be significant for maintaining rhythmicity and we hypothesize that it does so by transcriptionally regulating *Clk*.

Introduction

The canonical transforming growth factor-beta (TGF-β) pathway has been well studied with extracellular ligands forming a complex with transmembrane receptors to regulate transcription of target genes involved in cell proliferation, cell differentiation, cell death and various morphogenetic processes during development (Derynck and Akhurst,

2007). Cytokines of the TGF-β superfamily have been subdivided into TGF-βs, bone morphogenetic proteins (BMPs) and activins based on sequence similarity and consist of more than 30 secreted proteins (Feng and Derynck, 2005). There are common features in their signaling cascade wherein the receptors are serine-threonine kinases named type I and type II receptors that are ligand induced. The type II receptor kinases bind the ligand, which then phosphorylates the GS domain within the type-I receptor. Thus the active receptor complex phosphorylates two serines in the C-terminal SSXS motif of the receptor-regulated smad (R-Smad) proteins. This phosphorylation is essential for interaction with a co-smad as well as translocation to the nucleus to regulate target gene expression (Chen et al., 1996; Labbe et al., 1998; Yanagisawa et al., 1999).

In *Drosophila*, several members of the TGF-β superfamily have been identified. Decapentaplegic (Dpp), Screw (Scw), and Glass bottom boat (Gbb) belong to the BMP family and have been shown to specifically signal through type-I receptors Thickveins (Tkv) and Saxophone (Sax), whereas dActivin (dAct), Dawdle (Daw), Myoglianin (Myo), and Maverick (Mav) are members of Activin/TGF-β branch and propagate signal through only one type-I receptor, Baboon (Babo). Both subfamilies share the type II receptors: Punt (Put) and Wishful thinking (Wit)(Raftery and Sutherland, 1999). Smad2 (Smox) is the major R-Smad in *Drosophila* that is involved in the TGF- β signaling and is homologous to Smad2 and Smad 3 in vertebrates. The R-Smad involved in the BMP pathway is Mothers against dpp (Mad) and is related to vertebrate Smad1 and Smad 5. Interestingly, both the BMP and TGF- β pathways share a common co-Smad Medea

similar to Smad4 in vertebrates (Parker et al., 2004; Raftery and Sutherland, 1999).

Both activin/TGF- β pathways have been well characterized in vertebrate neurogenesis with important roles in development of post-mitotic neurons and in modulation of synapse (Krieglstein et al., 2011). In the majority of the mutants studied in *Drosophila*, a significant role of the TGF- β pathway in neuronal proliferation, wiring, axon guidance and remodeling of neurons during metamorphosis has been found (Parker et al., 2006; Serpe and O'Connor, 2006; Zheng et al., 2003; Zheng et al., 2006) in addition to its role in neuroblast proliferation in the larval brain (Zhu et al., 2008).

A key to neuronal assembly and communication is anterograde (communication from neurons to their postsynaptic targets) and retrograde (communication from target cells to the presynaptic neurons) signaling (Fitzsimonds and Poo, 1998). BMP is a well-conserved retrograde signaling pathway with receptors present on the presynaptic membrane influencing synaptic connectivity. This pathway has been well studied at the larval neuromuscular junction in *Drosophila* (Marques et al., 2002; McCabe et al., 2003). A significant finding of the presence of BMP signaling pathway in the small ventral lateral neurons in *Drosphila* brain was recently reported where activation of the pathway components caused lengthening of the circadian period (Beckwith et al., 2013). However, no role for TGF-β signaling in circadian clock in *Drosophila* has yet been reported.

The central clock in *Drosophila* is composed of two transcriptional feedback loops with genes *period* (*per*) and *timeless* (*tim*) being activated by Clock (CLK) and Cycle (CYC) and in turn these protein products negatively regulate *Clk* in the first loop. In the second loop, CLK and CYC activate the transcription of Vrille (VRI) and Pdp 1ε. VRI is a repressor of *Clk* whereas Pdp1ε activates *Clk*. The transcriptional and translational regulation of these central clock molecules gives rise to a 24-hour circadian period (Hardin, 2011). In addition to these interlocked feedback loops, CLK and CYC compete with clockwork orange (Cwo) to bind and regulate transcription of *per* and *tim* (Kadener et al., 2007; Matsumoto et al., 2007). Among the approximately 150 clock neurons that express the central clock components, the small ventral lateral neurons (s-LNvs) are considered to be core pacemaker neurons (Ewer et al., 1992; Helfrich-Forster, 1998; Peng et al., 2003; Renn et al., 1999). These neurons in addition to the large ventral lateral neurons (l-LNvs) express the neuropeptide pigment-dispersing factor (PDF) in adult *Drosophila* brain.

The autoregulatory feedback loops are well conserved with CLK and BMAL1 activating transcription of *per* and *cryptochrome* (*CRY*), which in turn negatively regulates CLK and BMAL1 in mammals (Ko and Takahashi, 2006). So far, the role of TGF-β/activin signaling in the circadian clock has only been reported in mammals. This signaling pathway is capable of resetting the circadian clock independently of *Per* and instead resets the clock through induction of *Dec1* (Kon et al., 2008). *Dec1* is a homolog of *clockwork orange* (*cwo*) in *Drosophila*. In this work, we have looked into TGF-β signaling in the *Drosophila* with respect to its role in setting the circadian period in PDF

neurons and also its role in the development of PDF neurons.

Materials and Methods

Fly strains

Flies were maintained on a standard cornmeal-yeast-agar medium at 25°C. The following lines were used in this study: *babo*^{fd4} allele, *babo*^{Df}, UAS-*babo (CA)*(Brummel et al., 1999), UAS-*babo*-*a*-miRNA, UAS-*babo*-*b*-miRNA, UAS-*babo*-*c*-miRNA (Awasaki et al., 2011), UAS-*punt* RNAi, UAS-*wit* RNAi, UAS-*dSmad2* RNAi, UAS-*medea* RNAi (generous gifts from Michael O'Connor) *pdf-GAL4* (Park et al., 2000), *tim-Gal4*, *tim-Gal4; pdfGal80* from M. Rosbash (Brandeis University), 1118-Gal4 (Blanchardon et al., 2001). For experiments using *babo*^{fd4}, *babo*^{Df}, *Smox*^{f4} alleles (Peterson et al., 2012), flies were allowed to lay eggs on grape juice agar plates supplemented with yeast as it has been previously shown that the larvae do not grow well on standard medium (Ghosh and O'Connor, 2014).

Locomotor Activity Assay

The locomotor activity of individual male flies was measured using Drosophila Activity Monitors (Trikinetics) and analyzed using ClockLab software (Actimetrics). Briefly, three-five day old flies were entrained to 12: 12 LD cycles for 4 days and then subjected to constant darkness for 7 days. Clocklab software generates chi square periodograms with significance that is set to $\alpha = 0.05$ and only flies with $\chi^2 \geq 10$ were used to analyze period.

Immunohistochemistry

Fly brains were dissected and fixed in 4% paraformaldehyde, 7.5% picric acid and phosphate buffer (0.1 M, pH 7.4) for 2 h at room temperature. Fixed tissues were washed in phosphate buffer followed by TNT (0.1 M Tris-HCl, 0.3M NaCl, 0.5% Triton X-100). The brains were blocked in 5% normal donkey serum (Jackson ImmunoResearch Laboratories) and subsequently incubated with primary antibody [rat anti-PDF (1:300)] at 4°C overnight. After washing with TNT, the brains were incubated with TRITC- or FITC-tagged secondary antibody at 1:200 for 1 h at room temperature. Following this, the brains were washed three times with TNT followed by phosphate buffer before being mounted in a quenching medium (0.5% n-propyl gallate in 90% glycerol and 10 mM phosphate buffer, pH 7.4). Fluorescent signals were captured using Olympus BX-61 microscope equipped with a CCD camera.

Results

Knockdown of Type I receptor babo$_a$ in PDF neurons causes circadian arrhythmicity

As a type-I receptor in the activin pathway, baboon (babo) regulates axon guidance in the embryo (Serpe and O'Connor, 2006) and neuron proliferation in the larval brain in addition to cell proliferation in imaginal disks (Brummel et al., 1999). We decided to look at the effect of knockdown of Type I receptor babo in PDF neurons. There are three different isoforms of babo (a, b and c) and they differ only in their extracellular ligand-

binding domains. They are expressed in different larval tissues emphasizing how tissues discriminate among the different ligands. The isoform $babo_a$ is majorly expressed in the brain whereas both $babo_a$ and $babo_b$ are expressed in the wing imaginal disc. The gut and fat body in larvae show the presence of isoform $babo_c$ (Jensen et al., 2009).

We tested the role all three isoforms of babo using targeted induction of miRNA depleting each of the isoforms (Awasaki et al., 2011) in the PDF neurons. We used four different GAL4 lines namely, *Pdf-80di gal4*, *Pdf-gal4*, *1118-Gal4* and *tim-Gal4* and performed *in situ* hybridization and immunohistochemistry to check for change in Pdf expression. As shown in the control (Figure 4.1A and A') Pdf is expressed both in the l-LNvs and s-LNvs in the adult brain. Depleting $babo_a$ isoform using Pdf-gal4 leads to detection of 2±1 s-LNvs (n=8) and all the 4 l-LNvs (Figure 4.1C and C'). When we used an enhancer trap Gal4 line, 1118 Gal4 that has expression in the PDF expressing ventral lateral neurons (Blanchardon et al., 2001), we could detect PDF expression in the l-LNvs but weaker PDF expression in 1± 2 s-LNvs (n=6) (Figure 4.1D and D').

In addition, we knocked down *babo-a* using a stronger Pdf-80di-Gal4 that includes a *Pdf* regulatory element (PRE) that drives PDF expression in the lateral neurons (Chapter 2 of this dissertation). Using this driver, we detected PDF expression in the l-LNvs but not in the s-LNvs indicated both by immunohistochemistry and *in situ* hybridization (Figure 4.1B and B'). Lastly, using *tim-Gal4*, a broad Gal4 driver also expressed in the PDF neurons, we detect PDF expression in all the 4 l-LNvs (Figure 4.1D and D') but not the

s-LNvs. These results strongly indicate transcriptional downregulation of *Pdf* in the s-LNvs suggesting a possible role for TGF-β signaling in these neurons.

Several studies have demonstrated s-LNvs as circadian pacemaker neurons essential for locomotor behavior (Grima et al., 2004; Lin et al., 2004; Peng et al., 2003; Renn et al., 1999). Hence, we performed locomotor behavior assay to determine if knockdown of $babo_a$ results in circadian arrhythmicity (Figure 4.2 and Table 4.1). Indeed under the control of *Pdf-Gal4* only 4 out of 25 flies were rhythmic with a period of $\tau = 24.75 \pm 1.44$ as compared to wild type flies (CS) which had a period of $\tau = 24.34 \pm 0.29$ (n=25). Whereas, under the control of *tim-gal4* flies were completely arrhythmic (n=24). Since lack of immunostaining in sLNvs is characteristic of a semi-dominant *Clock* mutant (Park et al., 2000), we compared the behavior of $babo_a$ knockdown in clock neurons to Clk^{JRK}. Under constant conditions, the *mi-*$babo_a$*:: tim* flies are completely arrhythmic similar to the circadian phenotype reported for Clk^{Jrk} (Allada et al., 1998). Clk^{Jrk} flies also exhibit abnormal rhythms under light-dark conditions and this is also true for the *mi-*$babo_a$*:: tim* flies. In addition to not detecting *Pdf* mRNA and PDF immunoreactivity in the s-LNvs, we also noticed abnormal dorsal projections as well as loss of optic lobe projections. In wild type flies, axonal projections from s-LNvs terminate in the dorsal protocerebrum.

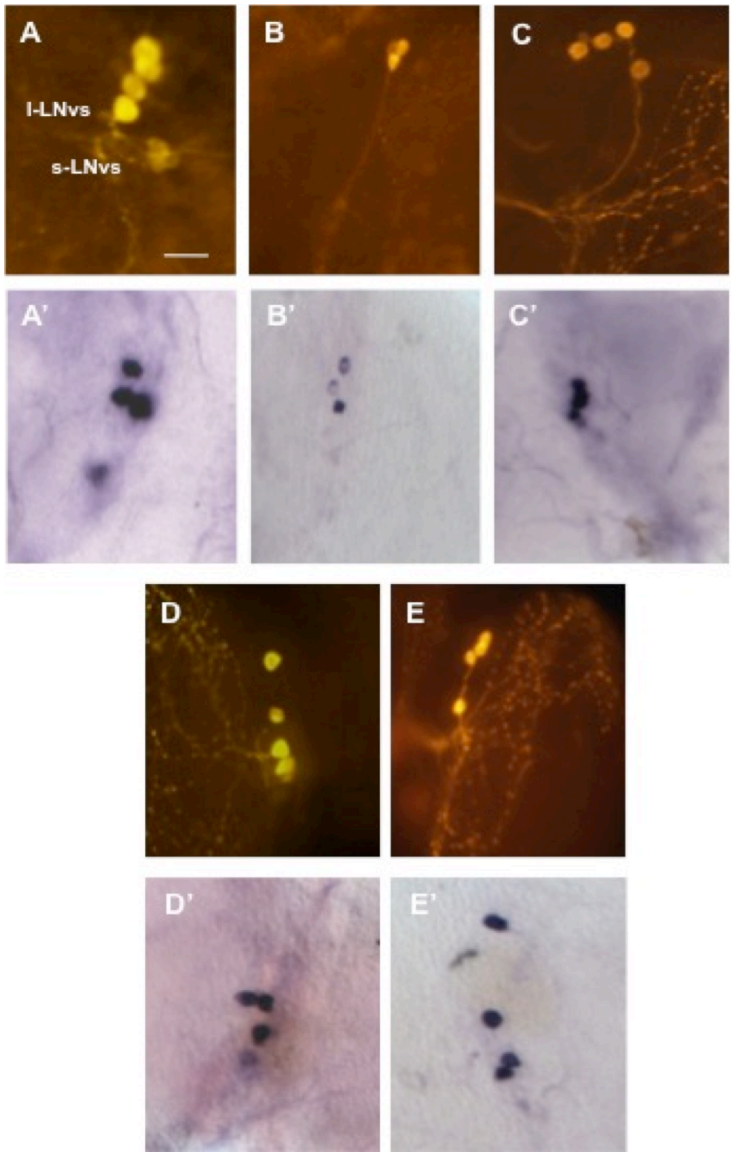


Figure 4.1 Expression of *Pdf* in response to knockdown of type I receptor *babo*$_a$.

(A-E) Pdf immunohistochemistry. (A'-E') *In situ* hybridization using *Pdf* probe in the adult brain. (A, A') Canton-S (n=6); (B, B') *Pdf-80D Gal4/+;; UAS-miRNA-babo*$_a$ /+ (n=8)*;* (C, C') yw; *Pdf-Gal4/+; UAS-miRNA-babo*$_a$/+ (n=8)*; (*D, D') *y w;; 1118-Gal4/ UAS-miRNA-babo*$_a$ (n=8); (E, E') yw; tim-*Gal4/+;; UAS-miRNA-babo*$_a$/+].

However, lack of expression in the s-LNvs when $babo_a$ is depleted in clock neurons indicates that these projections do not arise from the s-LNvs. This phenotype was previously noted in Clk^{Jrk} mutants (Park et al., 2000).

To further confirm if knockdown of $babo_a$ transcriptionally downregulates *Pdf* we looked at PDF immunoreactivity in *babo* mutants. The $babo^{fd4}$ / cyo, gfp allele lacks kinase domain (Zheng et al., 2003) whereas $babo^{Df}$ */ cyo, gfp* is a deficiency line that deletes the *babo* gene. Since both of these lines were not homozygous viable, we set up a cross between these two lines and selected for non-gfp trans heterozygous larvae either at L1 or L2 stage. These larvae were then allowed to grow on yeast paste and their larval CNS was stained for PDF. There was no PDF expression detected in the larval lateral neurons with remnants of dorsal projections stained indicating that type I receptor baboon plays a role in transcriptionally regulating *Pdf* (Figure 4.3). It is more likely that the TGF-β signaling might play a role in transcriptionally *Clk* that in turn affects *Pdf*.

Knockdown of baboon-b and c isoform did not affect *Pdf* expression and circadian rhythmicity

We tested two other *babo* isoforms $babo_b$ and $babo_c$ using Gal4 drivers *Pdf-Gal4* and *tim-Gal4*. Knocking down both these isoforms did not affect PDF immunoreactivity nor did they show any abnormal circadian phenotype (Figure 4.3 A-D and Table 4.1). This was expected, as $babo_a$ is the isoform that is mostly expressed in the brain (Jensen et al., 2009).

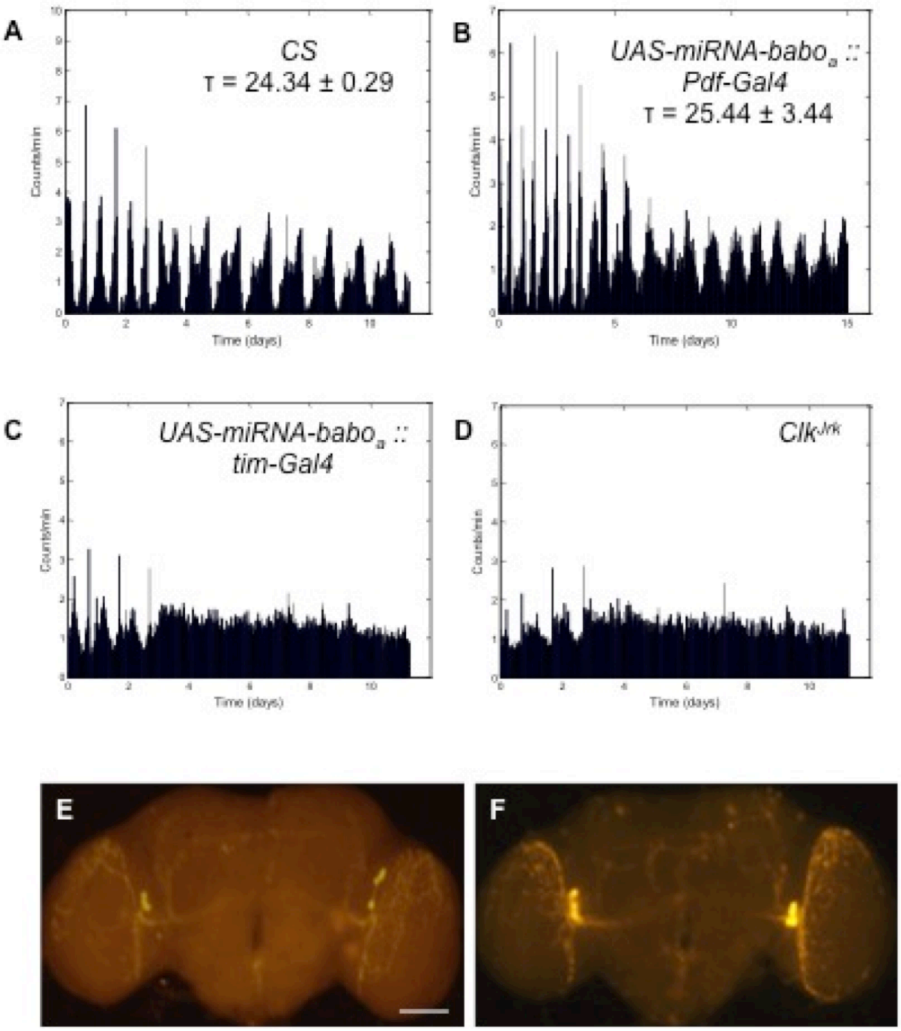


Figure 4.2 Knockdown of *babo$_a$* isoform leads to lack of PDF expression in the s-LNvs and arrhythmicity. Locomotor activity of the wild type flies (A) in comparison to the *Pdf-Gal4/+; UAS-mi-babo$_a$/+* (B) with just 4 flies out of 25 exhibiting rhythmic behavior under constant conditions. Arrhythmic behavior under constant conditions was observed in *tim-Gal4/+; UAS-mi-babo$_a$/+* (C) and *Clk^{Jrk}* (D). PDF immunoreactivity and abnormal dorsal and optic lobe projections was seen in *tim-Gal4/+; UAS-mi-babo$_a$/+* (E) *and Clk^{Jrk}* (F).

However, knockdown of *babo$_b$* and *babo$_c$* in the ventral lateral neurons using both the Gal4 drivers resulted in misrouting phenotype in n=7 adult brains (Figure 4.3A and C respectively) probably indicating that these isoforms may have a role in development of the s-LNv neurons. These observations indicate that transcriptional regulation of *Pdf* is only through one isoform of the Type I receptor and that the other two isoforms are important for fasciculation of the s-LNv axonal bundle and for acquisition of proper shape.

Cell autonomous regulation of *Pdf* by Type I receptor *babo$_a$* knockdown

We observed significant downregulation of *Pdf* after knocking down *babo$_a$* in the clock neurons using *tim-Gal4*. Since *tim-Gal4* drives expression in a broader set of neurons apart from the ventral lateral neurons, there is a possibility that downregulation occurs in a non-cell autonomous manner. To test this possibility we used *Pdf-Gal80* combined with *tim-Gal4* (Stoleru et al., 2004). This ensured Gal4 expression only in TIM positive and PDF negative neurons. As compared to the control, PDF immunoreactivity was restored in all the l-LNvs and s-LNvs (Figure 4.4) though not all the optic lobe projections were intact. These results provide evidence for LNv specific downregulation by Type I receptor babo$_a$.

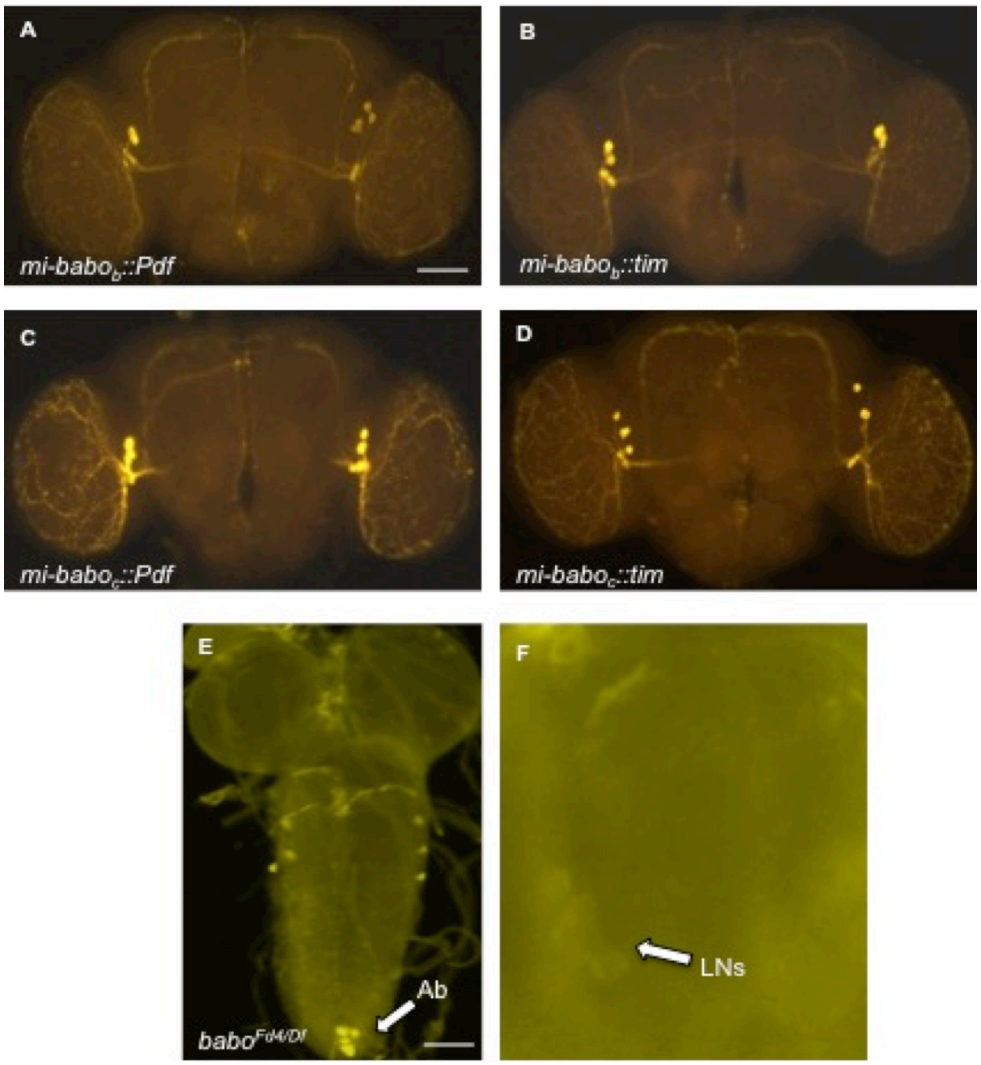


Figure 4.3 Knockdown of *babo$_b$* and *babo$_c$* led to misrouting phenotype. PDF immunostaining for the genotypes (A) *Pdf-Gal4/+; UAS-mi-babo$_b$/+;* (B) *tim-Gal4/+; UAS-mi-babo$_b$/+;* (C) *Pdf-Gal4/+; UAS-mi-babo$_c$/+* and (D) *tim-Gal4/+; UAS-mi-babo$_c$/+*. (E) Immunoreactivity for PDF in *babo^{Fd4}/babo^{Df}* larval brains shows weak staining in LNs (F) indicated by an arrow as compared to the PDF staining in the abdominal neurons (Ab) in the ventral nerve cord (E) indicated by an arrow.

A constitutively active form of babo causes overgrowth of s-LNv axonal projections

We overexpressed a constitutively active form of the babo receptor to further explore the role of this Type I receptor in the s-LNvs. Constitutive activation of babo has been shown to be involved in cell proliferation and overgrowth of wing discs (Brummel et al., 1999). Overexpression of the constitutively active form of the receptor in the PDF positive neurons resulted in the s-LNv projections not terminating in the dorsal protocerebrum but instead continued to grow. However, when expressed in the clock neurons using *tim-Gal4* there was no aberrant growth phenotype (Figure 4.4).

Punt and Wit play a role in the development of s-LNv neurons

Type I receptors require activation by Type II receptors to further get recognized by R-Smads (Chen et al., 1996; Labbe et al., 1998; Yanagisawa et al., 1999). Hence, we decided to test whether type II receptors Punt or Wit function to activate type I receptor babo. The gene *wishful thinking* (*wit*) is a homolog of BMP type II receptor in vertebrates and is known to mostly function as a presynaptic receptor at the neuromuscular junction in *Drosophila* (Marques et al., 2002). Recently, it was reported that Wit also functions in epithelial cell development in oocytes (Marmion et al., 2013). We tested for the role of *wit* in PDF neurons using *Pdf-Gal4* and *tim-Gal4* by using *wit* RNAi lines. Knocking down *wit* did not affect PDF immunoreactivity, however the staining intensity in the dorsal projections was weak (Figure 4.5A and A').

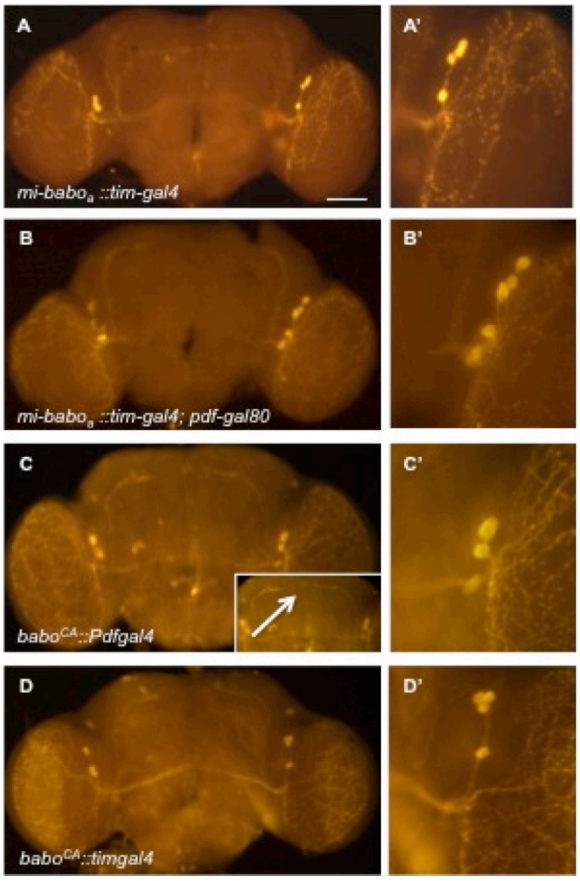


Figure 4.4 Cell autonomous role of *babo$_a$* in the PDF positive neurons. Presence of PDF immunostaining in the s-LNvs with the genotype (A) *tim-Gal4/+; UAS-mi-babo$_a$ /+* as compared to that of (B) *tim-Gal4/+; UAS-mi-babo$_a$ /pdf-gal80.* Overexpression of constitutively active babo receptor leads to overgrowth of the s-LNv dorsal projections when expressed in the PDF neurons (C) *Pdf-Gal4/+; UAS-babo^{CA}/+* whereas no aberrant phenotype was observed in flies with the genotype (D) *tim-Gal4/+; UAS-babo^{CA}/+.*

Interestingly, knockdown of *wit* in the clock neurons led to misrouting phenotype (Figure 4.5B and B'). We used *punt RNAi* line and drove it in PDF positive lateral neurons and detected 2±1 s-LNvs (n=8) with weaker staining in the dorsal projections (Figure 4.5D and D'). However, when *punt* was depleted in the clock neurons, we observed severe misrouting of the s-LNvs with no terminating dorsal projections (Figure 4.5D and D'). These data clearly indicate that probably both *wit* and *punt* play a role in development of PDF neurons. Knocking down led to misrouting of the s-LNv projections with *punt* depletion causing a stronger phenotype. This suggests that *punt* is more likely involved in maintaining axonal shape and at some point *punt* strongly influences *Pdf* downregulation enough to cause misrouting.

dSmad2 functions downstream of babo to control development of sLNvs

Drosophila Smad2 (dSmad2) mediates activin signaling and it has been shown previously that baboon signaling phosphorylates dSmad2 (Brummel et al., 1999). When expressed in the PDF neurons, knockdown of *dSmad2* led to misrouting phenotype (Figure 4.6A, A' and A''). However, when knocked down in clock neurons, there was a premature termination of the dorsal projections (Figure 4.6B, B' and B''), contrary to the phenotype when *dSmad2* was depleted in PDF positive lateral neurons. Under type I receptor baboon signaling, dSMad2 gets phosphorylated thus leading to formation of a heterodimer with Medea that is a co-Smad (Brummel et al., 1999). Knockdown of *Medea* in clock neurons is likely to downregulate *Pdf* expression in the s-LNvs. This was deduced from the weakly stained dorsal projections (Figure 4.6C, C' and C''). However, all four s-LNv neurons were detected in the brain samples (n=6).

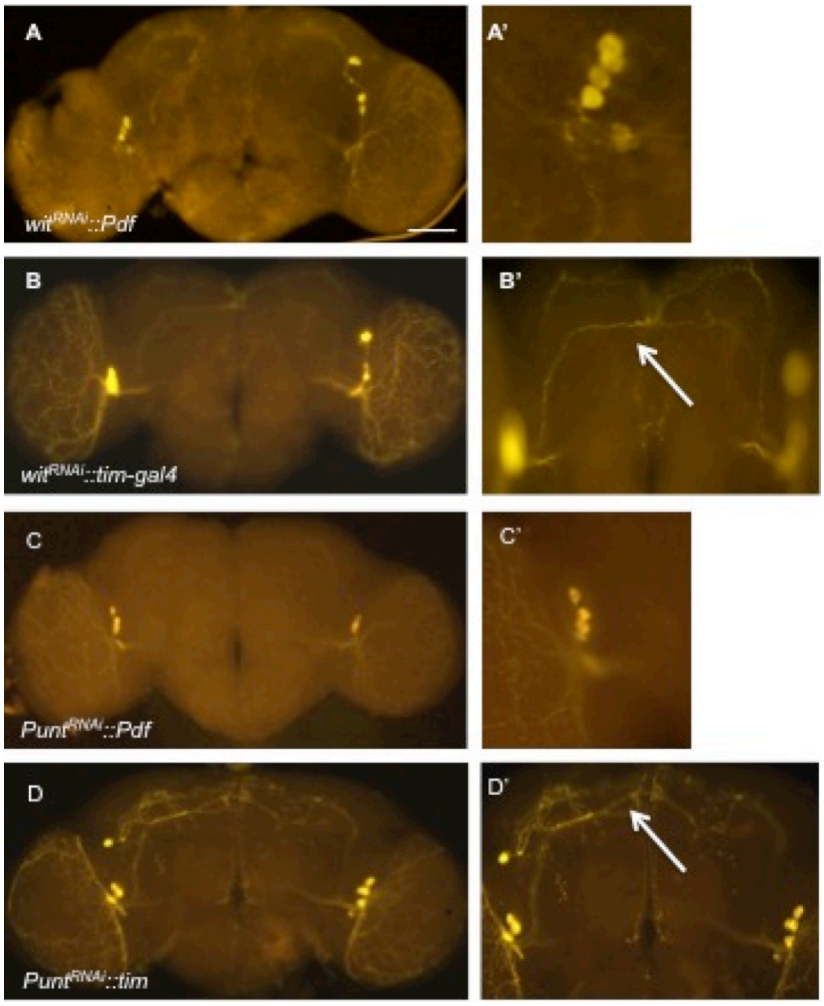


Figure 4.5 Type I receptors *punt* and *wit* affect PDF expression. Depletion of *wit* and *punt* in the PDF neurons led to weaker staining in the s-LNv dorsal projections (A) *Pdf-Gal4/+;UAS-wit*^{RNAi}*/+* (C) *Pdf-Gal4/+; UAS-punt*^{RNAi}*/+* respectively. Knocking down *wit* (B) *UAS-Dcr2/+; tim-Gal4/+; UAS-wit*^{RNAi}*/+* and *punt* (D) *UAS-Dcr2/+; tim-Gal4/+; UAS-punt*^{RNAi}*/+* in the clock neurons led to misrouting with the phenotype being more severe for *punt*.

Interestingly, knockdown of Medea in the PDF positive lateral neurons shows misrouting of the dorsal projections (Figure 4.6D, D' and D'') similar to dSMad2 knockdown (Figure 4.6A, A' and A''). These results clearly suggest that knockdown of dSmad2 and Medea leads to misrouting of the s-LNv axonal projections due to slight downregulation of *Pdf*.

Discussion

TGF-β signaling is highly conserved and mediates cell communication in metazoans with every component of the pathway represented in their genomes (Herpin et al., 2004). In this study, we specifically looked at the activin branch of the TGF- β signaling that acts through Smad2 in *Drosophila*. As compared to vertebrates, *Drosophila* has few ligands, receptors and Smad proteins (Huminiecki et al., 2009). Activin pathway mutants exhibit developmental defects and do not survive past pupal stage (Brummel et al., 1999; Peterson et al., 2012; Zheng et al., 2003) and hence most of the studies involve tissue specific manipulation of pathway components.

Neuronal connectivity and maintenance of functional phenotype of neurons is critical to proper functioning of the nervous system. However, we do not completely understand the mechanisms behind maintenance of neuronal phenotypes in differentiated neurons. Differentiation involves several pathways including the BMP and activin pathway (Hippenmeyer et al., 2004) where timely integration of signals controls neuronal connectivity and behavior.

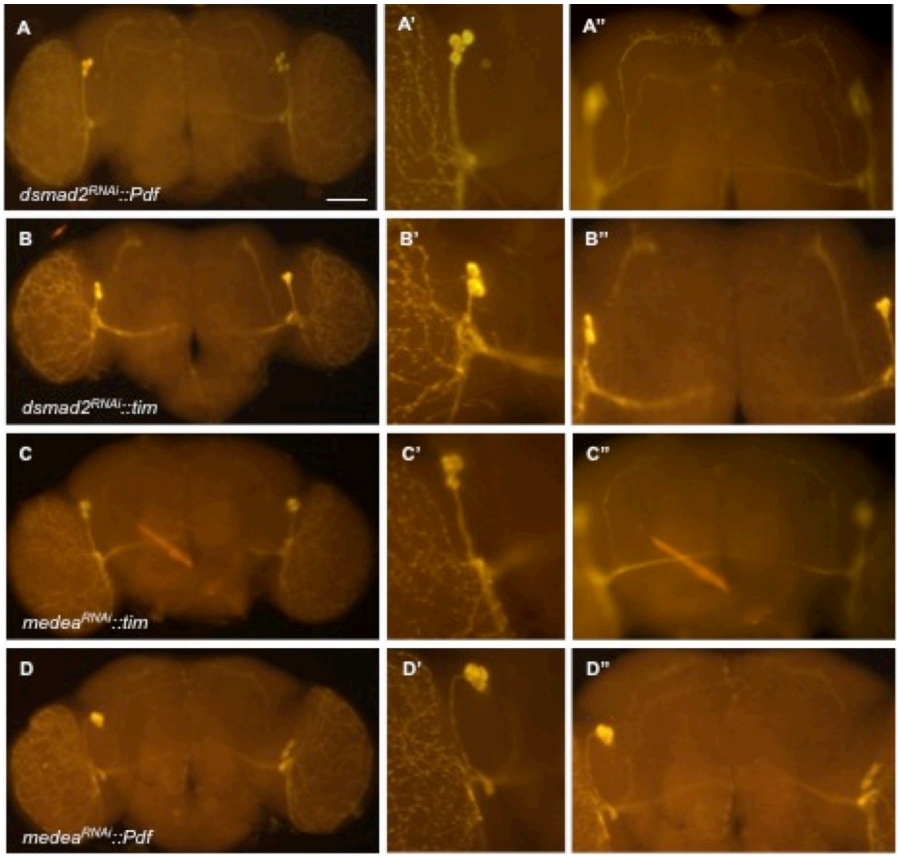


Figure 4.6 Knockdown of dSmad2 and Medea affect development of the PDF neurons. Depletion of *dSmad2* and *Medea* in the PDF positive neurons using *Pdf-Gal4* shows misrouting of the s-LNv dorsal projections. (A) *Pdf-Gal4/+; dSmad2^{RNAi}/+* (D) *Pdf-Gal4/+; UAS-Medea^{RNAi}/+*. Depletion of *dSmad2* in the clock neurons using tim-*Gal4/+; UAS-dSmad2^{RNAi}/+* leads to premature termination of s-LNv dorsal projections (B). However, flies with the genotype *tim-Gal4/+; UAS-Medea^{RNAi}/+* exhibit weaker staining in the dorsal projections (C).

Table 4.1: Locomotor activity assay for TGF-β components

Genotype	N	R	WR	AR	Period (h) Mean ± S.D
Wild-type	25	24	1	0	24.25 ± 0.31
UAS-mi-babo$_a$/Pdf-Gal4	25	4	1	20	25.44 ± 3.44
UAS-mi-babo$_a$/tim-Gal4	24	0	0	24	---
UAS-mi-babo$_b$/Pdf-Gal4	17	17	0	0	24.68 ± 2.81
UAS-mi-babo$_b$/tim-Gal4	15	14	1	0	24.07 ± 0.5
UAS-Dcr2/+; tim-Gal4/+; UAS-witRNAi/+	16	16	0	0	24.28 ± 0.26
UAS-Dcr2/+; tim-Gal4/+; UAS-punt^{RNAi}/+	17	14	3	0	24.24 ± 0.36

n, number of flies tested; R, rhythmic (power≥10); WR, weakly rhythmic 0<power<10); AR, arrhythmic.

One such well-known example is the neuronal connectivity in the circadian neuron cluster that controls behavior, physiology and metabolism in living organisms. In *Drosophila*, the BMP pathway exists in the PDF neurons that maintain circadian rhythmicity (Beckwith et al., 2013). However, no role for activin signaling has been reported and hence we decide to explore its role in regulating transcription and maintaining circadian phenotype.

Our results from eliminating type I receptor baboon in the PDF neurons and clock neurons clearly indicates the role of activity signaling in downregulating *Pdf*. We have also shown that only one of the isoforms $babo_a$ that is abundantly expressed in the brain mediates this downregulation. The locomotor behavior phenotype is arrhythmic on depletion of $babo_a$ in the PDF neurons. However, the arrhythmicity is severe on depletion of $babo_a$ in clock neurons. This indicates role of the other circadian neurons apart from the ventral lateral neurons. To confirm this, we employed *Pdf-Gal80* combined with *tim-Gal4* and the results clearly indicate the cell autonomous function of activin signaling in the PDF neurons.

To address which one of the type II receptors function to downregulate Pdf, we used RNAi lines available for *wit* and *punt* and drove them in either PDF positive lateral neurons or the clock neurons. Elimination of punt resulted in a much stronger phenotype using both *Pdf-Gal4* and *tim-Gal4*. There was weaker staining in the s-LNv terminals after *punt* knockdown in lateral neurons indicating some level of Pdf downregulation.

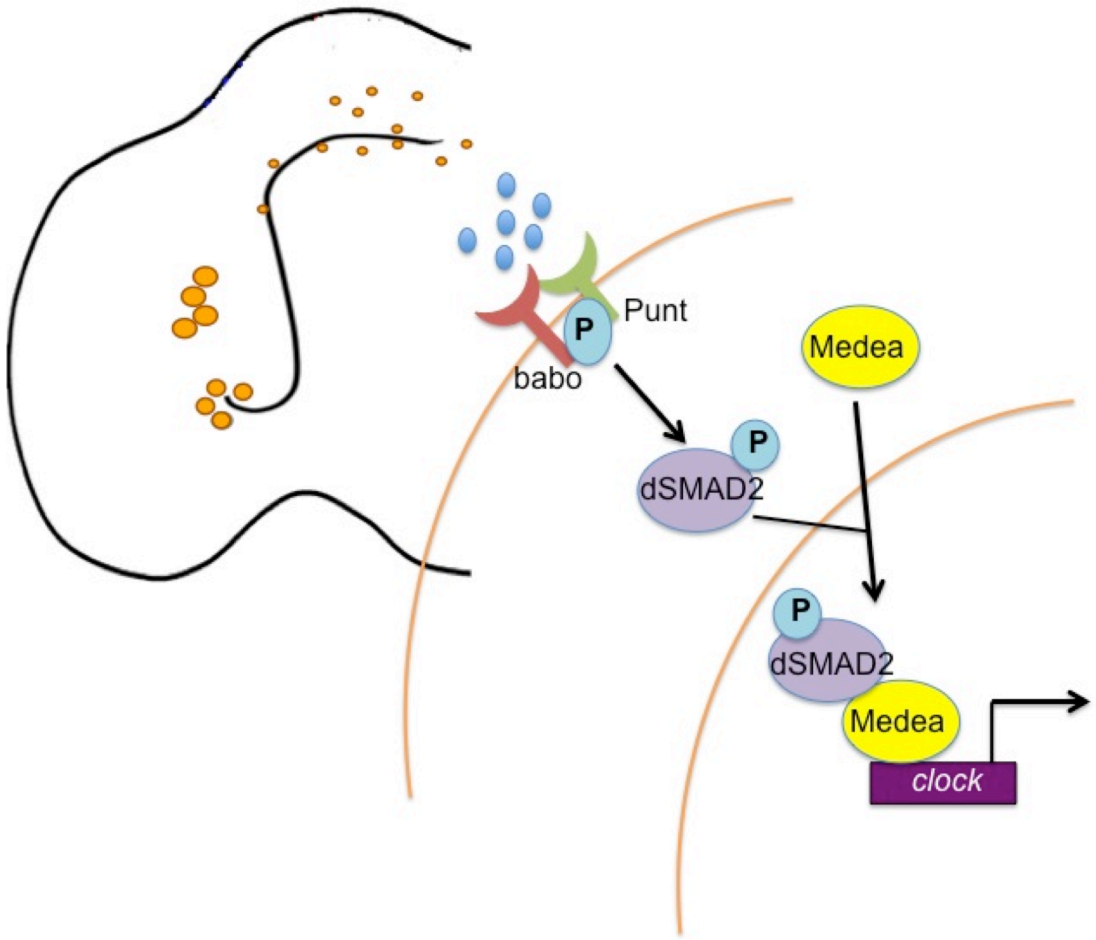


Figure 4.7 Model for TGF- β signaling in the PDF expressing s-LNvs. Ligand binds to type II receptor Punt or Wit on the membrane of s-LNvs, which then phosphorylates type I receptor babo to phosphorylate dSmad2. Phosphorylated dSMad2 and Medea form a complex and accumulate in the nucleus to activate the transcription of *Clock*.

However, the phenotype was much more severe when *punt* was knocked down in clock neurons with severe misrouting of the dorsal projections. Previously, it has been reported that loss of PDF leads to misrouting (Gorostiza and Ceriani, 2013) indicating the requirement of PDF in establishing the adult s-LNv circuitry.

The severe misrouting phenotype we observed indicates that activin signaling in the PDF circuit might play a crucial role apart from PDF itself. It is important to note that *wit* and *punt* are common type II receptors involved in both the activin and BMP pathways. Previous reports have identified *wit* as the type II receptor involved in the BMP signaling that regulates *Clk* transcription (Beckwith et al., 2013). Hence, knockdown of *wit* and the phenotype we detected might be due to involvement of BMP signaling and not activin pathway alone. However, the stronger phenotype for *punt* knockdown indicates that it might the major type II receptor functioning in the activin signaling in the PDF circuit.

Drosophila Smad2 functions in the activin pathway alone and is the sole transducer of this signaling pathway. Smad2 partners with Medea and regulates transcription of target genes. We eliminated *dSmad2* and *Medea* in the lateral neurons and found misrouting of the s-LNv projections clearly indicating the role of these two downstream effectors in the PDF neurons. Interestingly, elimination of these R-Smad and co-Smad in the clock neurons leads to weaker staining in the dorsal projections or premature termination of s-LNv terminals. Recently, baboon has been reported to directly activate Mad, BMP pathway specific R-Smad in addition to dSMad2. This occurs in the absence of BMP type I receptors indicating of a cross talk between the two signaling pathways (Peterson

et al., 2012). Based on our results, we deduce that Type I receptor baboon is crucial to activation of the TGF- β signaling in the PDF neurons and dSMad2 transduces this signal to possibly regulate *Clk* transcription that indirectly affects Pdf (Figure 4.7). We also hypothesize that there is a role for TGF- β signaling that is crucial to modeling of the adult PDF circuitry.

CHAPTER 5: MECHANISM FOR CAFFEINE RESISTANCE IN P*IGMENT DISPERSING FACTOR* (*PDF*) MUTANTS

Abstract

Caffeine, a psychostimulant produced from plants has insecticide properties with theobromine as the primary metabolite in *Drosophila*. Most of the studies have focused on the role of caffeine in influencing sleep or identifying gustatory receptors that respond to caffeine. Several microarray and RNA-seq studies have identified cyclical expression of xenobiotic-metabolizing proteins mainly cytochrome P450s (CYPS) that are under the influence of central clock factors. Caffeine is capable of inducing expression of *cyp6a2* and *cyp6a8* in *Drosophila*. However, the link between central clock factors and caffeine metabolism with respect to *cyp* gene regulation remains unexplored. PDF is a well-studied neuropeptide critical in maintaining circadian rhythms and is indirectly regulated by *Clk* and *Cyc*. It has been previously shown that PDF expressing small and large ventral lateral neurons show cyclical expression of *cyp6a2.* However, if *cyp6a8* is expressed in the PDF neurons is not known. When tested for caffeine-induced toxicity, *Pdf* null mutants (Pdf^{01}) were resistant to caffeine-induced fatality. Here, we show that Pdf^{01} exhibit a higher level of *cyp6a8* expression probably explaining their resistance to higher doses of caffeine. Also, we found that Pdf^{01} consume more caffeinated food over a long period of time. Furthermore, based on our results we speculate that activation of the PDF pathway is crucial to transcriptional regulation of the caffeine-induced *cyp6a8*. Our studies identify a critical role for PDF in modulating caffeine metabolism in flies.

Introduction

Most of the organisms have an endogenous circadian clock of approximately 24 hours, an adaption to the day and night cycles on Earth. These clock generated rhythms control physiology, metabolism and behavior of the organism. Metabolic homeostasis relies on synchrony between the circadian clock and individual cellular and organ clocks also known as peripheral clocks. In mammals, the molecular clock that operates in the suprachiasmatic nucleus (SCN) neurons and the peripheral clocks are similar, and the only difference is the way these clocks are entrained. The SCN neurons are entrained by light: dark cycles received from the retina (Aton and Herzog, 2005). However, the peripheral clocks are entrained by non-photic signals received from feeding-fasting rhythms that are in some cases independent of SCN (Schibler et al., 2003).

In *Drosophila*, the central clock is composed of transcriptional-translational feedback loops with heterodimers of Clock (CLK) and Cycle (CYC) that control transcription of Period (*per*) and Timeless (*tim*) and these proteins, in turn, inhibit CLK to keep circadian timing. Interestingly, peripheral clocks in different tissues have the same genes as that of the central oscillator (Giebultowicz and Hege, 1997; Krishnan et al., 1999). Cryptochrome (CRY) forms a part of the core clock in peripheral tissues as opposed to being a photoreceptor in the central clock (Krishnan et al., 2001; Levine et al., 2002). Disruption in circadian rhythms can have adverse effects on the metabolic function that lead to diabetes, cardiovascular diseases and some forms of cancer. Alterations in sleep pattern and short sleep duration has been shown to increase the risk of obesity and diabetes (Gangwisch, 2009).

The central clock drives rhythmic expression of several genes essential for metabolism, physiology and behavior and these genes are known as clock controlled genes (*ccgs*). Genome-wide transcriptional profiling has enabled the identification of rhythmically expressed genes and several enzymes across organisms (Keegan et al., 2007; Koike et al., 2012; Miller et al., 2007). Circadian rhythmicity within a metabolic pathway is dependent on the oscillations of enzymes or change in metabolite concentration. Detoxification enzymes were commonly thought to have no rhythmic expression until induced. However, microarray studies have revealed that several xenobiotic metabolizing genes are expressed rhythmically both in flies (Keegan et al., 2007) and in mammals (Yan et al., 2008). The detoxification process occurs in two stages where there is a change in the chemical structure followed by the second stage that involves cytochrome P450 monooxygenases (CYPs) (Feyereisen, 1999).

Cytochrome P450s (CYPs) are a diverse and superfamily of genes present in all organisms. There are four large clades of insect P450 genes: CYP2, CYP3, CYP4 and the mitochondrial P450 clade, each of which is further divided into sub-families thus making up a total of 85 different active *cyp* genes in *D. melanogaster* (Tijet et al., 2001). The effect of several toxic substances has been studied in *Drosophila*. Among those, the role of caffeine as a stress metabolite has been looked into for transcriptionally regulating *cyp* genes. Caffeine (1,3, 7- trimethylxanthine) is a neuroactive purine alkaloid produced in tea (*Camellia sinensis*) and coffee (*Coffea arabica*) among other plant species (Ashihara and Suzuki, 2004). Caffeine is capable of inducing increased heart rate (Zornik et al., 1999), inhibiting sleep (Shaw et al., 2000) and also has

mutagenic effects (Kuhlmann et al., 1968) in insects indicating several similarities in its function in vertebrates. Caffeine has been shown to increase cAMP levels on consumption in *Drosophila* (Bhaskara et al., 2008; Wang et al., 1998) through inhibition of phosphodiesterase (PDE). In mammals, antagonism of adenosine receptors is the pathway through which caffeine mediates its effect (Fredholm et al., 1999). Mammalian adenosine antagonists in *Drosophila* have shown to mimic effects of caffeine in sleep. *Drosophila* has a single adenosine receptor (DmelAdoR) and when expressed in a cell line was capable of increasing both calcium and cAMP levels (Dolezelova et al., 2007). However, when expressed in neuroblast cells, it failed to increase calcium levels and hence, it is debatable if caffeine acts through adenosine receptors in invertebrates (Kucerova et al., 2012).

In *Drosophila*, a few gustatory receptors especially Gr66a, Gr33a and Gr93a exhibit sensitivity to caffeine and respond to bitter taste-induced aversive behavior (Lee et al., 2009). In human liver, caffeine is metabolized by CYPs into three major dimethylxanthines namely, paraxanthine, theobromine and theophylline in addition to 1,3, 7–trimethyluric acid. Interestingly, all of these metabolite derivatives have different biological activities (Kot and Daniel, 2008). The predominant metabolite of caffeine is paraxanthine in humans, 1,3, 7–trimethyluric acid in rats and in monkeys it is theophylline (Bonati et al., 1984; Kot and Daniel, 2008). Interestingly, in *Drosophila* the major metabolite is theobromine and is metabolized by *Cyp6a8* (Coelho et al., 2015). It has been previously shown that caffeine is capable of inducing expression of two *cyp* genes namely *Cyp6a2* and *Cyp6a8*. However, this increased activation is not through

the adenosine receptor pathway but through increased cAMP levels (Bhaskara et al., 2008).

Interestingly, caffeine has been shown to promote wakefulness and the PDF expressing l-LNvs are wake promoting neurons (Parisky et al., 2008; Wu et al., 2009). Furthermore, microarray data has shown cyclical expression of several *cyp* genes in the PDF expressing ventral neuron (Kula-Eversole et al., 2010). In this study, we investigated whether PDF is involved in *cyp* gene regulation in response to caffeine feeding. This could explain the possible link between circadian rhythms and caffeine metabolism.

Materials and Methods

Drosophila strains and rearing conditions

All fly stocks were reared on standard cornmeal-yeast-agar medium and maintained at 25°C. Wild type Canton-S (CS) flies were used as a control for all the experiments. The following transgenic lines were employed in this study: per^{01}, tim^{01}, Clk^{Jrk} (Allada et al., 1998), $UAS\text{-}PKA^{inh}$ (Kiger et al., 1999), $w^{+};;Pdf^{01}$, *Pdf-Gal4*, Pdf^{Df}, Han^{3369} and Han^{5304} (Mertens et al., 2005).

Caffeine dose response

Caffeine-induced lethality was measured with different doses of caffeine. Flies were fed on 5% sucrose and 2% agar with either no caffeine or different doses of caffeine. Three replicates of each treatment with 45 males per genotype were performed at 25°C in 12:

12 hour Light: Dark (LD) conditions. Data (number of dead flies) were collected every 8 hours and survival rate was graphed. The average survival rates (%) for each genotype were tested in 3 independent experiments.

Feeding Behavior

The feeding assay was performed as described in (Xu et al., 2008). Caffeine was mixed into melted sucrose/agar food at a concentration of 1.2 mg/ml for all experiments except for the dose-response experiment where 0.5, 0.75, 1, 1.2, 2 and 3.5 mg/ml were used. After 24 hour starvation, all flies underwent 12:12 hour LD entrainment at 25°C for 3 days and were then transferred from cornmeal-yeast-agar food to food containing 5% sucrose, 1% agarose and 0.5 mg/ml blue dye [erioglaucine sodium salt] with either no caffeine or 1.2 mg/ml caffeine. These experiments were performed three times for each genotype. Each experiment had 25 flies assayed at two different time points ZT 0-2 and ZT 8-10. Immediately after feeding these flies were frozen on dry ice and the fly bodies were separated from the heads to prevent interference from eye pigment. The bodies were homogenized in 1X PBS buffer and centrifuged at 12,000 rpm for 25min followed by second 25 min centrifugation of the supernatant extracted. Absorbance was measured at 625 nm. Net absorbance was calculated by subtracting the absorbance from flies fed with normal food from the flies fed with blue food.

Capillary Feeder (CAFE) assay

The procedure for CAFE used in this experiment was modified from (Ja et al., 2007). Flies were entrained at 25°C for three 12: 12 hour LD cycles on 5% sucrose and 2% agarose food before being transferred to vials with 1% agarose that serves as water

source. 5 µl capillaries were filled with 5% sucrose and 5% yeast food containing 0.5 mg/ml red dye [sulforhodamine B]. For treatment, 1.2 mg/ml caffeine containing 0.5 mg/ml red dye [erioglaucine sodium salt] was added along with sucrose and yeast. The end of the capillary that was not inserted into the vial was dipped in mineral oil to slow the rate of evaporation. Evaporation rate was determined from a blanking vial containing no flies and change in volume in the micropipette was recorded.

Locomotor behavior assay

Three to five day old flies were individually placed in glass tubes containing 5% sucrose and 2% bactoagar food containing no caffeine, 0.2, 0.4, or 0.6 mg/ml caffeine. To assay the circadian period, these tubes were placed in *Drosophila* Activity Monitoring System (DAMS 3.8, TriKinetics). Twenty flies were tested per genotype and treatment group. The activity tubes were placed in 25°C incubator and were entrained for 3 days in 12: 12 light dark conditions and then subjected to constant darkness for 7 days. The data was collected and analyzed using Clocklab software. Clocklab software generates chi square periodograms with significance that is set to $\alpha = 0.05$ and only flies with $\chi^2 \geq 10$ were used to analyze period.

RT- PCR

Total RNA was extracted from fly heads using Trizol (Invitrogen) and treated with RNAse free DNase (Promega). AMV reverse transcriptase (Promega) was used to generate cDNAs. We used the following primers for *cyp6a8*: 5'-

GCTTTGAGACATCCTCCTCC 3' and 5'GCAGATGAGGGTATGATGA 3' with beta tubulin primers as an internal control.

Statistical Analysis

Statistical comparisons were made between *CS* and Pdf^{01} for the experiments on feeding behavior separately for food with sucrose and food with caffeine. We used two-tailed t-test and each figure shows Average ± SEM (*=p ≤ 0.05 and **= p ≤ 0.01).

Results

Pdf^{01} mutants are resistant to caffeine

Using *Drosophila prosaltans* it was previously determined that 2 mg/ml is the LD50 for caffeine in that organism (Itoyama and Bicudo, 1992). LD 50 is the lethal dose of a substance at which 50% of the organism die. Previous studies on the effect of caffeine in *Drosophila melanogaster* have used doses ranging from 0.2 mg/ml to 1 mg/ml and these have been based on the LD50 data from *Drosophila prosaltans*.

Caffeine has been shown to induce arousal in *Drosophila melanogaster* (Wu et al., 2009) and since large lateral neurons expressing Pigment dispersing factor (PDF) promote arousal (Parisky et al., 2008), we decided to test *Pdf* null mutants in our study. We used wild type flies Canton-S as control and tested for caffeine toxicity using different doses of caffeine ranging from the lowest dose of 0.2 mg/ml to extremely lethal dose of 3.5 mg/ml. 0.2mg/ml and 0.5 mg/ml of caffeine did not show a significant

difference in initial five days. Results from the toxicity assay clearly indicate that survival rate is dose dependent with higher concentration of caffeine being more toxic and lethal to the flies.

As shown in Figure 5.1 Pdf^{01} show resistance in caffeine as compared to *CS* flies at all doses of caffeine except at 3.5 mg/ml. This is possibly due to 3.5 mg/ml of caffeine being an extremely lethal dose. Considering 2 mg/ml as LD50, *CS* flies are sensitive to increasing concentrations of caffeine. At 1 mg/ml of caffeine 50% of the flies survive after feeding on caffeine for 60 hours. However, Pdf^{01} show resistance to caffeine at 1mg/ml with just 10% of the flies dying after feeding on caffeine at the end of 60 hours.

Interestingly, we observed a significant difference when we use 1.2 mg/ml of caffeine with both these genotypes in the first 5 days of feeding on caffeine food. 50% of the *CS* flies survived at the end of 40 hours whereas 50% of Pdf^{01} survived by the end of 72 hours for 1.2 mg/ml of caffeine. Hence, we decided to test the rest of the genotypes used in this study for toxicity at 1.2-mg/ml caffeine. Pdf^{Df} lacks the *Pdf* gene locus and has been previously described (Renn et al., 1999). In order to further confirm if Pdf^{01} mutants are indeed resistant to higher concentration of caffeine, we decided to test Pdf^{Df} flies. We crossed Pdf^{Df} males to Pdf^{01} female flies and the progeny showed increased resistance as compared to Pdf^{01} further supporting that loss of *Pdf* leads to increased caffeine resistance (Figure 5.2).

PDF neuropeptide signals through PDF receptor (PDFR), a G-protein coupled receptor that is positively coupled to cAMP (Hyun et al., 2005; Mertens et al., 2005). Previously, it was demonstrated that the PDF signaling pathway works through protein kinase A (PKA) to reset clock as well as through cAMP that is independent of PKA to control clock activity (Seluzicki et al., 2014). Hence, we decided to test two different *Pdfr* mutants namely Han^{3369} and Han^{5304}. Han^{5304} is a mutant allele that lacks all the seven transmembrane domains as well as the C-terminus whereas Han^{3369} deletes one of the transmembrane and C-terminus of the protein (Hyun et al., 2005). We also used PKA inhibitor and using the UAS-GAL4 system specifically inhibited PKA in the PDF neurons. In addition, we tested mutants of three important genes that form the central molecular clock in *Drosophila* namely per^{01}, tim^{01} and Clk^{Jrk} for caffeine toxicity at 1.2 mg/ml.

When exposed to 1.2 mg/ml of caffeine, Han^{3369} (one of the *Pdfr* mutants) showed increased caffeine resistance than Pdf^{01} mutants (Figure 5.2). In the circadian context, *Pdfr* mutants phenocopy the behavior of *Pdf* mutant showing lack of a morning activity peak and a phase advance in evening activity peak with arrhythmic behavior under constant conditions (Hyun et al., 2005). Hence, the resistance to caffeine in Han^{3369} mutants is expected. However, Han^{5304} was sensitive to caffeine as compared to Pdf^{01} mutants but not as sensitive as wild type flies (Figure 5.2). This could be possibly explained by the fact that Han^{5304} is a hypomorphic mutation and that leads to reduced level of the *Pdfr* gene activity (Klose et al., 2016).

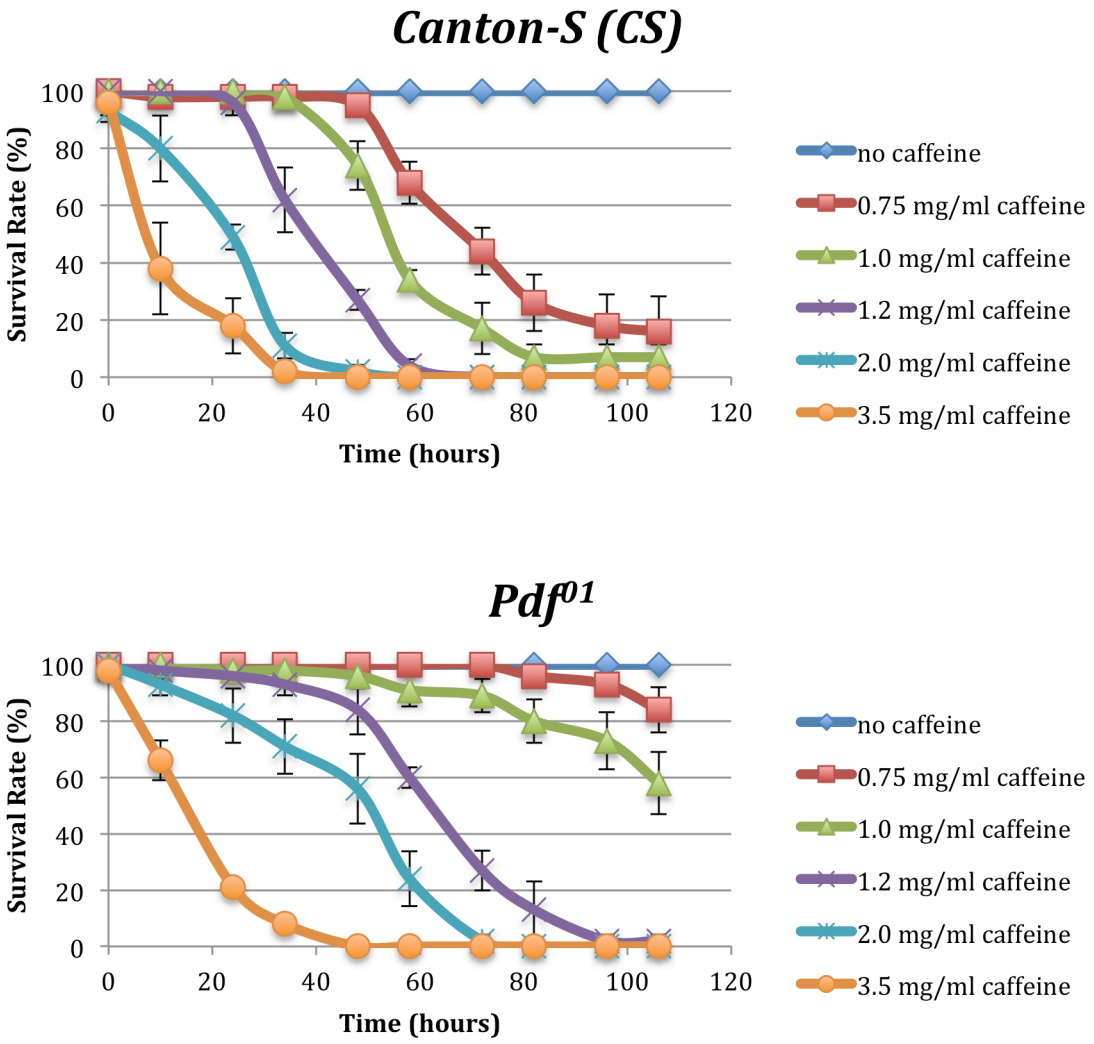


Figure 5.1 Average survival rate (%) for *CS* and *Pdf*^{01} at different concentrations of caffeine. X-axis represents time in hours each of the above two genotypes were fed caffeinated food. Y-axis represents the average survival rate (%) from n=45 for each concentration of caffeine per trial. Each data point is plotted as Mean ± S.E.M.

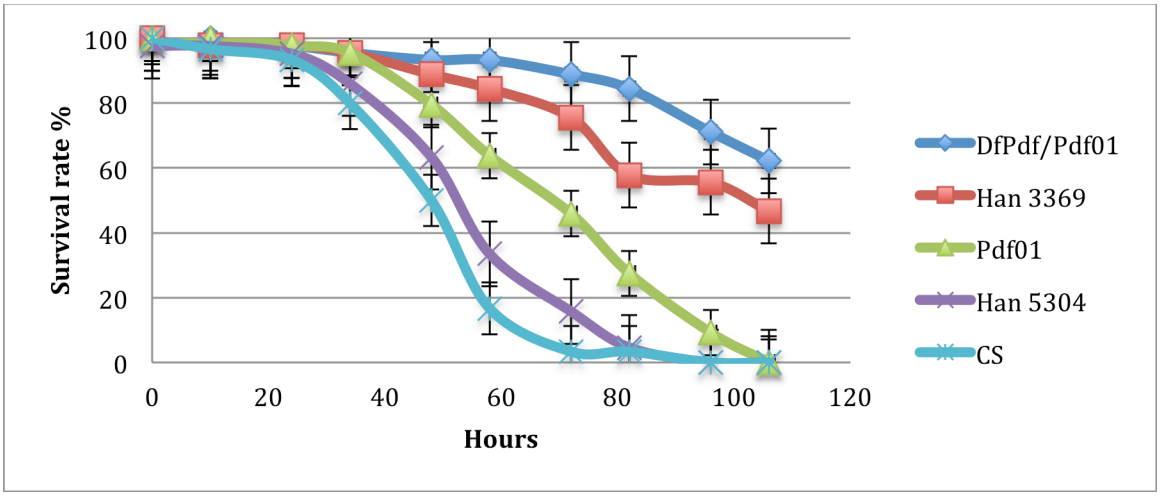
Interestingly, Clk^{Jrk} showed increased caffeine resistance as compared to Pdf^{01} but less resistant when compared to Pdf^{Df}/Pdf^{01} and Han^{3369}. Clk^{Jrk} is semidominant mutation that results from a premature stop codon that leads to loss of the activation domain of CLK (Allada et al., 1998). It is not a null mutant such as per^{01} and tim^{01}which show complete loss of function. Both per^{01} and tim^{01} mutants were sensitive to caffeine and especially tim^{01} and per^{S} flies showed increased sensitivity compared to the wild type flies (Figure 5.2). The per^{S} mutation leads to shorter circadian period length and was mapped to an approximately 30 amino acid domain of PER (Baylies et al., 1992; Rutila et al., 1992). These data indicate that caffeine tolerance requires function of PDF but is not influenced by the *Drosophila* central clock proteins with the exception of Clk^{Jrk} when compared to Pdf^{01}. However, we rule out the increased resistance exhibited by Clk^{Jrk} as Pdf^{Df}/Pdf^{01} flies are more resistant.

We looked into the function of the cAMP-dependent protein kinase A (PKA) by inhibiting it in the PDF neurons and testing the flies for their response to 1.2 mg/ml of caffeine. cAMP activates PKA activity by binding to its regulatory (R) subunit, and this binding releases the catalytic (C) subunit which then phosphorylates different substrates (Taylor, 1989). Inhibition of PKA in the PDF neurons led to a high tolerance for 1.2 mg/ml of caffeine with 50% of the flies surviving at the end of 120 hours of feeding on caffeine. These results are similar to the high tolerance exhibited by Pdf^{Df}/Pdf^{01} flies indicating that PDF signaling pathway plays a significant role in caffeine resistance.

Pdf^{01} consume more food as compared to *CS* flies

When feeding on caffeine if there are any internal changes in the metabolic state of the flies, it can lead to alterations in feeding behavior. Capillary feeder (CAFE) assay measures the amount of food ingested (Ja et al., 2007) over time even for several days. Cumulative ingestion by 25 individual male flies of two different genotypes was calculated over 3 days. We determined that there were differences in the food intake using 1.2 mg/ml of caffeine. Over time *Pdf*^{01} consumed more caffeinated food as compared to the *CS* flies.

In addition to the CAFE assay, we measured feeding in *CS* and *Pdf*^{01} flies by subjecting them to LD cycles and after 3 days of entrainment; these flies were subjected to constant conditions and were allowed to feed on normal food and caffeinated food for every 2 hours. We subjected these flies to normal food and caffeinated food at six different time points. *Pdf*^{01} consumed less food with sucrose at all other time points during the day except at CT 4-6 as compared to that of *CS* flies (Figure 5.4). However, *Pdf*^{01} consumed more caffeine food at all time points except at CT 12-16 and CT 18-20 (Figure 5.4). This trend further confirms that *Pdf*^{01} eat more caffeinated food as compared to wild type flies over a period of 24 hours. This is consistent with the CAFE assay data (Figure 5.3).



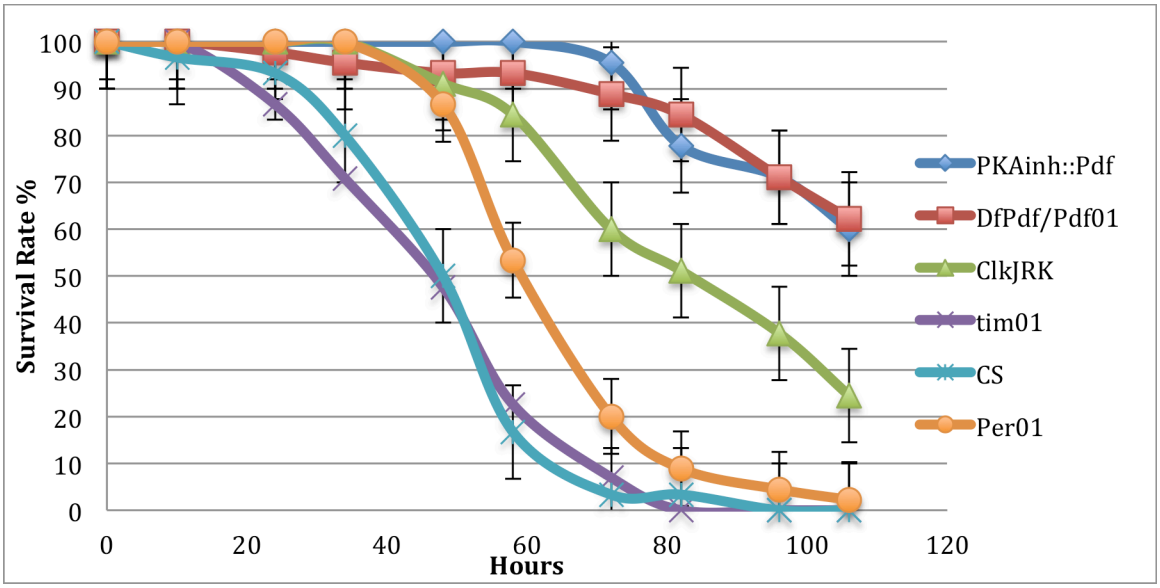
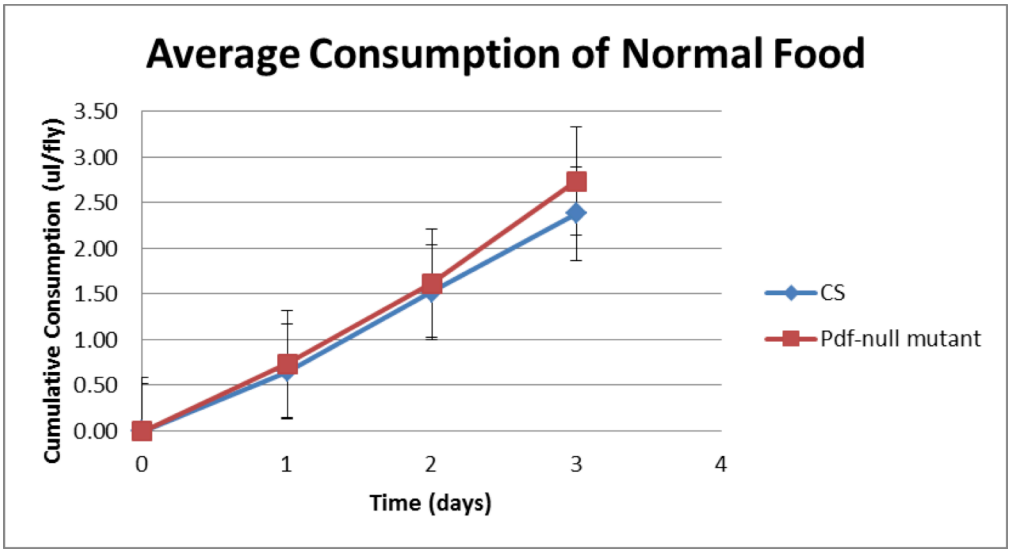


Figure 5.2 Average survival rates of different genotypes in 1.2 mg/ml caffeine

Based on the average survival rate plotted as percentage, it is clear that Pdf^{Df}/Pdf^{01} flies exhibited increased resistance as compared to the wild type and central clock mutants. Each data point is plotted as Mean ± S.E.M.



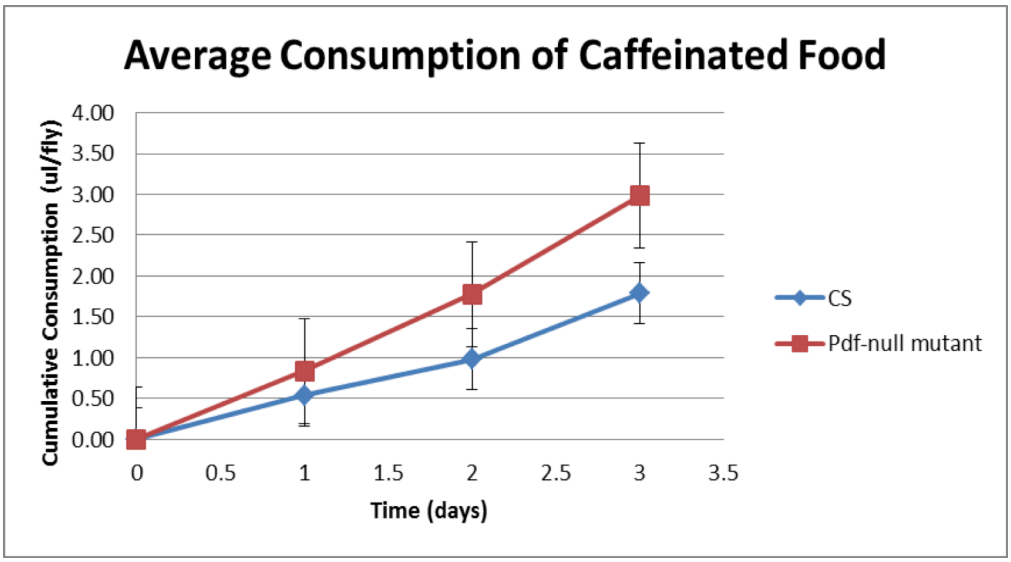


Figure 5.3 Measurement of food consumption using CAFE assay. Cumulative food intake by 25 individual male flies fed on either yeast and sucrose or combination of yeast, sucrose and caffeine. *Pdf*^{01} show higher consumption of food with caffeine as compared to the CS flies. All values are given as Mean ± S.E.M.

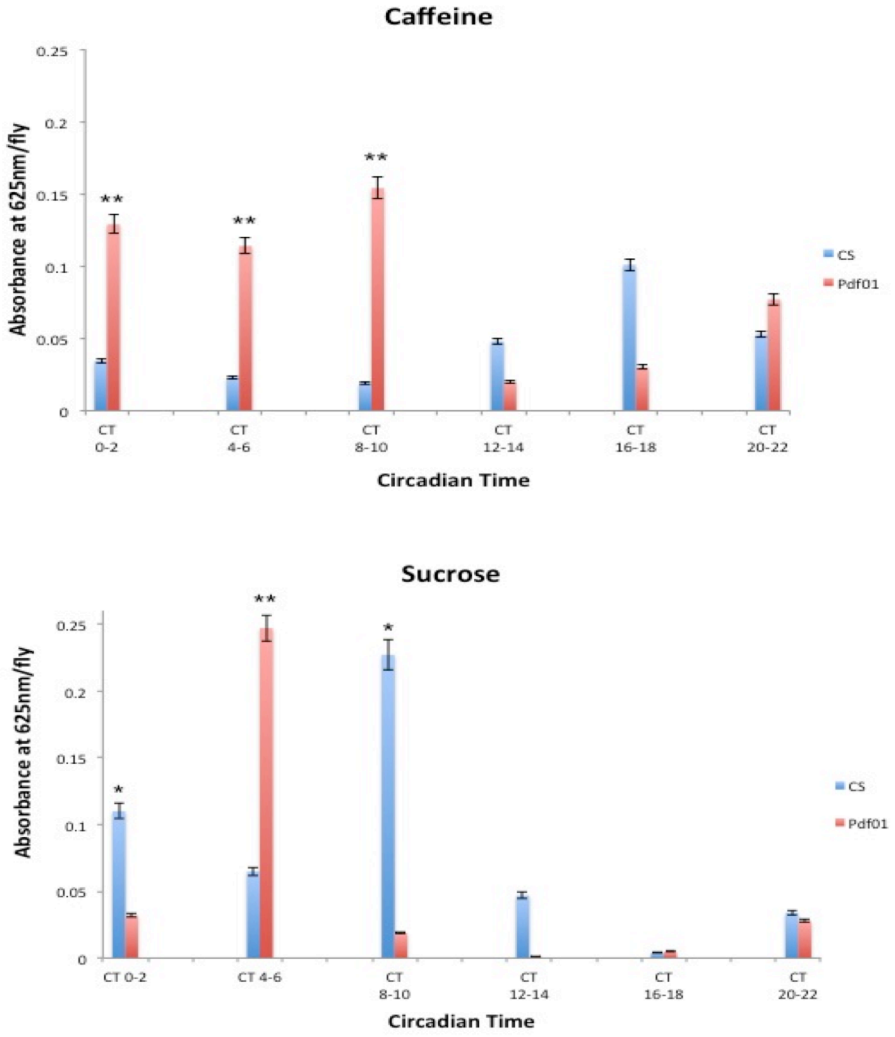


Figure 5.4 Measurement of food consumption using feeding assay. X-axis represents food consumed during 2-hour intervals at different times in a day. Y-axis represents amount of food consumed that is measured in terms of absorbance per fly. Significant differences in food consumption between *CS* and Pdf^{01} flies at the same time point were observed using two-tailed t-test. * represents p value ≤ 0.05 and ** p ≤ 0.01.

Wild type and *Pdf*^{01} mutants exhibit lengthening of circadian period with increasing concentrations of caffeine

Previously, when wild type flies were subjected to caffeine, there was an observed increase in their circadian period (Wu et al., 2009). We wanted to assess the circadian behavior of *Pdf*^{01} flies when exposed to caffeine at varying concentrations. We tested 20 flies per caffeine treatment for both wild type and *Pdf*^{01}. These flies were entrained for 4 LD cycles and then subjected to constant darkness for 10 days. We observed that *CS* flies showed increased activity with increasing caffeine concentration. We also observed an increase in circadian period of 1 hour at 0.4mg/ml caffeine as compared to when they were fed on non-caffeinated food (Figure 5.5). *Pdf*^{01} lack morning peak and have advanced evening peak under LD conditions and arrhythmicity gradually increases after 3-4 days of constant conditions (Park and Hall, 1998; Renn et al., 1999). *Pdf*^{01} also exhibit period extension at 0.4 mg/ml and increased activity with increasing caffeine concentration (Figure 5.5). This pattern in *Pdf*^{01} flies when fed on caffeinated food is due to increased overall activity in response to caffeine. However, we were not able to test for higher doses of caffeine, as the CS flies wouldn't survive the LD cycle. Also, we did not observe any significant arrhythmicity in the flies that were fed on 0.2 mg/ml and 0.4 mg/ml of caffeine for both the genotype.

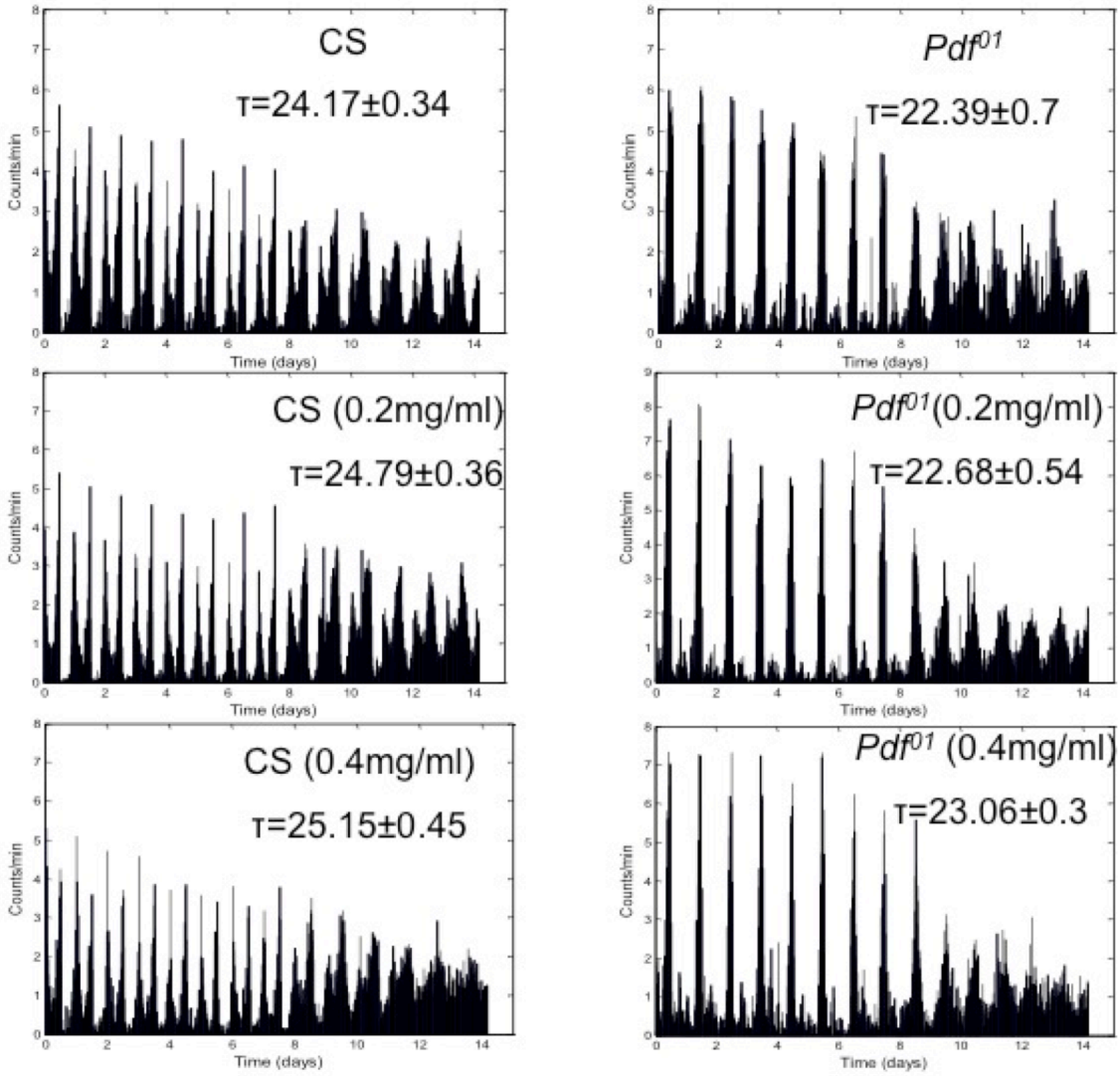


Figure 5.5. Locomotor activity for CS and *Pdf*^{01} flies. Activity profile for *CS* and *Pdf*^{01} flies fed on 0.2 mg/ml and 0.4 mg/ml of caffeine compared to no caffeine. Both *CS* and *Pdf*^{01} flies exhibited increase in the circadian period at different concentrations of caffeine. Circadian period is calculated as Average ± S.D. and represented by tau (τ). N=20 flies were tested per genotype for each concentration of caffeine.

Pdf^{01} show increased expression of caffeine induced *Cyp6a8*

To better understand the mechanism for caffeine resistance we tested changes in the expression of the gene *cyp6a8*. We used semiquantitative RT-PCR and found higher expression of and *cyp6a8* in *Pdf*^{01} as compared to wild type flies, thus providing a possible model for explaining caffeine resistance. We quantified the relative band density for *Pdf*^{01} and *CS* lanes using ImageJ gel analysis tool and significant difference was observed between the two genotypes for *cyp6a8* expression. This is however, a crude method to analyze difference in *cyp6a8* expression and real time quantification will be necessary to confirm these results.

Discussion

Caffeine is one of the most widely used secondary metabolites derived from plants. Plants have used caffeine as a chemical defense, and this function has been exploited through its use as a pesticide (Nathanson, 1984). Various studies in insects have found similar effects of caffeine as well in vertebrates. In Drosophila, caffeine is known to inhibit sleep. It has played in role in bitter taste induced aversive behavior that has led to the identification of gustatory receptors (Moon et al., 2009; Wu et al., 2009). The central clock drives rhythmic expression of several clock-controlled genes (*ccgs*). Genome wide transcriptional profiling has enabled the identification of several detoxification enzymes that metabolize xenobiotics, which were thought to have no rhythmic expression until induced (Keegan et al., 2007; Koike et al., 2012; Miller et al., 2007).

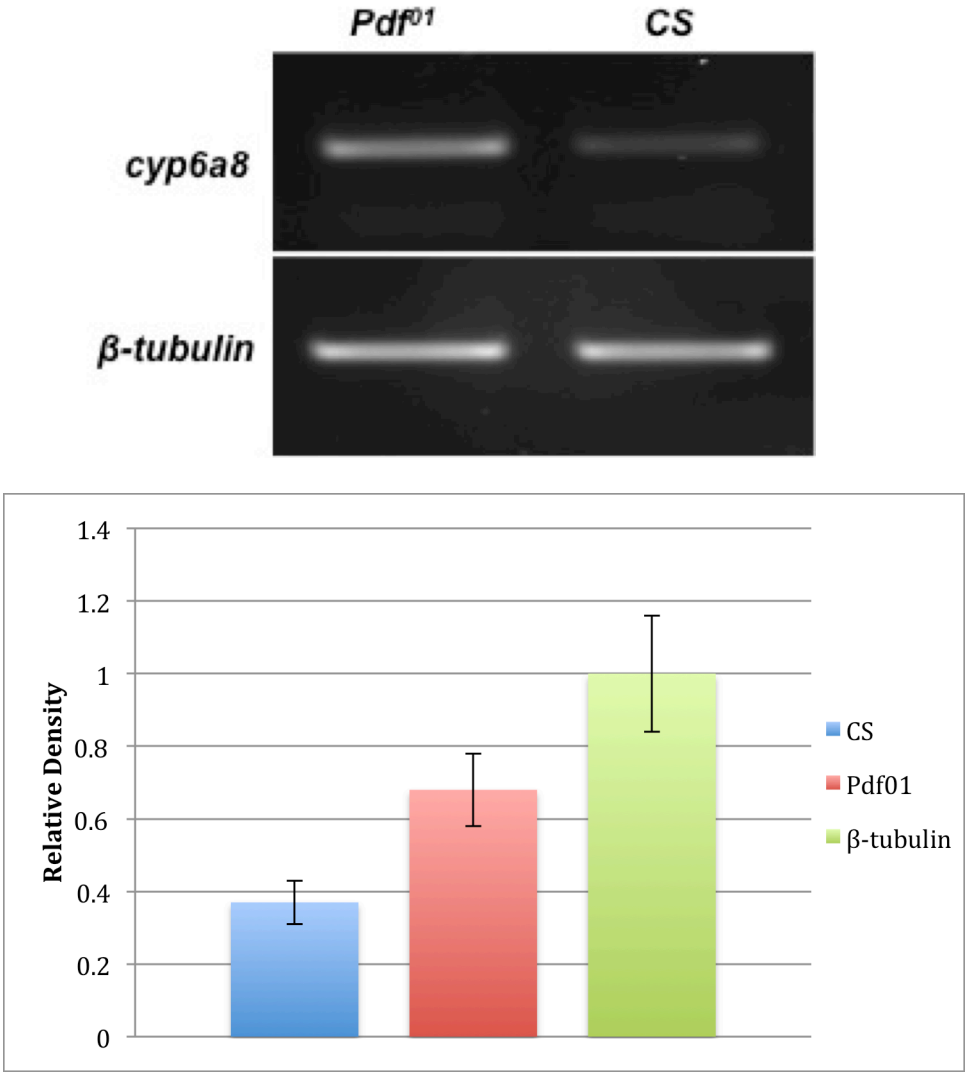


Figure 5.6 RT-PCR results show higher expression of *cyp6a8*. Top panel shows *cyp6a8* expression for *CS* and *Pdf*^{01} flies and bottom panel shows the loading control. Relative density was calculated using ImageJ gel analysis method. Relative density represents expression levels of *cyp6a8* for CS and *Pdf*^{01} flies relative to β-tubulin loading control (n=3). Data set is plotted as Mean ± S.E.M.

Cytochrome P540s play a key role in metabolism of xenobiotics including caffeine. In fact, in *Drosophila*, *cyp6a2* and *cyp6a8* are transcriptionally induced by caffeine (Bhaskara et al., 2008). A microarray study identified cycling genes in the ventral lateral neurons (LNvs) in the Drosophila brain. These neurons express the neuropeptide pigment-dispersing factor (PDF). *Cyp6a2* is differentially expressed in the small and large LNvs, but no cyclical expression was shown for *cyp6a8* (Kula-Eversole et al., 2010).

We decided to test the potential link between PDF and caffeine induced cyp genes and testing for he effect of varying doses of caffeine and their effect on survival. We tested wild type flies along with Pdf^{01} mutants and found that with increasing doses of caffeine, Pdf^{01} flies were more resistant to caffeine-induced toxicity. Based on this initial study, we decided to test several central clock proteins and their role in caffeine toxicity. Since, *Clk* and *Cyc* indirectly regulate *Pdf*, we initially thought that central clock mutants should show similar phenotype to Pdf^{01} flies. Intriguingly, per^{01} and tim^{01} were more sensitive to caffeine-induced toxicity. However, when we tested Clk^{Jrk} flies, they were resistant as compared to Pdf^{01} but were less resistant than Pdf^{01}/Pdf^{Df} flies. These results strongly suggest that lack of PDF causes flies to be more resistant to toxic doses of caffeine and there is no role for the central clock proteins in this process.

We further explored the mechanism behind resistance to toxic doses of caffeine and hence tested for CYP gene expression using RT-PCR in wild type and Pdf^{01} flies. Caffeine has been shown to induce two particular cyp genes *cyp6a2* and *cyp6a8*. Our

results indicate higher *cyp6a8* expression in Pdf^{01} flies as compared to wild type flies, thus providing a possible model for explaining caffeine resistance. PDF is a neuropeptide that serves as the clock output signal. Though it is known that central clock regulates feeding and metabolism (Xu et al., 2008), it is not clear if there is a feedback from metabolism to the clock. Caffeine is known in *Drosophila* to promote arousal through dopaminergic neurons (Nall et al., 2016). We tested for the link between PDF and caffeine metabolism by analyzing feeding behavior of Pdf^{01} and compared it to wild-type flies. We fed the flies both normal food and caffeinated food and found that the cumulative consumption for Pdf^{01} was higher over a period of 3 days. Interestingly, when we analyzed food consumption every 2 hours, we see a similar trend with Pdf^{01} flies consuming more caffeinated food over a 24-hour period. Previously, it has been shown that flies with a disrupted fat body clock consume more food (Xu et al., 2008). Based on this we hypothesize a crucial role for PDF in metabolism and feeding.

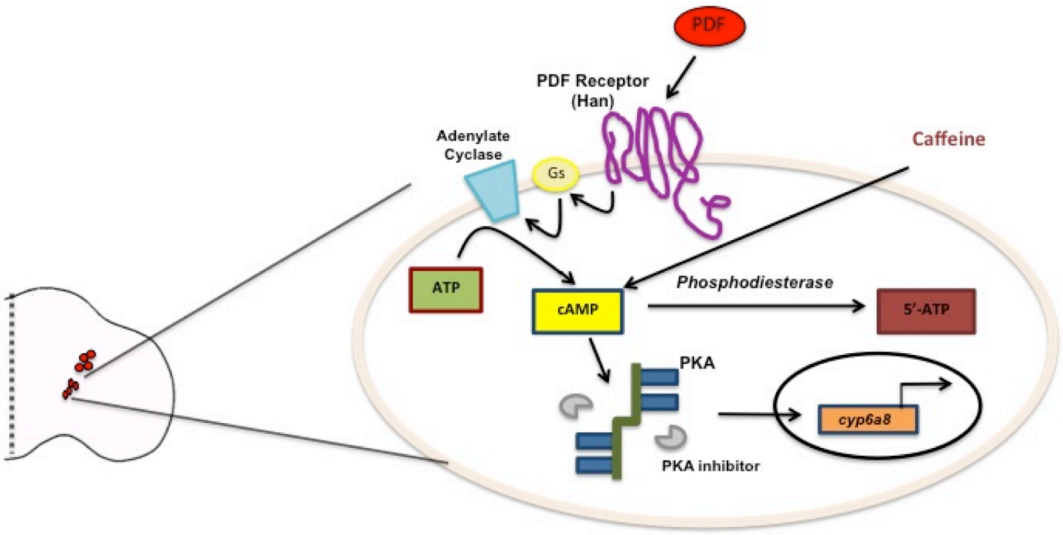


Figure 5.7 Model for the role of PDF pathway in regulating caffeine induced gene *cyp 6a8*. In the lateral neurons, PDF binds to Pdf receptor to activate the downstream signaling cascade. This leads to increase in cAMP, which further leads to activation of PKA and transcriptional regulation of cyp6a8. Caffeine is also capable of increasing cAMP.

CHAPTER 6: CONCLUSIONS

The collection of work outlined here attempts to address few important questions in the field of circadian rhythms and development in *Drosophila melanogaster*. Firstly, how is a neuropeptide PDF that is critical to maintaining circadian rhythm regulated? Secondly what functional role does scro, a homeodomain transcription factor play in addition to regulating *Pdf*? Thirdly, what is the role of TGF- β signaling in PDF neurons? Lastly, if the PDF signaling pathway regulates caffeine induced *cyp* genes thus playing a role in metabolism. PDF forms a hierarchy in the circadian network where timely integration of signals controls neuronal connectivity and behavior. The work presented here provides a novel and significant insight into each of these questions.

PDF has been extensively studied within the clock circuit. Through our studies, we identified a cis-regulatory region in the *Pdf* promoter that we call *Pdf* regulatory element (PRE). PRE is a 13 bp repeat with a 9 bp spacer region that is conserved among other *Drosophila* species. PRE is crucial for Pdf expression in the ventral lateral neurons in the brain. We identified a homeodomain transcription factor scarecrow (*scro*) that binds to PRE. We found *scro* to be crucial in restricting *Pdf* expression and that it plays the role of a negative regulator in non-PDF neurons in the brain. Though we were successful in finding a negative regulator of PDF, we still do not know what activates PDF and helps its maintenance in the ventral lateral neurons. CHIP-seq could be a useful technique to identify the proteins that bind to PRE and thus can enhance our understanding of PDF regulation.

We tried to address the role of TGF- β signaling in PDF neurons. To this end, we found the role of Type I receptor baboon to be crucial to transcriptionally regulating *Pdf*. However, the role of other pathway components was ambiguous. Recently, baboon has been reported to directly activate Mad, BMP pathway specific R-Smad in addition to dSMad2. This occurs in the absence of BMP type I receptors indicating of a cross talk between the two signaling pathways (Peterson et al., 2012). Based on this, it is difficult to conclude that the results we observe are due to TGF- β signaling alone. In addition, the target sites for dSmad2 in the *Drosophila* genome is unknown and hence, it will be interesting to know if the central clock proteins or PDF is a target of dSmad2.

PDF signaling is crucial to maintaining circadian rhythmicity but its role in metabolism hasn't been looked into. We tested Pdf^{01} mutants for the metabolite caffeine and found them to be resistant to higher doses of caffeine. This led us to investigate the mechanism and we found cytochrome (cyp) genes upregulated in Pdf^{01}. Recent reports suggest the cyclical changes in these metabolizing enzymes that were once thought to remain constant. In addition, microarray data found the caffeine-induced *cyp6a2* to cycle in the *Pdf* neurons. Through our experiments we have ruled out the role of central clock components in caffeine resistance and we think this is unique to PDF. However, we need to look into how does the PDF pathway activate the transcription of *cyp* genes and also find the transcription factors that play a key role in this activation.

Lastly, we wanted to characterize the function of *scro* in addition to its role in *Pdf* regulation. Since, our data suggested that *scro* might be a cell fate regulator, we used

the eye, wing and genital disc to test the role of *scro*. Our studies focus on overexpression of *scro* as CRISPR mutants we generated were homozygous lethal at embryo stage. When expressed in the wing and genital disc, *scro* was capable of transforming the tissues implicating its role in regulating segmental identity in *Drosophila*. Based on preliminary evidence, we hypothesize *scro* interacts with microRNA iab4 in the Bithorax complex of Hox genes to regulate these genes.

LIST OF REFERENCES

Allada, R., White, N.E., So, W.V., Hall, J.C., and Rosbash, M. (1998). A mutant Drosophila homolog of mammalian Clock disrupts circadian rhythms and transcription of period and timeless. Cell *93*, 791-804.

Ashihara, H., and Suzuki, T. (2004). Distribution and biosynthesis of caffeine in plants. Frontiers in bioscience : a journal and virtual library *9*, 1864-1876.

Aton, S.J., Colwell, C.S., Harmar, A.J., Waschek, J., and Herzog, E.D. (2005). Vasoactive intestinal polypeptide mediates circadian rhythmicity and synchrony in mammalian clock neurons. Nature neuroscience *8*, 476-483.

Aton, S.J., and Herzog, E.D. (2005). Come together, right...now: synchronization of rhythms in a mammalian circadian clock. Neuron *48*, 531-534.

Awasaki, T., Huang, Y., O'Connor, M.B., and Lee, T. (2011). Glia instruct developmental neuronal remodeling through TGF-beta signaling. Nature neuroscience *14*, 821-823.

Bahn, J.H., Lee, G., and Park, J.H. (2009). Comparative analysis of Pdf-mediated circadian behaviors between Drosophila melanogaster and D. virilis. Genetics *181*, 965-975.

Baker, N.E. (2001). Cell proliferation, survival, and death in the Drosophila eye. Seminars in cell & developmental biology *12*, 499-507.

Baylies, M.K., Vosshall, L.B., Sehgal, A., and Young, M.W. (1992). New short period mutations of the Drosophila clock gene per. Neuron *9*, 575-581.

Beckwith, E.J., Gorostiza, E.A., Berni, J., Rezaval, C., Perez-Santangelo, A., Nadra, A.D., and Ceriani, M.F. (2013). Circadian period integrates network information through activation of the BMP signaling pathway. PLoS biology *11*, e1001733.

Benveniste, R.J., and Taghert, P.H. (1999). Cell type-specific regulatory sequences control expression of the Drosophila FMRF-NH2 neuropeptide gene. Journal of neurobiology *38*, 507-520.

Benveniste, R.J., Thor, S., Thomas, J.B., and Taghert, P.H. (1998). Cell type-specific regulation of the Drosophila FMRF-NH2 neuropeptide gene by Apterous, a LIM homeodomain transcription factor. Development *125*, 4757-4765.

Bhaskara, S., Chandrasekharan, M.B., and Ganguly, R. (2008). Caffeine induction of Cyp6a2 and Cyp6a8 genes of Drosophila melanogaster is modulated by cAMP and D-JUN protein levels. Gene *415*, 49-59.

Blanchardon, E., Grima, B., Klarsfeld, A., Chelot, E., Hardin, P.E., Preat, T., and Rouyer, F. (2001). Defining the role of Drosophila lateral neurons in the control of

circadian rhythms in motor activity and eclosion by targeted genetic ablation and PERIOD protein overexpression. The European journal of neuroscience *13*, 871-888.

Blau, J., and Young, M.W. (1999). Cycling vrille expression is required for a functional Drosophila clock. Cell *99*, 661-671.

Bonati, M., Latini, R., Tognoni, G., Young, J.F., and Garattini, S. (1984). Interspecies comparison of in vivo caffeine pharmacokinetics in man, monkey, rabbit, rat, and mouse. Drug metabolism reviews *15*, 1355-1383.

Bradbury, A.F., and Smyth, D.G. (1991). Peptide amidation. Trends in biochemical sciences *16*, 112-115.

Brand, A.H., and Perrimon, N. (1993). Targeted gene expression as a means of altering cell fates and generating dominant phenotypes. Development *118*, 401-415.

Brummel, T., Abdollah, S., Haerry, T.E., Shimell, M.J., Merriam, J., Raftery, L., Wrana, J.L., and O'Connor, M.B. (1999). The Drosophila activin receptor baboon signals through dSmad2 and controls cell proliferation but not patterning during larval development. Genes & development *13*, 98-111.

Busser, B.W., Bulyk, M.L., and Michelson, A.M. (2008). Toward a systems-level understanding of developmental regulatory networks. Current opinion in genetics & development *18*, 521-529.

Carr, M., Cotton, S., Rogers, D.W., Pomiankowski, A., Smith, H., and Fowler, K. (2006). Assigning sex to pre-adult stalk-eyed flies using genital disc morphology and X chromosome zygosity. BMC developmental biology *6*, 29.

Carre, A., Szinnai, G., Castanet, M., Sura-Trueba, S., Tron, E., Broutin-L'Hermite, I., Barat, P., Goizet, C., Lacombe, D., Moutard, M.L*., et al.* (2009). Five new TTF1/NKX2.1 mutations in brain-lung-thyroid syndrome: rescue by PAX8 synergism in one case. Human molecular genetics *18*, 2266-2276.

Chen, X., Rubock, M.J., and Whitman, M. (1996). A transcriptional partner for MAD proteins in TGF-beta signalling. Nature *383*, 691-696.

Coelho, A., Fraichard, S., Le Goff, G., Faure, P., Artur, Y., Ferveur, J.F., and Heydel, J.M. (2015). Cytochrome P450-dependent metabolism of caffeine in Drosophila melanogaster. PloS one *10*, e0117328.

Cowden, J., and Levine, M. (2003). Ventral dominance governs sequential patterns of gene expression across the dorsal-ventral axis of the neuroectoderm in the Drosophila embryo. Developmental biology *262*, 335-349.

Danner, S., and Belasco, J.G. (2001). T7 phage display: a novel genetic selection system for cloning RNA-binding proteins from cDNA libraries. Proceedings of the National Academy of Sciences of the United States of America *98*, 12954-12959.

Darlington, T.K., Wager-Smith, K., Ceriani, M.F., Staknis, D., Gekakis, N., Steeves, T.D., Weitz, C.J., Takahashi, J.S., and Kay, S.A. (1998). Closing the circadian loop: CLOCK-induced transcription of its own inhibitors per and tim. Science *280*, 1599-1603.

Davidson, E.H., and Levine, M.S. (2008). Properties of developmental gene regulatory networks. Proceedings of the National Academy of Sciences of the United States of America *105*, 20063-20066.

Deplancke, B. (2009). Experimental advances in the characterization of metazoan gene regulatory networks. Briefings in functional genomics & proteomics *8*, 12-27.

Derynck, R., and Akhurst, R.J. (2007). Differentiation plasticity regulated by TGF-beta family proteins in development and disease. Nature cell biology *9*, 1000-1004.

Dolezelova, E., Nothacker, H.P., Civelli, O., Bryant, P.J., and Zurovec, M. (2007). A Drosophila adenosine receptor activates cAMP and calcium signaling. Insect biochemistry and molecular biology *37*, 318-329.

Dubruille, R., and Emery, P. (2008). A plastic clock: how circadian rhythms respond to environmental cues in Drosophila. Molecular neurobiology *38*, 129-145.

Dunlap, J.C. (1999). Molecular bases for circadian clocks. Cell *96*, 271-290.

Ebbs, M.L., and Amrein, H. (2007). Taste and pheromone perception in the fruit fly Drosophila melanogaster. Pflugers Archiv : European journal of physiology *454*, 735-747.

Edery, I. (2011). A master CLOCK hard at work brings rhythm to the transcriptome. Genes & development *25*, 2321-2326.

Eipper, B.A., Myers, A.C., and Mains, R.E. (1985). Peptidyl-glycine alpha-amidation activity in tissues and serum of the adult rat. Endocrinology *116*, 2497-2504.

Ewer, J., Frisch, B., Hamblen-Coyle, M.J., Rosbash, M., and Hall, J.C. (1992). Expression of the period clock gene within different cell types in the brain of Drosophila adults and mosaic analysis of these cells' influence on circadian behavioral rhythms. The Journal of neuroscience : the official journal of the Society for Neuroscience *12*, 3321-3349.

Fan, Y., Wang, S., Hernandez, J., Yenigun, V.B., Hertlein, G., Fogarty, C.E., Lindblad, J.L., and Bergmann, A. (2014). Genetic models of apoptosis-induced proliferation

decipher activation of JNK and identify a requirement of EGFR signaling for tissue regenerative responses in Drosophila. PLoS genetics *10*, e1004131.

Fang, Y., Sathyanarayanan, S., and Sehgal, A. (2007). Post-translational regulation of the Drosophila circadian clock requires protein phosphatase 1 (PP1). Genes & development *21*, 1506-1518.

Feng, X.H., and Derynck, R. (2005). Specificity and versatility in tgf-beta signaling through Smads. Annual review of cell and developmental biology *21*, 659-693.

Fernandez, L.P., Lopez-Marquez, A., and Santisteban, P. (2015). Thyroid transcription factors in development, differentiation and disease. Nature reviews Endocrinology *11*, 29-42.

Feyereisen, R. (1999). Insect P450 enzymes. Annual review of entomology *44*, 507-533.

Fitzsimonds, R.M., and Poo, M.M. (1998). Retrograde signaling in the development and modification of synapses. Physiological reviews *78*, 143-170.

Fredholm, B.B., Battig, K., Holmen, J., Nehlig, A., and Zvartau, E.E. (1999). Actions of caffeine in the brain with special reference to factors that contribute to its widespread use. Pharmacological reviews *51*, 83-133.

Freeman, M. (1996). Reiterative use of the EGF receptor triggers differentiation of all cell types in the Drosophila eye. Cell *87*, 651-660.

Gangwisch, J.E. (2009). Epidemiological evidence for the links between sleep, circadian rhythms and metabolism. Obesity reviews : an official journal of the International Association for the Study of Obesity *10 Suppl 2*, 37-45.

Gehring, W.J., Qian, Y.Q., Billeter, M., Furukubo-Tokunaga, K., Schier, A.F., Resendez-Perez, D., Affolter, M., Otting, G., and Wuthrich, K. (1994). Homeodomain-DNA recognition. Cell *78*, 211-223.

Gelbart, W.M., Emmert, D.B. (2013). Flybase High Throughput Expression Pattern Data.

Ghosh, A.C., and O'Connor, M.B. (2014). Systemic Activin signaling independently regulates sugar homeostasis, cellular metabolism, and pH balance in Drosophila melanogaster. Proceedings of the National Academy of Sciences of the United States of America *111*, 5729-5734.

Giebultowicz, J.M. (2000). Molecular mechanism and cellular distribution of insect circadian clocks. Annual review of entomology *45*, 769-793.

Giebultowicz, J.M., and Hege, D.M. (1997). Circadian clock in Malpighian tubules. Nature *386*, 664.

Glossop, N.R., Lyons, L.C., and Hardin, P.E. (1999). Interlocked feedback loops within the Drosophila circadian oscillator. Science *286*, 766-768.

Gorostiza, E.A., and Ceriani, M.F. (2013). Retrograde bone morphogenetic protein signaling shapes a key circadian pacemaker circuit. The Journal of neuroscience : the official journal of the Society for Neuroscience *33*, 687-696.

Gratz, S.J., Cummings, A.M., Nguyen, J.N., Hamm, D.C., Donohue, L.K., Harrison, M.M., Wildonger, J., and O'Connor-Giles, K.M. (2013). Genome engineering of Drosophila with the CRISPR RNA-guided Cas9 nuclease. Genetics *194*, 1029-1035.

Gratz, S.J., Ukken, F.P., Rubinstein, C.D., Thiede, G., Donohue, L.K., Cummings, A.M., and O'Connor-Giles, K.M. (2014). Highly specific and efficient CRISPR/Cas9-catalyzed homology-directed repair in Drosophila. Genetics *196*, 961-971.

Greig, S., and Akam, M. (1995). The role of homeotic genes in the specification of the Drosophila gonad. Current biology : CB *5*, 1057-1062.

Grima, B., Chelot, E., Xia, R., and Rouyer, F. (2004). Morning and evening peaks of activity rely on different clock neurons of the Drosophila brain. Nature *431*, 869-873.

Hao, H., Allen, D.L., and Hardin, P.E. (1997). A circadian enhancer mediates PER-dependent mRNA cycling in Drosophila melanogaster. Molecular and cellular biology *17*, 3687-3693.

Hardin, P.E. (2006). Essential and expendable features of the circadian timekeeping mechanism. Current opinion in neurobiology *16*, 686-692.

Hardin, P.E. (2011). Molecular genetic analysis of circadian timekeeping in Drosophila. Advances in genetics *74*, 141-173.

Harvey, R.P. (1996). NK-2 homeobox genes and heart development. Developmental biology *178*, 203-216.

Hay, B.A., Maile, R., and Rubin, G.M. (1997). P element insertion-dependent gene activation in the Drosophila eye. Proceedings of the National Academy of Sciences of the United States of America *94*, 5195-5200.

Hay, B.A., Wassarman, D.A., and Rubin, G.M. (1995). Drosophila homologs of baculovirus inhibitor of apoptosis proteins function to block cell death. Cell *83*, 1253-1262.

Hayashi, S., and Scott, M.P. (1990). What determines the specificity of action of Drosophila homeodomain proteins? Cell *63*, 883-894.

He, L., Wang, M., Gao, M., and Zhou, J. (1992). Expression of c-fos protein in serotonergic neurons of rat brainstem following electro-acupuncture. Acupuncture & electro-therapeutics research *17*, 243-248.

Helfrich-Forster, C. (1995). The period clock gene is expressed in central nervous system neurons which also produce a neuropeptide that reveals the projections of circadian pacemaker cells within the brain of Drosophila melanogaster. Proceedings of the National Academy of Sciences of the United States of America *92*, 612-616.

Helfrich-Forster, C. (1997). Development of pigment-dispersing hormone-immunoreactive neurons in the nervous system of Drosophila melanogaster. The Journal of comparative neurology *380*, 335-354.

Helfrich-Forster, C. (1998). Robust circadian rhythmicity of Drosophila melanogaster requires the presence of lateral neurons: a brain-behavioral study of disconnected mutants. Journal of comparative physiology A, Sensory, neural, and behavioral physiology *182*, 435-453.

Helfrich-Forster, C., and Homberg, U. (1993). Pigment-dispersing hormone-immunoreactive neurons in the nervous system of wild-type Drosophila melanogaster and of several mutants with altered circadian rhythmicity. The Journal of comparative neurology *337*, 177-190.

Helfrich-Forster, C., Shafer, O.T., Wulbeck, C., Grieshaber, E., Rieger, D., and Taghert, P. (2007). Development and morphology of the clock-gene-expressing lateral neurons of Drosophila melanogaster. The Journal of comparative neurology *500*, 47-70.

Hermann-Luibl, C., Yoshii, T., Senthilan, P.R., Dircksen, H., and Helfrich-Forster, C. (2014). The ion transport peptide is a new functional clock neuropeptide in the fruit fly Drosophila melanogaster. The Journal of neuroscience : the official journal of the Society for Neuroscience *34*, 9522-9536.

Herpin, A., Lelong, C., and Favrel, P. (2004). Transforming growth factor-beta-related proteins: an ancestral and widespread superfamily of cytokines in metazoans. Developmental and comparative immunology *28*, 461-485.

Hewes, R.S., and Taghert, P.H. (2001). Neuropeptides and neuropeptide receptors in the Drosophila melanogaster genome. Genome research *11*, 1126-1142.

Hippenmeyer, S., Kramer, I., and Arber, S. (2004). Control of neuronal phenotype: what targets tell the cell bodies. Trends in neurosciences *27*, 482-488.

Holland, P.W., Booth, H.A., and Bruford, E.A. (2007). Classification and nomenclature of all human homeobox genes. BMC biology *5*, 47.

Huminiecki, L., Goldovsky, L., Freilich, S., Moustakas, A., Ouzounis, C., and Heldin, C.H. (2009). Emergence, development and diversification of the TGF-beta signalling pathway within the animal kingdom. BMC evolutionary biology *9*, 28.

Hyun, S., Lee, Y., Hong, S.T., Bang, S., Paik, D., Kang, J., Shin, J., Lee, J., Jeon, K., Hwang, S.*, et al.* (2005). Drosophila GPCR Han is a receptor for the circadian clock neuropeptide PDF. Neuron *48*, 267-278.

Itoyama, M., and Bicudo, H. (1992). Effects of caffeine on fecundity, egg laying capacity, development time and longevity in Drosophila prosaltans. Rev Bras Genet *15*, 303-321.

Iyer, E.P., Iyer, S.C., Sullivan, L., Wang, D., Meduri, R., Graybeal, L.L., and Cox, D.N. (2013). Functional genomic analyses of two morphologically distinct classes of Drosophila sensory neurons: post-mitotic roles of transcription factors in dendritic patterning. PloS one *8*, e72434.

Ja, W.W., Carvalho, G.B., Mak, E.M., de la Rosa, N.N., Fang, A.Y., Liong, J.C., Brummel, T., and Benzer, S. (2007). Prandiology of Drosophila and the CAFE assay. Proceedings of the National Academy of Sciences of the United States of America *104*, 8253-8256.

Jagla, K., Bellard, M., and Frasch, M. (2001). A cluster of Drosophila homeobox genes involved in mesoderm differentiation programs. BioEssays : news and reviews in molecular, cellular and developmental biology *23*, 125-133.

Jennings, B.H., Pickles, L.M., Wainwright, S.M., Roe, S.M., Pearl, L.H., and Ish-Horowicz, D. (2006). Molecular recognition of transcriptional repressor motifs by the WD domain of the Groucho/TLE corepressor. Molecular cell *22*, 645-655.

Jensen, P.A., Zheng, X., Lee, T., and O'Connor, M.B. (2009). The Drosophila Activin-like ligand Dawdle signals preferentially through one isoform of the Type-I receptor Baboon. Mechanisms of development *126*, 950-957.

Jong-cheol Lee , K.-H.K., Yoon Jeong Lee , Siuk Yoo (2014). NK2-specific domain is responsible for cell death upon ectopic expression of VND in various Drosophila tissues. Genes & genomics *36*, 1-10.

Kadener, S., Stoleru, D., McDonald, M., Nawathean, P., and Rosbash, M. (2007). Clockwork Orange is a transcriptional repressor and a new Drosophila circadian pacemaker component. Genes & development *21*, 1675-1686.

Kaneko, M. (1998). Neural substrates of Drosophila rhythms revealed by mutants and molecular manipulations. Current opinion in neurobiology *8*, 652-658.

Kaneko, M., and Hall, J.C. (2000). Neuroanatomy of cells expressing clock genes in Drosophila: transgenic manipulation of the period and timeless genes to mark the perikarya of circadian pacemaker neurons and their projections. The Journal of comparative neurology *422*, 66-94.

Karch, F., Galloni, M., Sipos, L., Gausz, J., Gyurkovics, H., and Schedl, P. (1994). Mcp and Fab-7: molecular analysis of putative boundaries of cis-regulatory domains in the bithorax complex of Drosophila melanogaster. Nucleic acids research *22*, 3138-3146.

Kaufman, T.C., Lewis, R., and Wakimoto, B. (1980). Cytogenetic Analysis of Chromosome 3 in DROSOPHILA MELANOGASTER: The Homoeotic Gene Complex in Polytene Chromosome Interval 84a-B. Genetics *94*, 115-133.

Keegan, K.P., Pradhan, S., Wang, J.P., and Allada, R. (2007). Meta-analysis of Drosophila circadian microarray studies identifies a novel set of rhythmically expressed genes. PLoS computational biology *3*, e208.

Keisman, E.L., Christiansen, A.E., and Baker, B.S. (2001). The sex determination gene doublesex regulates the A/P organizer to direct sex-specific patterns of growth in the Drosophila genital imaginal disc. Developmental cell *1*, 215-225.

Kiger, J.A., Jr., Eklund, J.L., Younger, S.H., and O'Kane, C.J. (1999). Transgenic inhibitors identify two roles for protein kinase A in Drosophila development. Genetics *152*, 281-290.

Kim, Y., and Nirenberg, M. (1989). Drosophila NK-homeobox genes. Proceedings of the National Academy of Sciences of the United States of America *86*, 7716-7720.

Klose, M., Duvall, L.B., Li, W., Liang, X., Ren, C., Steinbach, J.H., and Taghert, P.H. (2016). Functional PDF Signaling in the Drosophila Circadian Neural Circuit Is Gated by Ral A-Dependent Modulation. Neuron *90*, 781-794.

Ko, C.H., and Takahashi, J.S. (2006). Molecular components of the mammalian circadian clock. Human molecular genetics *15 Spec No 2*, R271-277.

Koike, N., Yoo, S.H., Huang, H.C., Kumar, V., Lee, C., Kim, T.K., and Takahashi, J.S. (2012). Transcriptional architecture and chromatin landscape of the core circadian clock in mammals. Science *338*, 349-354.

Koizumi, K., Lintas, C., Nirenberg, M., Maeng, J.S., Ju, J.H., Mack, J.W., Gruschus, J.M., Odenwald, W.F., and Ferretti, J.A. (2003). Mutations that affect the ability of the vnd/NK-2 homeoprotein to regulate gene expression: transgenic alterations and tertiary

structure. Proceedings of the National Academy of Sciences of the United States of America *100*, 3119-3124.

Kon, N., Hirota, T., Kawamoto, T., Kato, Y., Tsubota, T., and Fukada, Y. (2008). Activation of TGF-beta/activin signalling resets the circadian clock through rapid induction of Dec1 transcripts. Nature cell biology *10*, 1463-1469.

Kot, M., and Daniel, W.A. (2008). The relative contribution of human cytochrome P450 isoforms to the four caffeine oxidation pathways: an in vitro comparative study with cDNA-expressed P450s including CYP2C isoforms. Biochemical pharmacology *76*, 543-551.

Krieglstein, K., Zheng, F., Unsicker, K., and Alzheimer, C. (2011). More than being protective: functional roles for TGF-beta/activin signaling pathways at central synapses. Trends in neurosciences *34*, 421-429.

Krishnan, B., Dryer, S.E., and Hardin, P.E. (1999). Circadian rhythms in olfactory responses of Drosophila melanogaster. Nature *400*, 375-378.

Krishnan, B., Levine, J.D., Lynch, M.K., Dowse, H.B., Funes, P., Hall, J.C., Hardin, P.E., and Dryer, S.E. (2001). A new role for cryptochrome in a Drosophila circadian oscillator. Nature *411*, 313-317.

Kucerova, L., Broz, V., Fleischmannova, J., Santruckova, E., Sidorov, R., Dolezal, V., and Zurovec, M. (2012). Characterization of the Drosophila adenosine receptor: the effect of adenosine analogs on cAMP signaling in Drosophila cells and their utility for in vivo experiments. Journal of neurochemistry *121*, 383-395.

Kuhlmann, W., Fromme, H.G., Heege, E.M., and Ostertag, W. (1968). The mutagenic action of caffeine in higher organisms. Cancer research *28*, 2375-2389.

Kula-Eversole, E., Nagoshi, E., Shang, Y., Rodriguez, J., Allada, R., and Rosbash, M. (2010). Surprising gene expression patterns within and between PDF-containing circadian neurons in Drosophila. Proceedings of the National Academy of Sciences of the United States of America *107*, 13497-13502.

Kumar, J.P. (2012). Building an ommatidium one cell at a time. Developmental dynamics : an official publication of the American Association of Anatomists *241*, 136-149.

Kvon, E.Z., Kazmar, T., Stampfel, G., Yanez-Cuna, J.O., Pagani, M., Schernhuber, K., Dickson, B.J., and Stark, A. (2014). Genome-scale functional characterization of Drosophila developmental enhancers in vivo. Nature *512*, 91-95.

Labbe, E., Silvestri, C., Hoodless, P.A., Wrana, J.L., and Attisano, L. (1998). Smad2 and Smad3 positively and negatively regulate TGF beta-dependent transcription through the forkhead DNA-binding protein FAST2. Molecular cell *2*, 109-120.

Lear, B.C., Merrill, C.E., Lin, J.M., Schroeder, A., Zhang, L., and Allada, R. (2005). A G protein-coupled receptor, groom-of-PDF, is required for PDF neuron action in circadian behavior. Neuron *48*, 221-227.

Lee, G., Hall, J.C., and Park, J.H. (2002). Doublesex gene expression in the central nervous system of Drosophila melanogaster. Journal of neurogenetics *16*, 229-248.

Lee, G.G., Kikuno, K., Nair, S., and Park, J.H. (2013). Mechanisms of postecdysis-associated programmed cell death of peptidergic neurons in Drosophila melanogaster. The Journal of comparative neurology *521*, 3972-3991.

Lee, Y., Moon, S.J., and Montell, C. (2009). Multiple gustatory receptors required for the caffeine response in Drosophila. Proceedings of the National Academy of Sciences of the United States of America *106*, 4495-4500.

Levi, F., and Schibler, U. (2007). Circadian rhythms: mechanisms and therapeutic implications. Annual review of pharmacology and toxicology *47*, 593-628.

Levine, J.D., Funes, P., Dowse, H.B., and Hall, J.C. (2002). Advanced analysis of a cryptochrome mutation's effects on the robustness and phase of molecular cycles in isolated peripheral tissues of Drosophila. BMC neuroscience *3*, 5.

Lewis, E.B. (1978). A gene complex controlling segmentation in Drosophila. Nature *276*, 565-570.

Lin, Y., Stormo, G.D., and Taghert, P.H. (2004). The neuropeptide pigment-dispersing factor coordinates pacemaker interactions in the Drosophila circadian system. The Journal of neuroscience : the official journal of the Society for Neuroscience *24*, 7951-7957.

Marin, I., and Baker, B.S. (1998). The evolutionary dynamics of sex determination. Science *281*, 1990-1994.

Marmion, R.A., Jevtic, M., Springhorn, A., Pyrowolakis, G., and Yakoby, N. (2013). The Drosophila BMPRII, wishful thinking, is required for eggshell patterning. Developmental biology *375*, 45-53.

Marques, G., Bao, H., Haerry, T.E., Shimell, M.J., Duchek, P., Zhang, B., and O'Connor, M.B. (2002). The Drosophila BMP type II receptor Wishful Thinking regulates neuromuscular synapse morphology and function. Neuron *33*, 529-543.

Martinek, S., Inonog, S., Manoukian, A.S., and Young, M.W. (2001). A role for the segment polarity gene shaggy/GSK-3 in the Drosophila circadian clock. Cell *105*, 769-779.

Matsumoto, A., Ukai-Tadenuma, M., Yamada, R.G., Houl, J., Uno, K.D., Kasukawa, T., Dauwalder, B., Itoh, T.Q., Takahashi, K., Ueda, R.*, et al.* (2007). A functional genomics strategy reveals clockwork orange as a transcriptional regulator in the Drosophila circadian clock. Genes & development *21*, 1687-1700.

Maury, E., Ramsey, K.M., and Bass, J. (2010). Circadian rhythms and metabolic syndrome: from experimental genetics to human disease. Circulation research *106*, 447-462.

McCabe, B.D., Marques, G., Haghighi, A.P., Fetter, R.D., Crotty, M.L., Haerry, T.E., Goodman, C.S., and O'Connor, M.B. (2003). The BMP homolog Gbb provides a retrograde signal that regulates synaptic growth at the Drosophila neuromuscular junction. Neuron *39*, 241-254.

McDonald, M.J., Rosbash, M., and Emery, P. (2001). Wild-type circadian rhythmicity is dependent on closely spaced E boxes in the Drosophila timeless promoter. Molecular and cellular biology *21*, 1207-1217.

McGinnis, W., Garber, R.L., Wirz, J., Kuroiwa, A., and Gehring, W.J. (1984a). A homologous protein-coding sequence in Drosophila homeotic genes and its conservation in other metazoans. Cell *37*, 403-408.

McGinnis, W., Levine, M.S., Hafen, E., Kuroiwa, A., and Gehring, W.J. (1984b). A conserved DNA sequence in homoeotic genes of the Drosophila Antennapedia and bithorax complexes. Nature *308*, 428-433.

McGuire, S.E., Le, P.T., Osborn, A.J., Matsumoto, K., and Davis, R.L. (2003). Spatiotemporal rescue of memory dysfunction in Drosophila. Science *302*, 1765-1768.

Mertens, I., Vandingenen, A., Johnson, E.C., Shafer, O.T., Li, W., Trigg, J.S., De Loof, A., Schoofs, L., and Taghert, P.H. (2005). PDF receptor signaling in Drosophila contributes to both circadian and geotactic behaviors. Neuron *48*, 213-219.

Miklos, G.L., and Rubin, G.M. (1996). The role of the genome project in determining gene function: insights from model organisms. Cell *86*, 521-529.

Miller, B.H., McDearmon, E.L., Panda, S., Hayes, K.R., Zhang, J., Andrews, J.L., Antoch, M.P., Walker, J.R., Esser, K.A., Hogenesch, J.B.*, et al.* (2007). Circadian and CLOCK-controlled regulation of the mouse transcriptome and cell proliferation. Proceedings of the National Academy of Sciences of the United States of America *104*, 3342-3347.

Miyasako, Y., Umezaki, Y., and Tomioka, K. (2007). Separate sets of cerebral clock neurons are responsible for light and temperature entrainment of Drosophila circadian locomotor rhythms. Journal of biological rhythms *22*, 115-126.

Moon, S.J., Lee, Y., Jiao, Y., and Montell, C. (2009). A Drosophila gustatory receptor essential for aversive taste and inhibiting male-to-male courtship. Current biology : CB *19*, 1623-1627.

Murad, A., Emery-Le, M., and Emery, P. (2007). A subset of dorsal neurons modulates circadian behavior and light responses in Drosophila. Neuron *53*, 689-701.

Murali, T., Pacifico, S., Yu, J., Guest, S., Roberts, G.G., 3rd, and Finley, R.L., Jr. (2011). DroID 2011: a comprehensive, integrated resource for protein, transcription factor, RNA and gene interactions for Drosophila. Nucleic acids research *39*, D736-743.

Muraro, N.I., Pirez, N., and Ceriani, M.F. (2013). The circadian system: plasticity at many levels. Neuroscience *247*, 280-293.

Nagoshi, E., Sugino, K., Kula, E., Okazaki, E., Tachibana, T., Nelson, S., and Rosbash, M. (2010). Dissecting differential gene expression within the circadian neuronal circuit of Drosophila. Nature neuroscience *13*, 60-68.

Nall, A.H., Shakhmantsir, I., Cichewicz, K., Birman, S., Hirsh, J., and Sehgal, A. (2016). Caffeine promotes wakefulness via dopamine signaling in Drosophila. Scientific reports *6*, 20938.

Nassel, D.R., Shiga, S., Mohrherr, C.J., and Rao, K.R. (1993). Pigment-dispersing hormone-like peptide in the nervous system of the flies Phormia and Drosophila: immunocytochemistry and partial characterization. The Journal of comparative neurology *331*, 183-198.

Nassel, D.R., and Winther, A.M. (2010). Drosophila neuropeptides in regulation of physiology and behavior. Progress in neurobiology *92*, 42-104.

Nathanson, J.A. (1984). Caffeine and related methylxanthines: possible naturally occurring pesticides. Science *226*, 184-187.

Nitabach, M.N., and Taghert, P.H. (2008). Organization of the Drosophila circadian control circuit. Current biology : CB *18*, R84-93.

Nitabach, M.N., Wu, Y., Sheeba, V., Lemon, W.C., Strumbos, J., Zelensky, P.K., White, B.H., and Holmes, T.C. (2006). Electrical hyperexcitation of lateral ventral pacemaker neurons desynchronizes downstream circadian oscillators in the fly circadian circuit and induces multiple behavioral periods. The Journal of neuroscience : the official journal of the Society for Neuroscience *26*, 479-489.

Parisky, K.M., Agosto, J., Pulver, S.R., Shang, Y., Kuklin, E., Hodge, J.J., Kang, K., Liu, X., Garrity, P.A., Rosbash, M.*, et al.* (2008). PDF cells are a GABA-responsive wake-promoting component of the Drosophila sleep circuit. Neuron *60*, 672-682.

Park, J.H., and Hall, J.C. (1998). Isolation and chronobiological analysis of a neuropeptide pigment-dispersing factor gene in Drosophila melanogaster. Journal of biological rhythms *13*, 219-228.

Park, J.H., Helfrich-Forster, C., Lee, G., Liu, L., Rosbash, M., and Hall, J.C. (2000). Differential regulation of circadian pacemaker output by separate clock genes in Drosophila. Proceedings of the National Academy of Sciences of the United States of America *97*, 3608-3613.

Parker, L., Ellis, J.E., Nguyen, M.Q., and Arora, K. (2006). The divergent TGF-beta ligand Dawdle utilizes an activin pathway to influence axon guidance in Drosophila. Development *133*, 4981-4991.

Parker, L., Stathakis, D.G., and Arora, K. (2004). Regulation of BMP and activin signaling in Drosophila. Progress in molecular and subcellular biology *34*, 73-101.

Peng, Y., Stoleru, D., Levine, J.D., Hall, J.C., and Rosbash, M. (2003). Drosophila free-running rhythms require intercellular communication. PLoS biology *1*, E13.

Peterson, A.J., Jensen, P.A., Shimell, M., Stefancsik, R., Wijayatonge, R., Herder, R., Raftery, L.A., and O'Connor, M.B. (2012). R-Smad competition controls activin receptor output in Drosophila. PloS one *7*, e36548.

Picot, M., Cusumano, P., Klarsfeld, A., Ueda, R., and Rouyer, F. (2007). Light activates output from evening neurons and inhibits output from morning neurons in the Drosophila circadian clock. PLoS biology *5*, e315.

Raftery, L.A., and Sutherland, D.J. (1999). TGF-beta family signal transduction in Drosophila development: from Mad to Smads. Developmental biology *210*, 251-268.

Rao, K.R. (2001). Crustacean pigmentary effector hormones: chemistry and functions of RPCF, PDH, and related peptides. Amer Zool *41*, 364-379.

Rao, K.R., and Riehm, J.P. (1993). Pigment-dispersing hormones. Annals of the New York Academy of Sciences *680*, 78-88.

Renn, S.C., Park, J.H., Rosbash, M., Hall, J.C., and Taghert, P.H. (1999). A pdf neuropeptide gene mutation and ablation of PDF neurons each cause severe abnormalities of behavioral circadian rhythms in Drosophila. Cell *99*, 791-802.

Rieger, D., Shafer, O.T., Tomioka, K., and Helfrich-Forster, C. (2006). Functional analysis of circadian pacemaker neurons in Drosophila melanogaster. The Journal of neuroscience : the official journal of the Society for Neuroscience *26*, 2531-2543.

Robbins, E., and Marcus, P.I. (1963). Dynamics of Acridine Orange-Cell Interaction. I. Interrelationships of Acridine Orange Particles and Cytoplasmic Reddening. The Journal of cell biology *18*, 237-250.

Robinett, C.C., Vaughan, A.G., Knapp, J.M., and Baker, B.S. (2010). Sex and the single cell. II. There is a time and place for sex. PLoS biology *8*, e1000365.

Ronshaugen, M., Biemar, F., Piel, J., Levine, M., and Lai, E.C. (2005). The Drosophila microRNA iab-4 causes a dominant homeotic transformation of halteres to wings. Genes & development *19*, 2947-2952.

Rosenfeld, M.G., Lunyak, V.V., and Glass, C.K. (2006). Sensors and signals: a coactivator/corepressor/epigenetic code for integrating signal-dependent programs of transcriptional response. Genes & development *20*, 1405-1428.

Rutila, J.E., Edery, I., Hall, J.C., and Rosbash, M. (1992). The analysis of new short-period circadian rhythm mutants suggests features of D. melanogaster period gene function. Journal of neurogenetics *8*, 101-113.

Rutila, J.E., Suri, V., Le, M., So, W.V., Rosbash, M., and Hall, J.C. (1998). CYCLE is a second bHLH-PAS clock protein essential for circadian rhythmicity and transcription of Drosophila period and timeless. Cell *93*, 805-814.

Sanchez, L., and Guerrero, I. (2001). The development of the Drosophila genital disc. BioEssays : news and reviews in molecular, cellular and developmental biology *23*, 698-707.

Sanchez-Herrero, E., Vernos, I., Marco, R., and Morata, G. (1985). Genetic organization of Drosophila bithorax complex. Nature *313*, 108-113.

Schibler, U., Ripperger, J., and Brown, S.A. (2003). Peripheral circadian oscillators in mammals: time and food. Journal of biological rhythms *18*, 250-260.

Scott, M.P., and Weiner, A.J. (1984). Structural relationships among genes that control development: sequence homology between the Antennapedia, Ultrabithorax, and fushi tarazu loci of Drosophila. Proceedings of the National Academy of Sciences of the United States of America *81*, 4115-4119.

Scott, M.P., Weiner, A.J., Hazelrigg, T.I., Polisky, B.A., Pirrotta, V., Scalenghe, F., and Kaufman, T.C. (1983). The molecular organization of the Antennapedia locus of Drosophila. Cell *35*, 763-776.

Seluzicki, A., Flourakis, M., Kula-Eversole, E., Zhang, L., Kilman, V., and Allada, R. (2014). Dual PDF signaling pathways reset clocks via TIMELESS and acutely excite target neurons to control circadian behavior. PLoS biology *12*, e1001810.

Serpe, M., and O'Connor, M.B. (2006). The metalloprotease tolloid-related and its TGF-beta-like substrate Dawdle regulate Drosophila motoneuron axon guidance. Development *133*, 4969-4979.

Shafer, O.T., Helfrich-Forster, C., Renn, S.C., and Taghert, P.H. (2006). Reevaluation of Drosophila melanogaster's neuronal circadian pacemakers reveals new neuronal classes. The Journal of comparative neurology *498*, 180-193.

Shafer, O.T., Kim, D.J., Dunbar-Yaffe, R., Nikolaev, V.O., Lohse, M.J., and Taghert, P.H. (2008). Widespread receptivity to neuropeptide PDF throughout the neuronal circadian clock network of Drosophila revealed by real-time cyclic AMP imaging. Neuron *58*, 223-237.

Shaw, P.J., Cirelli, C., Greenspan, R.J., and Tononi, G. (2000). Correlates of sleep and waking in Drosophila melanogaster. Science *287*, 1834-1837.

Sopory, S., Kwon, S., Wehrli, M., and Christian, J.L. (2010). Regulation of Dpp activity by tissue-specific cleavage of an upstream site within the prodomain. Developmental biology *346*, 102-112.

Stanewsky, R., Kaneko, M., Emery, P., Beretta, B., Wager-Smith, K., Kay, S.A., Rosbash, M., and Hall, J.C. (1998). The cryb mutation identifies cryptochrome as a circadian photoreceptor in Drosophila. Cell *95*, 681-692.

Stoleru, D., Peng, Y., Agosto, J., and Rosbash, M. (2004). Coupled oscillators control morning and evening locomotor behaviour of Drosophila. Nature *431*, 862-868.

Taghert, P.H., Roberts, M.E., Renn, S.C., and Jacobs, P.S. (2000). Metamorphosis of tangential visual system neurons in Drosophila. Developmental biology *222*, 471-485.
Taylor, S.S. (1989). cAMP-dependent protein kinase. Model for an enzyme family. The Journal of biological chemistry *264*, 8443-8446.

Teleman, A.A., and Cohen, S.M. (2000). Dpp gradient formation in the Drosophila wing imaginal disc. Cell *103*, 971-980.

Tijet, N., Helvig, C., and Feyereisen, R. (2001). The cytochrome P450 gene superfamily in Drosophila melanogaster: annotation, intron-exon organization and phylogeny. Gene *262*, 189-198.

Uhler, J., Zhang, H., Syu, L.J., and Mellerick, D.M. (2007). The Nk-2 box of the Drosophila homeodomain protein, Vnd, contributes to its repression activity in a Groucho-dependent manner. Mechanisms of development *124*, 1-10.

Vanden Broeck, J. (2001). Neuropeptides and their precursors in the fruitfly, Drosophila melanogaster. Peptides *22*, 241-254.

Wang, X., Liu, L., Xia, S., Feng, C., and Guo, A. (1998). Relationship between visual learning/memory ability and brain cAMP level in Drosophila. Science in China Series C, Life sciences / Chinese Academy of Sciences *41*, 503-511.

Weatherbee, S.D., Halder, G., Kim, J., Hudson, A., and Carroll, S. (1998). Ultrabithorax regulates genes at several levels of the wing-patterning hierarchy to shape the development of the Drosophila haltere. Genes & development *12*, 1474-1482.

Willoughby, L., Chung, H., Lumb, C., Robin, C., Batterham, P., and Daborn, P.J. (2006). A comparison of Drosophila melanogaster detoxification gene induction responses for six insecticides, caffeine and phenobarbital. Insect biochemistry and molecular biology *36*, 934-942.

Wu, M.N., Ho, K., Crocker, A., Yue, Z., Koh, K., and Sehgal, A. (2009). The effects of caffeine on sleep in Drosophila require PKA activity, but not the adenosine receptor. The Journal of neuroscience : the official journal of the Society for Neuroscience *29*, 11029-11037.

Xu, K., Zheng, X., and Sehgal, A. (2008). Regulation of feeding and metabolism by neuronal and peripheral clocks in Drosophila. Cell metabolism *8*, 289-300.

Yamaguchi, T., Hosono, Y., Yanagisawa, K., and Takahashi, T. (2013). NKX2-1/TTF-1: an enigmatic oncogene that functions as a double-edged sword for cancer cell survival and progression. Cancer cell *23*, 718-723.

Yan, J., Wang, H., Liu, Y., and Shao, C. (2008). Analysis of gene regulatory networks in the mammalian circadian rhythm. PLoS computational biology *4*, e1000193.

Yanagisawa, J., Yanagi, Y., Masuhiro, Y., Suzawa, M., Watanabe, M., Kashiwagi, K., Toriyabe, T., Kawabata, M., Miyazono, K., and Kato, S. (1999). Convergence of transforming growth factor-beta and vitamin D signaling pathways on SMAD transcriptional coactivators. Science *283*, 1317-1321.

Yoshii, T., Heshiki, Y., Ibuki-Ishibashi, T., Matsumoto, A., Tanimura, T., and Tomioka, K. (2005). Temperature cycles drive Drosophila circadian oscillation in constant light that otherwise induces behavioural arrhythmicity. The European journal of neuroscience *22*, 1176-1184.

Yoshii, T., Todo, T., Wulbeck, C., Stanewsky, R., and Helfrich-Forster, C. (2008). Cryptochrome is present in the compound eyes and a subset of Drosophila's clock neurons. The Journal of comparative neurology *508*, 952-966.

Yu, Z., Syu, L.J., and Mellerick, D.M. (2005). Contextual interactions determine whether the Drosophila homeodomain protein, Vnd, acts as a repressor or activator. Nucleic acids research *33*, 1-12.

Zaffran, S., Das, G., and Frasch, M. (2000). The NK-2 homeobox gene scarecrow (scro) is expressed in pharynx, ventral nerve cord and brain of Drosophila embryos. Mechanisms of development *94*, 237-241.

Zheng, X., Wang, J., Haerry, T.E., Wu, A.Y., Martin, J., O'Connor, M.B., Lee, C.H., and Lee, T. (2003). TGF-beta signaling activates steroid hormone receptor expression during neuronal remodeling in the Drosophila brain. Cell *112*, 303-315.

Zheng, X., Zugates, C.T., Lu, Z., Shi, L., Bai, J.M., and Lee, T. (2006). Baboon/dSmad2 TGF-beta signaling is required during late larval stage for development of adult-specific neurons. The EMBO journal *25*, 615-627.

Zhu, C.C., Boone, J.Q., Jensen, P.A., Hanna, S., Podemski, L., Locke, J., Doe, C.Q., and O'Connor, M.B. (2008). Drosophila Activin- and the Activin-like product Dawdle function redundantly to regulate proliferation in the larval brain. Development *135*, 513-521.

Zornik, E., Paisley, K., and Nichols, R. (1999). Neural transmitters and a peptide modulate Drosophila heart rate. Peptides *20*, 45-51.

APPENDIX

Groucho (Gro) is a transcriptional co-repressor and is involved in regulating several genes involved in *Drosophila* development. In the case of VND, a member of the NK2 family, GRO has been shown to interact with the N-terminal TN domain as previously stated in Chapter 2 of this thesis. However, our genetic data indicate that SCRO-mediated *Pdf* repression does not involve GRO. In order to look into the function of *Gro* in Pdf and clock neurons, we overexpressed it using *Pdf-Gal4* and *tim-Gal4*. The s-LNv projections usually terminate in the dorsal brain but in the case of ectopic expression of *Gro* this does not seem to be true. Interestingly, overexpression of *Gro* leads to overgrowth of s-LNv dorsal projections. This suggests a role for *Gro* in development of the s-LNv projections (Figure A1). It probably interacts with a DNA binding protein that is involved in development of s-LNv axonal projections. In addition, we also looked into the function of Gro in the developing eye. When we ectopically expressed *Gro* using *GMR-Gal4*, we observed a much severe phenotype than what we observed for *scro* (Figure 3.2). This clearly indicates a much broader role for *Gro* during development.

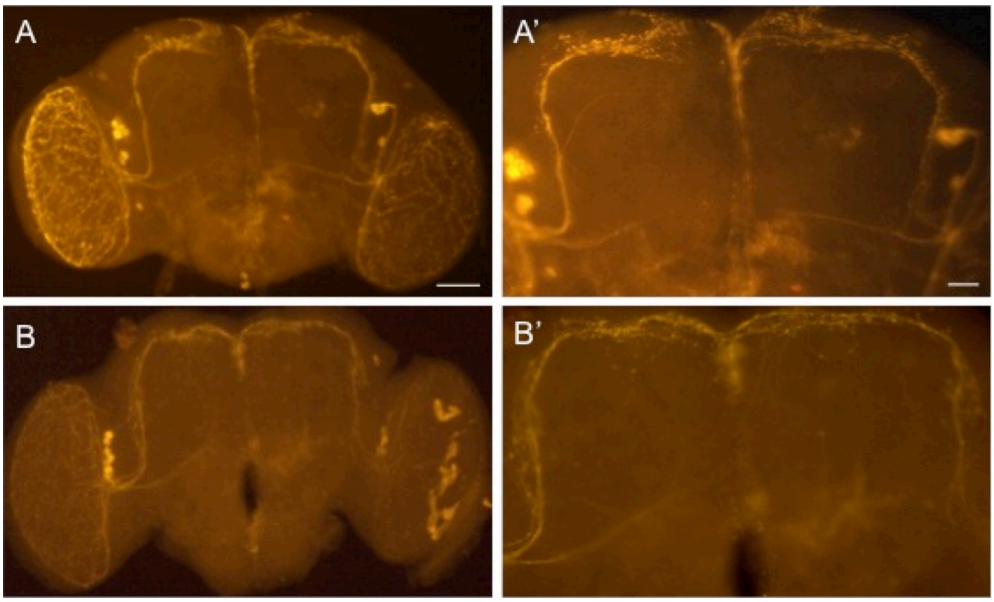


Figure A1: Overexpression of *Gro* led to aberrant phenotype of the s-LNv dorsal projections. (A and A') *Pdf-Gal4/+; UAS-Gro/+* showed continual growth of dorsal projections with a fork at the end of these axonal projections. The phenotype differs for ectopic expression of *Gro* in the clock neurons. (B and B') *tim-Gal4/+; UAS-Gro/+* have continued dorsal projections with no fork.

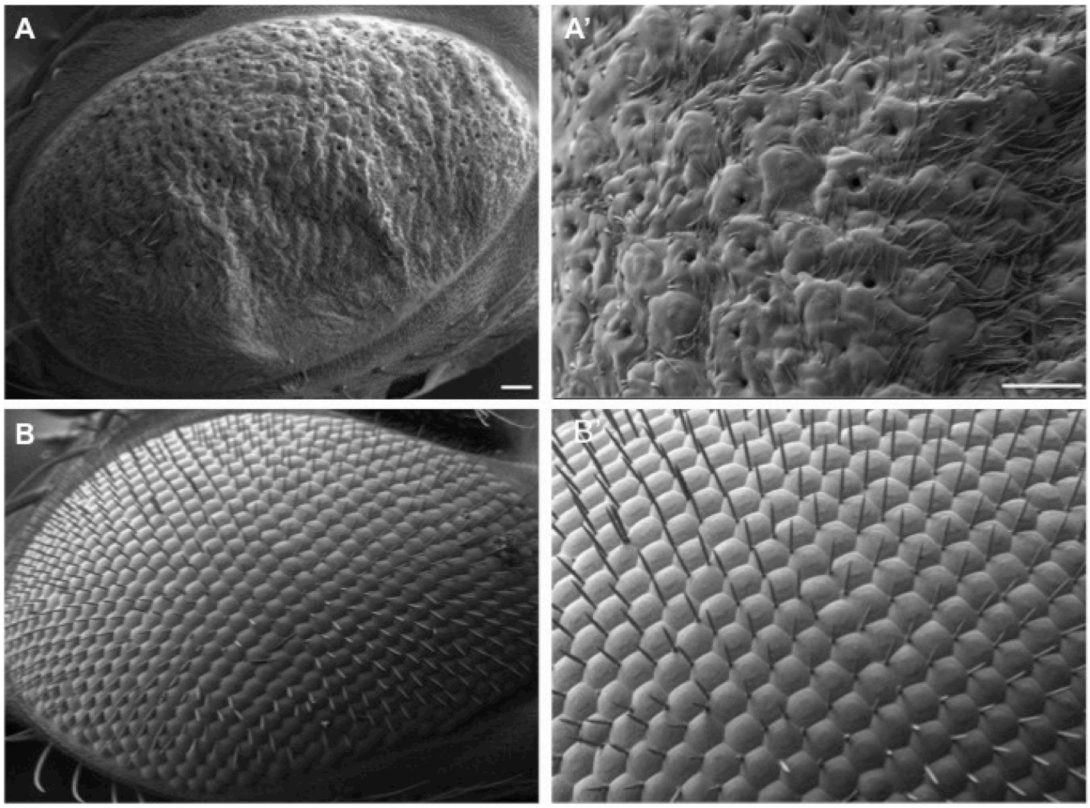


Figure A2: Ectopic expression of *Gro* led to abnormal eye phenotype. SEM images depicting eye phenotype. (A and A') *GMR-Gal4/+;; UAS-Gro/+* flies with lack of ommatidia and holes in the eye with a lot of extra bristles. In comparison, the wild type flies have eyes with intact ommatidia and bristles (B and B').

VITA

Sudershana Nair grew up in Mumbai, India. She took up Life Sciences during her undergraduate years in University of Mumbai and graduated with Bachelor of Science degree in Biochemistry and Zoology. She continued her graduate study in University of Mumbai in Biochemistry and was awarded with a Masters in Science degree in 2007. She joined the University of Tennessee, Knoxville in August 2009 to pursue her doctoral studies in the field of *Drosophila* neurogenetics. She joined Dr. Jae H. Park's laboratory at the University of Tennessee, Knoxville in May 2010 and started her work on investigating regulation of the neuropeptide pigment-dispersing factor. In 2016, she was awarded the James and Dora Wright fellowship for excellence in research.